MULTIREFERENCE COUPLED CLUSTER THEORY

by

FRANCESCO EVANGELISTA

(Under the Direction of Henry F. Schaefer III)

ABSTRACT

In this dissertation we have developed and applied the state-specific multireference coupled cluster theory suggested by Mukherjee and co-workers (Mk-MRCC). For model systems, Mk-MRCC is found to provide more accurate results than competitor theories at all levels of truncation of the cluster operator. The first production-level code for Mukherjee multireference coupled cluster singles and doubles (Mk-MRCCSD) computations has been written. A crucial element for the development of Mk-MRCC into a computational tool was the realization that the coupling terms appearing in the equations could be written in a simple closed form. Mk-MRCCSD results are reported for the singlet-triplet splittings in *ortho*-, *meta*-, and *para*-benzyne, coming within 1.5 kcal mol^{-1} of experiment in all cases. We also report the first implementation with correct scaling of the Mk-MRCC method with singles, doubles, and approximate iterative triples Mk-MRCCSDT-*n*, (*n* = 1a,1b,2,3) as well as full triples (Mk-MRCCSDT). In all model systems the various Mk-MRCCSDT-*n* approaches recover on average between 59% and 73% of the full triples effect.

INDEX WORDS: multireference coupled cluster theory, bond dissociation, diradicals, thermochemistry, benzynes

MULTIREFERENCE COUPLED CLUSTER THEORY

by

FRANCESCO EVANGELISTA

FORB, Università di Pisa, Pisa, Italy, 2004

A Dissertation Submitted to the Graduate Faculty of The University of Georgia in Partial

Fulfillment of the Requirements for the Degree

DOCTOR OF PHILOSOPHY

ATHENS, GEORGIA

2008

MULTIREFERENCE COUPLED CLUSTER THEORY

by

FRANCESCO EVANGELISTA

Major Professor: Henry F. Schaefer III

Committee: Wesley D. Allen
                    Steven P. Lewis

Electronic Version Approved:

Maureen Grasso
Dean of the Graduate School
The University of Georgia
December 2008

To my wife Rhiannon.

theory, I found the subject fascinating. In my visit to CC(Q)C I was given a lot of material to read and brought it back with me to Vasto, in Italy. What was going on at CC(Q)C was interesting but it looked challenging. Without the summer fellowship program in 2003 I would have probably never applied to the University of Georgia. I would like to thank Nate DeYonker and Michael Schuurman who were in charge of the program in 2003.

I would like to thank Dr. Fritz Schaefer for giving me the opportunity to work in his group. I was given a great deal of time and resources that I never dreamed to be able to get during a Ph.D. program. During these four years I enjoyed working with Dr. Wesley Allen on multireference coupled cluster. I am particularly thankful for all the times he pushed me to look deeper into problems. Dr. Yukio Yamaguchi guided me into the world of scientific programming with his insights and extremely useful lecture notes. A special thank goes to Dr. Andrew Simmonett, I really enjoyed all the evenings we spent programming PSIMRCC. Dr. Justin Turney has been a good friend and constant source of insight and help.

The few conversations with Ed Valeev that I had at the beginning of my Ph.D. work were essential to the success of my studies. During my Ph.D. program I enjoyed collaborating with Professor Jürgen Gauss. Special thanks go to Professor Debashis Mukherjee. He has been a great guide and a mentor.

TABLE OF CONTENTS

INTRODUCTION AND LITERATURE REVIEW

1.1 INTRODUCTION

Studying multireference open-shell atomic and molecular systems such as radicals, biradicals and excited electronic states is a challenge for both experimentation and theory. From the experimental point of view, these chemical species are highly reactive and short-lived.[1] Despite the enormous progress made by the quantum chemistry community, multireference open-shells are still problematic because the wave function is not dominated by a single electron configuration.

The coupled cluster method in its single-reference formulation (SRCC) is now established as the most accurate theoretical level to study the electronic structure of atoms and molecules. For well-behaved systems (i.e., closed-shell and most high-spin open-shell molecules), SRCC achieves experimental accuracy for molecular thermochemistry and kinetics.[2] In contrast, the failures of single-reference coupled cluster methods for open-shell molecular systems with a multireference wave function are well documented.

The purpose of this thesis is the development of multireference coupled cluster theory into a robust and versatile tool for the study of diradicals and excited states. In this introduction I will focus on defining the nature of a multireference wave function, giving a brief review of

coupled cluster theory, and discussing the problems connect to the generalization of coupled cluster theory to the multireference case.

1.2 DEFINING MULTIREFERENCE

In this section we seek to define the concept of multireference character of a wave function. To this end, we will expand the exact electronic wave function $|\Psi\rangle$ in a one-particle spin-orbital basis set $\{\psi_p(x)\}$ of dimension M, with x a composite index for spatial ($\mathbf{r}$) and spin (s) variables, i.e. $x = \{\mathbf{r}, s\}$. The electronic Hamiltonian in the Born-Oppenheimer approximation may be written using the second quantization creation ($\hat{a}^\dagger$) and annihilation operators ($\hat{a}$) as[3]

$$\hat{H} = \sum_{pq} h_{pq} \hat{a}_p^\dagger \hat{a}_q + \frac{1}{4} \sum_{pqrs} \langle pq||rs\rangle \hat{a}_p^\dagger \hat{a}_q^\dagger \hat{a}_s \hat{a}_r \, , \tag{1.1}$$

where the labels p, q, r, and s run over the entire spin-orbital basis set, and the one- and two-electron integrals are defined as

$$\begin{aligned} h_{pq} &= \int dx \, \psi_p^*(x) \hat{h}(x) \psi_q(x), \\ \langle pq|rs\rangle &= \int dx \, dx' \, \psi_p^*(x) \psi_q^*(x') \frac{1}{|\mathbf{r} - \mathbf{r}'|} \psi_r(x) \psi_s(x'), \end{aligned} \tag{1.2}$$

while the antisymmetrized two-electron integral used in Eq. (1.1) are defined $\langle pq||rs\rangle = \langle pq|rs\rangle - \langle pq|sr\rangle$.

If $|\Psi\rangle$ is normalized, the energy is given by the expectation value of the Hamiltonian operator

$$E = \langle \Psi | \hat{H} | \Psi \rangle$$

$$= \sum_{pq} h_{pq} \langle \Psi | \hat{a}_p^\dagger \hat{a}_q | \Psi \rangle + \frac{1}{4} \sum_{pqrs} \langle pq || rs \rangle \langle \Psi | \hat{a}_p^\dagger \hat{a}_q^\dagger \hat{a}_s \hat{a}_r | \Psi \rangle \qquad (1.3)$$

$$= \sum_{pq} h_{pq} \gamma_q^p + \frac{1}{4} \sum_{pqrs} \langle pq || rs \rangle \gamma_{rs}^{pq},$$

where the quantities $\gamma_q^p = \langle \Psi | \hat{a}_p^\dagger \hat{a}_q | \Psi \rangle$ and $\gamma_{rs}^{pq} = \langle \Psi | \hat{a}_p^\dagger \hat{a}_q^\dagger \hat{a}_s \hat{a}_r | \Psi \rangle$ appearing in the above

equation are elements of the one- and two-particle reduced density matrices γ_1 and γ_2. These

quantities allow us to rewrite the energy expression in a more compact way and are going to be

used to classify electronic states into open- and closed-shell. From Eq. (1.3) it is evident that γ_1

and γ_2 contain all the information necessary to compute the energy of a system of electrons.

The diagonal elements of γ_1 (γ_p^p) give the probability of finding an electron in spin-orbital p,

while $\frac{1}{2} \gamma_{pq}^{pq}$ gives the probability of finding an electron pair in spin-orbitals p and q.

The contribution of γ_2 to the electronic energy is composed of one- and two-body terms.

To separate these two effects it is convenient to introduce the two-particle density cumulant λ_2

defined as $\gamma_{rs}^{pq} = \gamma_r^p \gamma_s^q - \gamma_s^p \gamma_r^q + \lambda_{rs}^{pq}$. In essence, λ_{rs}^{pq} is the non-trivial component of the

two-particle density matrix, as it is defined as the difference of γ_2 and the two-particle density

matrix for independent particles obeying Fermi statistics, $\gamma_s^p \gamma_r^q - \gamma_r^p \gamma_s^q$. The energy can now be

written in terms of γ_1 and λ_2

$$E = \frac{1}{2} \sum_{pq} (h_{pq} + f_{pq}^\gamma) \gamma_{pq} + \frac{1}{4} \sum_{pqrs} \langle pq || rs \rangle \lambda_{rs}^{pq}, \qquad (1.4)$$

where the generalized Fock matrix f_{pq}^γ is given by $f_{pq}^\gamma = h_{pq} + \sum_{rs} \langle pr || sq \rangle \gamma_s^r$. Now all the

contribution of the Coulomb correlation is contained in the second term of Eq. (1.4) and is

separated from the energy contribution of the one-particle density matrix. For an independent particle model (i.e. Hartree−Fock theory), only the first term of Eq. (1.4) contributes to the energy and λ_2 is zero.

Since the energy of the exact wave function is invariant with respect to a unitary rotation of the spin-orbitals, we will work in the basis that diagonalizes the one-particle density matrix. The corresponding spin-orbitals are then called natural orbitals, and the one-particle density can be characterized simply by the eigenvalues, or spin-orbital occupation numbers, of each orbital p,

$$n_p = \left\langle \Psi \left| \hat{a}_p^\dagger \hat{a}_p \right| \Psi \right\rangle .$$

To illustrate the importance of γ_1 and λ_2 in our definition of open- and closed-shell states, we will consider a simple example: the dissociation of H_2 in a minimal basis set. The minimal basis set for H_2 consists of two normalized $1s$ atomic orbitals centered on each H atom, $\chi_A(\mathbf{r})$ and $\chi_B(\mathbf{r})$. From these two atomic orbital the symmetry adapted molecular orbitals φ_1 (σ bonding) and φ_2 (σ^* antibonding) can be formed,

$$\varphi_1(\mathbf{r}) = \frac{\chi_A(\mathbf{r}) + \chi_B(\mathbf{r})}{\sqrt{2(1 + S_{AB})}}, \quad \varphi_2(\mathbf{r}) = \frac{\chi_A(\mathbf{r}) - \chi_B(\mathbf{r})}{\sqrt{2(1 - S_{AB})}}, \tag{1.5}$$

where the overlap integral S_{AB} is defined as

$$S_{AB} = \int \chi_A(\mathbf{r}) \chi_B(\mathbf{r}) \, d\mathbf{r} . \tag{1.6}$$

Within the minimal basis set, the exact ground state wave function of H_2 is a linear combination of two electronic configurations

$$\left| \Psi \right\rangle = c_1 \left| \Phi_1 \right\rangle + c_2 \left| \Phi_2 \right\rangle , \tag{1.7}$$

where $|\Phi_1\rangle = \hat{a}_1^\dagger \hat{a}_{\bar{1}}^\dagger |-\rangle$, $|\Phi_2\rangle = \hat{a}_2^\dagger \hat{a}_{\bar{2}}^\dagger |-\rangle$, and $|-\rangle$ is the true vacuum. In writing these two configurations we have used a bar above the orbital indices to indicate an electron in a beta spin-orbital. For this wave function the one-particle density matrix is

$$\gamma_q^p = \gamma_{\bar{q}}^{\bar{p}} = \begin{bmatrix} c_1^2 & 0 \\ 0 & c_2^2 \end{bmatrix}, \tag{1.8}$$

while the non-zero spin blocks of the two-body density cumulant is

$$\lambda_{r\bar{s}}^{p\bar{q}} = \begin{bmatrix} c_1^2(1-c_1^2) & c_1 c_2 (1-c_1 c_2) \\ c_1 c_2 (1-c_1 c_2) & c_2^2(1-c_2^2) \end{bmatrix}. \tag{1.9}$$

At the equilibrium geometry, the ground state wave function of H$_2$ is dominated by $|\Phi_1\rangle$, which means that $c_1 \approx 1$ and the second configuration has a small coefficients, that is $|c_2| < \varepsilon \ll 1$. Then γ_1 is

$$\gamma_q^p = \gamma_{\bar{q}}^{\bar{p}} = \begin{bmatrix} 1 & 0 \\ 0 & 0 \end{bmatrix} + O(\varepsilon^2), \tag{1.10}$$

which shows that that γ_1 is idempotent, that is $\gamma_1 \gamma_1 = \gamma_1$, in other words, the eigenvalues of γ_1 are either zero or one. λ_2 is given instead by

$$\lambda_{r\bar{s}}^{p\bar{q}} = \begin{bmatrix} 0 & c_2 \\ c_2 & 0 \end{bmatrix} + O(\varepsilon^2), \tag{1.11}$$

and its trace is equal to zero, up to linear terms in c_k. This case shows that when the wave function is dominated by one configuration the main contribution to the correlation is given by the first term of Eq. (1.4), with the contribution of Coulomb correlation to the energy entering at order $O(\varepsilon)$.

For dissociated H_2 the two electronic configurations are degenerate and the wave functions is characterized by $c_1 = -c_2 = 2^{-1/2}$. In this case we have

$$\gamma_q^p = \gamma_{\bar{q}}^{\bar{p}} = \begin{bmatrix} \frac{1}{2} & 0 \\ 0 & \frac{1}{2} \end{bmatrix}, \tag{1.12}$$

so that $\boldsymbol{\gamma}_1$ is no longer idempotent, since $\boldsymbol{\gamma}_1\boldsymbol{\gamma}_1 = \frac{1}{2}\boldsymbol{\gamma}_1$. The two-body density cumulant is

$$\lambda_{rs}^{p\bar{q}} = \begin{bmatrix} \frac{1}{4} & \frac{-3}{2} \\ \frac{-3}{2} & \frac{1}{4} \end{bmatrix}, \tag{1.13}$$

and the trace of $\boldsymbol{\lambda}_2$ is equal to $\frac{1}{2}$. For this example the Coulomb correlation energy is no longer a first-order correction, but instead a zeroth-order contribution.

These two examples represent the limiting case of single- and multireference systems and suggest that the properties of $\boldsymbol{\gamma}_1$ and $\boldsymbol{\lambda}_2$ may be used to classify electronic states into open- and closed-shell. Here I will follow the classification introduced by Kutzelnigg.[4] Closed-shell states are characterized by two properties: (1) they are non-degenerate and transform as a one-dimensional irrep of the molecular symmetry group. Degenerate sets of natural spin orbitals have the same occupation number, (2) The one-particle density matrix $\boldsymbol{\gamma}_1$ is near-idempotent ($\boldsymbol{\gamma}_1\boldsymbol{\gamma}_1 \cong \boldsymbol{\gamma}_1$) and therefore its eigenvalues are approximately 0 or 1. The occupation number may be used to sort the spin-orbitals in two categories: elements in the first group $\{\psi_i\}$ are characterized by occupation $n_i \cong 1$ and are called (doubly) occupied while orbitals in the second category $\{\psi_a\}$ have zero occupation $n_a \cong 0$ and are called virtual. For closed-shell states a zeroth-order approximation to the wave function is given by a Slater determinant built out of all the occupied spin-orbitals

$$\left|\Psi^{(0)}\right\rangle = \left|\Phi\right\rangle = \prod_i^{occ} \hat{a}_i^\dagger \left|-\right\rangle . \tag{1.14}$$

Open-shell states do not satisfy one or both of these properties. This leads to three types of open-shell states: (1) A non-degenerate state with non-idempotent γ_1. (2) A degenerate state with a near idempotent γ_1. (3) A degenerate state with a non-idempotent γ_1. Case (1) is distinguished from the closed-shell case by the fact there is a distinct group of orbitals $\{\psi_x\}$ with occupation $0 < n_x < 1$. These systems may be characterized by the trace of the two-particle density cumulant λ_2

$$\mathrm{Tr}(\lambda_2) = \sum_p^{all} n_p(1-n_p) \cong \sum_x^{act} n_x(1-n_x) . \tag{1.15}$$

$\mathrm{Tr}(\lambda_2)$ is a measure of electron correlation and it is zero for a Slater determinant. For N_{act} active electrons, the largest value $\mathrm{Tr}(\lambda_2)$ can assume is $N_{act}/4$. A correct zeroth-order wave functions for this type of open-shell states is the product of the closed-shell determinant built from occupied orbitals times all possible combinations of active electrons

$$\left|\Psi^{(0)}\right\rangle = \prod_i^{occ} \hat{a}_i^\dagger \left[C_{xy\cdots} \sum_{xy\cdots}^{act} \hat{a}_x^\dagger \hat{a}_y^\dagger \cdots \right] \left|-\right\rangle = \sum_{\mu=1}^{d} \left|\Phi_\mu\right\rangle c_\mu , \tag{1.16}$$

where the coefficients $C_{xy\cdots}$ weight the different combinations of active electrons. Notice that this wave function can be conveniently written as a generic expansion in terms of d Slater determinants Φ_μ times a coefficient c_μ. Open-shell states of type (2) and (3) are less relevant to our work and will not be discussed here.

1.3 THE SINGLE-REFERENCE COUPLED CLUSTER APPROACH

A basic assumption of most post-Hartree–Fock methods is that the exact electronic wave function $|\Psi\rangle$ can be expressed as the sum of a reference Slater determinant $|\Phi\rangle$ built from a set of optimized orbitals (i.e. Hartree–Fock orbitals), plus a correction $|\Xi\rangle$ which accounts for electron correlation

$$|\Psi\rangle = |\Phi\rangle + |\Xi\rangle. \tag{1.17}$$

Because a single Slater determinant cannot account for Coulomb correlation $[\gamma_2 = 0]$ the correction $|\Xi\rangle$ is effectively accounting for this missing contribution.

In coupled cluster theory the exact wave function is expressed via the exponential ansatz

$$|\Psi\rangle = e^{\hat{T}}|\Phi\rangle, \tag{1.18}$$

where $|\Phi\rangle$ is a reference closed-shell or open-shell Slater determinant, and $\hat{T}$ is an excitation operator truncated at a certain level n

$$\hat{T} = \sum_{k=1}^{n} \hat{T}_n . \tag{1.19}$$

Each individual component of the cluster operator is expressed introducing the cluster amplitudes $t_{ij\cdots}^{ab\cdots}$ defined as $t_{ij\cdots}^{ab\cdots} = \langle \Phi_{ij\cdots}^{ab\cdots} | \hat{T} | \Phi \rangle$, so that $\hat{T}_n$ is given by

$$\hat{T}_n = \frac{1}{(n!)^2} \sum_{ij\cdots}^{\text{occ}} \sum_{ab\cdots}^{\text{vir}} t_{ij\cdots}^{ab\cdots} \underbrace{\cdots \hat{a}_b^{\dagger} \hat{a}_j \hat{a}_a^{\dagger} \hat{a}_i}_{n\text{-th level excitation}} . \tag{1.20}$$

The cluster amplitudes thus defined are antisymmetric with respect to the interchange of upper or lower indices. After expanding the exponential ansatz [Eq. (1.18)] we can now identify the correction $|\Xi\rangle$ with the terms containing linear and higher powers of $\hat{T}$

$$|\Psi\rangle = |\Phi\rangle + \hat{T}|\Phi\rangle + \underbrace{\frac{1}{2!}\hat{T}^2|\Phi\rangle + \ldots}_{|\Xi\rangle} \qquad (1.21)$$

To determine $\hat{T}$ and the energy the coupled cluster ansatz in introduced in the Schrödinger equation

$$\hat{H}e^{\hat{T}}|\Phi\rangle = Ee^{\hat{T}}|\Phi\rangle. \qquad (1.22)$$

It is convenient to premultiply Eq. (1.22) by $\exp(-\hat{T})$ to get the equivalent equation

$$e^{-\hat{T}}\hat{H}e^{\hat{T}}|\Phi\rangle = \bar{H}|\Phi\rangle = E|\Phi\rangle, \qquad (1.23)$$

where the similarity transformed Hamiltonian $\bar{H} = e^{-\hat{T}}\hat{H}e^{\hat{T}}$ has been introduced. This form of the coupled cluster equations has the advantage that all terms are connected, therefore showing that energy and other physical properties are guaranteed to scale properly with the size of the system. By applying the Baker-Campbell-Hausdorff formula[5] we can expand $\bar{H}$ in terms of commutators of $\hat{H}$ and $\hat{T}$

$$\begin{aligned}
e^{-\hat{T}}\hat{H}e^{\hat{T}} = \hat{H} &+ \left[\hat{H},\hat{T}\right] \\
&+ \frac{1}{2!}\left[\left[\hat{H},\hat{T}\right],\hat{T}\right] \\
&+ \frac{1}{3!}\left[\left[\left[\hat{H},\hat{T}\right],\hat{T}\right],\hat{T}\right] \\
&+ \frac{1}{4!}\left[\left[\left[\left[\hat{H},\hat{T}\right],\hat{T}\right],\hat{T}\right],\hat{T}\right].
\end{aligned} \qquad (1.24)$$

Two conditions contribute to the truncation of $\bar{H}$ at four nested commutators: (1) the fact that $\hat{T}$ is a pure excitation operator, and (2) the two-particle nature of the Hamiltonian. Projecting Eq. (1.23) on the left with the reference determinant $\langle\Phi|$ we get an equation for the energy

$$E = \langle\Phi|\bar{H}|\Phi\rangle. \qquad (1.25)$$

Sufficiency conditions to determine the cluster amplitudes are derived by projecting Eq. (1.23) on the manifold of excited determinants $M = \left\{ \left| \Phi_{ij\cdots}^{ab\cdots} \right\rangle, \left| \Phi_{ij\cdots}^{ab\cdots} \right\rangle \in \hat{T} \left| \Phi \right\rangle \right\}$:

$$\left\langle \Phi_{ij\cdots}^{ab\cdots} \left| \bar{H} \right| \Phi \right\rangle = 0. \tag{1.26}$$

Truncating the cluster operator to single and double excitations (n = 2) defines the coupled cluster method with singles and doubles (CCSD). When CCSD is augmented by a perturbative estimate of the effect of triple excitations we get the CCSD(T) method, the "gold standard" of quantum chemistry.

1.4 FAILURE OF SINGLE-REFERENCE COUPLED CLUSTER THEORY FOR MULTIREFERENCE SYSTEMS

In the preceding section we saw that the correction accounting for electron correlation may be written as

$$\left| \Xi \right\rangle = \hat{T} \left| \Phi \right\rangle + \frac{1}{2!} \hat{T}^2 \left| \Phi \right\rangle + \dots \tag{1.27}$$

This assumption clearly breaks down for a multireference system. Suppose the zeroth-order wave function $\left| \Psi^{(0)} \right\rangle$ to be an equally weighted sum of a reference determinant $\left| \Phi \right\rangle$ and a doubly excited determinant $\left| \Phi_{k\bar{k}}^{c\bar{c}} \right\rangle$

$$\left| \Psi^{(0)} \right\rangle = \frac{1}{\sqrt{2}} \left(\left| \Phi \right\rangle - \left| \Phi_{k\bar{k}}^{c\bar{c}} \right\rangle \right). \tag{1.28}$$

Then a cluster analysis of the wavefunction would give the double excitation amplitude $t_{k\bar{k}}^{c\bar{c}}$ a value of ca. −1. When this happens, disconnected quadruples (e.g. deriving from the square of the cluster operator) containing excitations from orbital pair k to the virtual orbital c will be overestimated, in turn affecting all other cluster amplitudes. As a consequence, when we apply

CCSD and CCSD(T) to a system with multireference character these methods can incur in a significant error.

1.5 MULTIREFERENCE COUPLED CLUSTER FORMALISMS

The generalization of the single-reference ansatz to the multireference case is neither straightforward nor unique. For a review of the major formalisms the reader should consult the introduction to Chapter II. Here I would like to emphasize the ideas contained in the various formalisms advanced in the literature. The first complication introduced when extending a single-reference theory to the multireference case is the partitioning of the orbitals in three spaces: core, active and external. These in turn are used to define a set of Slater determinants or configuration state functions Φ_μ with $\mu = 1 \dots d$, called the model space. Core orbitals are doubly occupied in all functions belonging to the model space, while active orbitals are partially occupied and external orbitals are unoccupied.

Two basic paradigms have been advanced in multireference coupled cluster theory. Both seek to express an exact electronic state $|\Psi_\alpha\rangle$ by the action of a wave operator $\hat{\Omega}$ on a zeroth-order wave function $|\Psi_\alpha^{(0)}\rangle$

$$|\Psi_\alpha\rangle = \hat{\Omega}|\Psi_\alpha^{(0)}\rangle, \tag{1.29}$$

where the zeroth-order wave function is a linear combination of model space determinants

$$|\Psi_\alpha^{(0)}\rangle = \sum_{\mu=1}^{d} c_\mu^{(\alpha)} |\Phi_\mu\rangle. \tag{1.30}$$

In the first paradigm the wave operator is parameterized by a single exponential operator[6]

$$\hat{\Omega} = e^{\hat{S}}, \tag{1.31}$$

so that the final wave function is internally contracted

$$\left| \Psi_\alpha \right\rangle = e^{\hat{S}} \sum_{\mu=1}^{d} c_\mu^{(\alpha)} \left| \Phi_\mu \right\rangle. \tag{1.32}$$

In practice this form is problematic because $\hat{S}$ cannot be defined as a pure excitation operator and thus leads to a non-terminating expansion of the similarity-transformed Hamiltonian $e^{-\hat{S}} \hat{H} e^{\hat{S}}$. This problems was first addressed in Fock-space multireference coupled cluster (FS-MRCC) theory[7] by taking the normal ordered part of $\exp(\hat{S})$, that is

$$\hat{\Omega}_{\text{FS-MRCC}} = \left\{ e^{\hat{S}} \right\}. \tag{1.33}$$

The ansatz of Eq. (1.33) eliminates contractions among cluster operators themselves, which do not arise in the single-reference case.

In Fock-space multireference coupled cluster theory, the Fermi vacuum is a *N*-electron state $\left| \Phi \right\rangle$. Particle non-conserving operators are used to reach ionized or electron attached states with multireference character. The model space then is augmented with all possible occupations of the active orbitals and divided into sectors (*m,n*) according to how many electrons are added and removed from $\left| \Phi \right\rangle$. The wave operator includes operator from different sectors of the Fock space,

$$\hat{S} = \hat{S}^{(m,n)} = \sum_{\substack{k=0...m \\ l=0...n}} \hat{T}^{(k,l)}, \tag{1.34}$$

where $\hat{T}^{(k,l)}$ are cluster operators for a the (*k,l*) sector and include excitations cluster operators truncated at level *n*

$$\hat{T}^{(k,l)} = \hat{T}_1^{(k,l)} + \hat{T}_2^{(k,l)} + \ldots + \hat{T}_n^{(k,l)}. \tag{1.35}$$

Fock space coupled cluster is best suited to compute differential properties like excitation energies, electron affinities and ionization potentials. On the contrary, the computation of potential energy surfaces is plagued by the intruder state problem, caused by determinants outside the zeroth-order wave function which interact strongly with the model space in certain areas of the potential energy surface.

Another formalism based on Eq. (1.31) was recently advanced by Mukherjee and co-workers. These developments are based on extended normal ordering with respect to a multireference vacuum[8,9] which facilitates the evaluation of the expectation values of an operator $\hat{O}$ with respect to vacuum $\left| \Psi^{(0)} \right\rangle$. The internally contracted MRCC of Mukherjee[8] starts from an operator $\hat{S}$ containing redundant set of excitations, which is transformed to a linearly independent operator by singular value decomposition. Although this formalism is promising, so far the complexity of extended normal ordering has hindered its development.

The second MRCC paradigm is based on the wave operator ansatz of Jeziorski and Monkhorst[10]

$$\hat{\Omega}_{\mathrm{JM}} = \sum_{\mu=1}^{d} e^{\hat{T}^{\mu}} \left| \Phi_{\mu} \right\rangle \left\langle \Phi_{\mu} \right|, \tag{1.36}$$

where the cluster operators $\hat{T}^{\mu}$ are excitation operators that promote electrons from the occupied to the virtual orbital space of Φ_{μ} and are typically truncated at a certain excitation level n,

$$\hat{T}^{\mu} = \hat{T}_1^{\mu} + \hat{T}_2^{\mu} + \ldots + \hat{T}_n^{\mu}. \tag{1.37}$$

The wave function obtained from the JM ansatz is

$$|\Psi\rangle = \hat{\Omega}_{\mathrm{JM}}\left|\Psi^{(0)}\right\rangle = \sum_{\mu=1}^{d} e^{\hat{T}^{\mu}}\left|\Phi_{\mu}\right\rangle c_{\mu}^{(\alpha)}, \tag{1.38}$$

and is a linear combination of exponential functions obtained from reference determinants Φ_{μ} spanning a d-dimensional model space. This form of the wave function is basically an uncontracted version of Eq. (1.32). The energy of the JM wave function is obtained as an eigenvalue of the effective Hamiltonian matrix

$$H_{\mu\nu}^{\mathrm{eff}} = \left\langle\Phi_{\mu}\left|\hat{H}e^{\hat{T}^{\nu}}\right|\Phi_{\nu}\right\rangle, \tag{1.39}$$

while the expansion coefficients $[c_{\mu}^{(\alpha)}]$ entering Eq. (1.38) are derived from the corresponding eigenvector,

$$\sum_{\nu=1}^{d} H_{\mu\nu}^{\mathrm{eff}} c_{\nu}^{(\alpha)} = E_{\alpha} c_{\mu}^{(\alpha)}. \tag{1.40}$$

So far we have not specified a set of conditions for the cluster operators $\hat{T}^{\mu}$. In state-universal MRCC (SU-MRCC) theory the cluster amplitudes are obtained via the Bloch equation and lead to the set of equations

$$\left\langle\Phi_{ij\cdots}^{ab\cdots}(\mu)\left|\bar{H}_{\mu}\right|\Phi_{\mu}\right\rangle = \sum_{\nu(\neq\mu)}\left\langle\Phi_{ij\cdots}^{ab\cdots}(\mu)\left|e^{-\hat{T}^{\mu}}e^{\hat{T}^{\nu}}\right|\Phi_{\nu}\right\rangle H_{\mu\nu}^{\mathrm{eff}} \quad (\mu=1,2,\ldots,d), \tag{1.41}$$

which are coupled via the terms $\left\langle\Phi_{ij\cdots}^{ab\cdots}(\mu)\left|e^{-\hat{T}^{\mu}}e^{\hat{T}^{\nu}}\right|\Phi_{\nu}\right\rangle$. Notice that there is no reference to a particular state in Eq. (1.41). This is characteristic of state-universal theories, as they aim at determining a manifold of states in one computation. State-universal coupled cluster suffers from the intruder state problem, and because the same set of parameters is used to describe a manifold of states, it is inherently less accurate than single-reference CC.[11]

1.6   STATE-SPECIFIC MULTIREFERENCE COUPLED CLUSTER THEORY

State-specific theories aim at solving the problems encountered in SU-MRCC by treating one state at a time through a JM wave operator. This simplification introduces the problem of sufficiency conditions, because the number of equations that can be derived by introducing a state-specific wave operator into the Schrödinger equation is smaller than the number of cluster amplitudes contained in the $\hat{T}^{\mu}$ operators. In particular, a redundancy exists among the amplitudes related to any determinant that can be generated from multiple references within the chosen excitation level cutoff. Since the amplitudes are underdetermined, one must introduce supplementary conditions, and as this choice is not unequivocal, various theories have been advanced.

The Brillouin-Wigner (BW) MRCC method was first derived using the BW form of the Bloch equation.[12,13] This formalism solves the problem of intruder states but has one major deficiency – it is not size extensive. While size-extensivity corrections form BW-MRCC have been advanced, these either reintroduce the problem of intruder states or make the theory non-exact.[14,15] On the contrary, the state-specific MRCC method of Mukherjee (Mk-MRCC)[8,16] is rigorously size extensive and intruder free.

Prior to the beginning of my thesis, Mk-MRCC was never compared against other theories or used in conjunction with large basis sets, as there were no production level implementations. Moreover, the coupling terms appearing in the Mk-MRCC equations were considered to be intractable, and this argument perhaps discouraged its further development by the quantum chemistry community.

1.7   PROSPECTUS

In chapter 2 we report the first general implementation of SU-MRCC, BW-MRCC, and Mk-MRCC within a new arbitrary-order string-based code. These methods were applied to the study of potential energy curves of model systems and benchmarked against single-reference coupled cluster and full configuration interaction results. This work was decisive to prove the superiority of the Mk-MRCC over BW-MRCC and SU-MRCC. Chapter 3 deals with a general derivation of the "same vacuum" coupling terms found in Mk-MRCC. We report the implementation of the Mukherjee MRCC method with single and double excitations (Mk-MRCCSD) together with benchmark applications to the dissociation of F_2 and the harmonic vibrational frequencies of ozone. An initial application of Mk-MRCCSD to the singlet-triplet splitting problem in *ortho*-, *meta*-, and *para*-benzyne exemplifies the potential of this method. Chapter 4 deals with the introduction of approximate and full triple excitations in Mk-MRCC. A family of approximate methods (Mk-MRCCSDT-*n*, *n* = 1a,1b,2,3) is advanced and their performance tested against full Mk-MRCCSDT. This contribution also represented the first implementation of full triple-excitations MRCC with proper scaling.

REFERENCES

[1]   H. Maskill, *The investigation of organic reactions and their mechanisms*. (Blackwell Pub., Oxford ; Ames, Iowa, 2006).

[2]   K. L. Bak, P. Jørgensen, J. Olsen, T. Helgaker, and W. Klopper, J. Chem. Phys. **112**, 9229 (2000).

[3]   T. D. Crawford and H. F. Schaefer, Rev. Comp. Chem. **14**, 33 (2000).

[4]   W. Kutzelnigg, in *Progress in theoretical chemistry and physics*, edited by J. Rychlewski (Kluwer Academic Publishers, Dordrecht ; Boston, 2003).

[5]   E. Merzbacher, *Quantum Mechanics*, 2 ed. (John Wiley and Sons, New York, 1970).

[6]   D. Mukherjee, R. K. Moitra, and A. Mukhopadhyay, Mol. Phys. **33**, 955 (1977).

[7]   I. Lindgren, Int. J. Quantum. Chem. Symp. **12**, 33 (1978).

[8]   U. S. Mahapatra, B. Datta, B. Bandyopadhyay, and D. Mukherjee, Adv. Quantum Chem. **30**, 163 (1998).

[9]   W. Kutzelnigg and D. Mukherjee, J. Chem. Phys. **107**, 432 (1997).

[10]   B. Jeziorski and H. J. Monkhorst, Phys. Rev. A **24**, 1668 (1981).

[11]   J. Paldus, P. Piecuch, L. Pylypow, and B. Jeziorski, Phys. Rev. A **47**, 2738 (1993).

[12]   J. Mášik, I. Hubač, and P. Mach, J. Chem. Phys. **108**, 6571 (1998).

[13]   J. Mášik and I. Hubač, Adv. Quantum. Chem. **31**, 75 (1999).

[14]   I. Hubač, J. Pittner, and P. Čársky, J. Chem. Phys. **112**, 8779 (2000).

[15]   J. Pittner, J. Chem. Phys. **118**, 10876 (2003).

[16]   U. S. Mahapatra, B. Datta, and D. Mukherjee, Mol. Phys. **94**, 157 (1998).

CHAPTER 2

HIGH-ORDER EXCITATIONS IN STATE-UNIVERSAL AND STATE-SPECIFIC MULTIREFERENCE COUPLED

CLUSTER THEORIES: MODEL SYSTEMS[†]

2.1 ABSTRACT

For the first time high-order excitations ($n > 2$) have been studied in three multireference couple cluster (MRCC) theories built on the wave operator formalism: (1) the state-universal (SU) method of Jeziorski and Monkhorst; (2) the state-specific Brillouin-Wigner (BW) coupled cluster method; and (3) the state-specific MRCC approach of Mukherjee (Mk). For the H4, P4, BeH_2, and H8 models, multireference coupled cluster wave functions, with complete excitations ranging from doubles to hextuples have been computed with a new arbitrary-order string-based code. Comparison is then made to corresponding single-reference (SR) coupled cluster and full configuration interaction (FCI) results. For the ground states the BW and Mk methods are found, in general, to provide more accurate results than the SU approach at all levels of truncation of the cluster operator. The inclusion of connected triple excitations reduces the Non-Parallelism Error (NPE) in singles and doubles MRCC energies by a factor of 2 to 10. In the BeH_2 and H8 models, the inclusion of all quadruple excitations yields absolute energies within 1 kcal mol^{-1} of the FCI limit. While the MRCC methods are very effective in multireference regions of the potential energy surfaces, they are outperformed by single-reference CC when one electronic configuration dominates.

2.2 INTRODUCTION

Multireference coupled cluster (MRCC) theories involve generalizations of the exponential *ansatz* used in the cluster expansion of the electronic wave function (Ψ) from a single reference determinant (Φ)[1-3]

$$|\Psi\rangle = \exp(\hat{T})|\Phi\rangle, \tag{1}$$

where the cluster operator $\hat{T}$ promotes electrons from the occupied to the virtual orbital space of the reference determinant and is typically truncated at a certain excitation level (n),

$$\hat{T} = \hat{T}_1 + \hat{T}_2 + \ldots + \hat{T}_n .$$ (2)

The solution of the Schrödinger equation using projection techniques and the *ansatz* of Eq. (1) leads to the well known single-reference coupled cluster (SRCC) methods.[2-5] The SRCC approach is a very successful[6,7] *ab initio* method because it is size extensive, size consistent, and recovers an high percentage of the correlation energy, even at the singly and doubly excited coupled cluster (SRCCSD) level. Moreover, accuracy can be improved systematically to the full configuration interaction (FCI) limit, simply by including higher excitations in Eq. (2) within the same formalism. The conventional SRCC approach has only one major drawback: it fails when the system contains quasidegenerate electronic configurations, because of the poor description of the zeroth-order wave function by the single-determinant reference (Φ). This limitation makes conventional SRCC methods inapplicable to a large subset of chemistry, including homolytic bond breaking, singlet diradicals, many transition metal compounds, certain types of excited electronic states, and various transition states for chemical reactions.

Genuine multireference coupled cluster methods address this problem by including all the relevant quasi-degenerate determinants in the zeroth-order wave function. There are at least three broad categories of multireference coupled cluster methods: Fock-space or valence-universal (VU), Hilbert space or state-universal (SU), and state-specific (SS) theories.

Fock-space methods can treat several states with different numbers of electrons in one computation and thus are capable of directly providing the electron affinities and ionization potentials of a molecular system.[8-11] In this approach a certain configuration $\left| \Psi_0^{(0,0)} \right\rangle$ is chosen to define a Fermi vacuum. The molecular orbital (MO) space is then divided into three subsets:

core, active, and unoccupied. The zeroth-order wave function is built from the Fermi vacuum by removing p electrons from the core orbitals and adding q electrons to the active orbitals. This subset of the Fock space is termed the (q,p) *sector*. In Fock space MRCC the excitation operator is separated into a particle non-conserving operator $\hat{S}$ that includes orbital relaxation, and a $\hat{T}$ operator that accounts for dynamical correlation. The wave function is based on the exponential *ansatz*

$$\left| \Psi^{(q,p)} \right\rangle = \exp(\hat{T})\{\exp(\hat{S})\}\left| \Psi_0^{(q,p)} \right\rangle , \tag{3}$$

where $\left| \Psi_0^{(q,p)} \right\rangle$ is a multireference zeroth-order wave function for the (q,p) sector of the Fock space, and $\{\exp(\hat{S})\}$ is the normal-ordered contribution from the exponential operator $\exp(\hat{S})$, containing excitations from the core and active orbitals.[10]

Hilbert space, or state-universal (SU), methods simultaneously treat entire sets of electronic states (the model space) with the same number of electrons, yielding an excitation energy spectrum within a single computation. In essence, these methods are multireference, multiroot schemes suitable for mapping a manifold of potential energy surfaces. Hilbert-space methods are usually based on the Jeziorski and Monkhorst[12] (JM) *ansatz* for the wave operator, because it allows the treatment of all reference determinants on an equal footing. The application of Hilbert-space methods has been plagued by intruder state problems,[13-15] occurring when a determinant outside the model space closely approaches the energy of a state inside this space at some point on a potential energy surface. Paldus and Li[15-19] have recently revised the original SUCC formulation of JM, giving explicit *t*-amplitude conditions (C-conditions) that preserve size extensivity in the case of general model spaces. In this manner one can carefully select the reference determinants to avoid intruders.

State-selective (SS) coupled cluster theories treat one state (α) at a time by building a state-specific wave operator and selecting one root of an effective Hamiltonian. These approaches are less susceptible to the intruder state problem and in some cases are more efficient computationally than the VU and SU schemes. Recent developments in SSMRCC theory include the work of Mukherjee and co-workers, who proposed a rigorously size-extensive formulation denoted here as MkCC.[20-25] This approach has been investigated both at the CCSD and CEPA (coupled electron pair approximation) levels, and applied to the H4, P4, BeH_2 models, as well as Li_2, F_2, and to several other diatomic molecules.[25] While the MkCC method has given encouraging results in these tests, it has not been used in conjunction with large basis sets, and it is currently not implemented into a production level program.

The state-specific version of Brillouin-Wigner MRCC theory (BWMRCC, or BWCC) advanced by Hubač, Pittner, and collaborators[26-31] is another SSMRCC formalism that is potentially applicable to a variety of problems. The theory in its original formulation is not size-extensive, but *a posteriori* and iterative corrections to reduce or eliminate size-extensivity errors have been developed.[28,32] BWCC is still under active investigation, with recent developments involving the use of general model spaces[33] and the partial inclusion of connected triple excitations in the cluster operator.[29]

Various MRCC theories built on a single-reference framework have been advanced, including the CASCC[34-37] approach, the reduced multireference (RMRCCSD) method,[38-46] active-space CC approaches,[47-53] orbital-optimized CC schemes,[54-56] higher-order, non-iterative corrections derived from the similarity-transformed Hamiltonian,[57-61] and a broad class of method-of-moments CC (MM-CC)[62-67] and renormalized CC methods.[68-73]

The main idea behind the many MM-CC variants developed by Piecuch and co-workers[62-79] is to compute non-iterative, state-specific energy corrections after the single-reference CC energy is converged,

$$\delta^{(SRCC)} = E^{FCI} - E^{(SRCC)}. \qquad (4)$$

The $\delta^{(SRCC)}$ term is considered as a functional Λ of both the exact wave function $|\Psi\rangle$ and the higher moments $\mathcal{M}_j^{(SRCC)}$ of the SRCC equations (left-projections of excited determinants of order j on the vector $e^{-\hat{T}}He^{\hat{T}}|\Phi\rangle$), i.e.,

$$\delta^{(SRCC)} = \Lambda[|\Psi\rangle, \mathcal{M}_j^{(SRCC)}, j > n], \qquad (5)$$

where n is the truncation level chosen for the initial SRCC computation. By replacing $|\Psi\rangle$ with various approximate wave functions, a hierarchy of increasingly accurate methods is achieved. The MM-CC method has been successfully applied to the study several organic reactions and excited states.[74-79]

The state-specific formulation of MRCC investigated by Adamowicz and co-workers[34,35] is based on a complete active space (CAS) reference. Although this approach is based conceptually on a wave function rather than a wave operator *ansatz*, it can provide accurate descriptions of multireference systems. For the CAS(2,2)CCSD case the wave function takes the form

$$\left|\Psi_{CAS(2,2)CCSD}\right\rangle = \exp[\hat{T}_1 + \hat{T}_2 + \hat{T}_3(^{Abc}_{Ijk}) + \hat{T}_4(^{ABcd}_{IJkl})](1 + \hat{C}_1 + \hat{C}_2)|0\rangle. \qquad (6)$$

Here the linear operators $\hat{C}_1$ and $\hat{C}_2$ produce the determinants that belong to the CAS space while $\hat{T}_3(^{Abc}_{Ijk})$ and $\hat{T}_4(^{ABcd}_{IJkl})$ are higher excitation cluster operators with restrictions on certain orbital indices (I,A,…). This SSMRCC approach has been investigated by several authors. [34-37]

Very recently Hanrath[80,81] has introduced another wave function *ansatz* based on the JM wave operator and through the reindexing of the amplitudes was able to obtain a state-selective theory. The approach is size consistent, and preliminary results indicate that it is a potential competitor for other SSMRCC theories.

The field of coupled cluster research has benefited from the introduction of computer-aided manipulation of equations and generation of code, and the solution of the coupled cluster equations by means of determinantal algorithms. These advances are exemplified in the early work on automatic processing of diagrams by Paldus and Wong,[82,83] and the automatic generation of CC code by Janssen[84] and Li and Paldus,[85] as well as the more recent arbitrary order CC[86] and Tensor Contraction Engine[87,88] of Hirata and co-workers, the general CC advances of Kállay,[37,89,90] the general model space CC of Olsen,[36] the general MRCC code of Abrams and Sherrill,[91] and the code for automated generation of CC diagrams by Lyakh, Ivanov and Adamowicz.[35] These investigations have considered the SRCC and the SSMRCC methods described by Adamowicz,[34,35] but have avoided the SU, VU and the SSMRCC wave operator formalisms.

The aim of this paper is to study the effect of higher excitations in genuine SU and SS multireference coupled cluster theories based on the wave operator formalism. In this research we have employed string algorithms[36,92] with the coupled cluster expansion of wave functions to investigate the SUMRCC method of Jeziorski and Monkhorst,[12] the SSBWMRCC approach of Hubač *et al.*,[26-31] and the SSMRCC method of Mukherjee and co-workers.[20-24] First the theoretical foundations of these methods will be reviewed. Second, we provide details of our new computer code for arbitrary-order MRCC benchmarking. Finally, we report the first high-order ($n > 2$) MRCC results for the four classic models: H4, P4, BeH_2 and H8.

2.3 WAVE OPERATOR MRCC FORMALISMS

In this section a brief summary is provided of the wave operator formalism used to construct the SU and SS theories.[12,22,93] We limit our considerations to a complete model space (CMS) consisting of the set of determinants belonging to a complete active space (CAS), $M_0 = \mathrm{span}\{|\Phi_\mu\rangle : \mu = 1, 2, \ldots, d\}$. These d Slater determinants are built from a set of spatial orbitals $\{|\varphi_i\rangle : i = 1, 2, \ldots, N\}$ times a spin function. A projection operator, $\hat{P}$, is associated with the model space

$$\hat{P} = \sum_{\mu=1}^{d} |\Phi_\mu\rangle\langle\Phi_\mu|, \tag{7}$$

and $\hat{Q}$ is a projector on the determinants (Φ_q) in the corresponding orthogonal complement of M_0, indicated by the symbol $M^\perp$. The projector $\hat{Q}$ is then

$$\hat{Q} = 1 - \hat{P} = \sum_{q \in M^\perp} |\Phi_q\rangle\langle\Phi_q|. \tag{8}$$

The exact wave function is obtained from the action of a wave operator $\hat{\Omega}$ on $|\Psi_\alpha^P\rangle$, namely

$$|\Psi_\alpha\rangle = (\hat{P} + \hat{Q})|\Psi_\alpha\rangle = |\Psi_\alpha^P\rangle + \hat{Q}|\Psi_\alpha\rangle = \hat{\Omega}|\Psi_\alpha^P\rangle. \tag{9}$$

The wave operator satisfies the Schrödinger equation for all d eigenstates (SU theory) or for one eigenstate α (SS theories), i.e.,

$$\hat{H}\hat{\Omega}|\Psi_\alpha^P\rangle = E_\alpha\hat{\Omega}|\Psi_\alpha^P\rangle. \tag{10}$$

The effective Hamiltonian, assuming intermediate normalization, is

$$\hat{H}^{\mathrm{eff}} = \hat{P}\hat{H}\hat{\Omega}\hat{P}, \tag{11}$$

which provides the exact energy (E_α) of all states of interest, as well as the expansion coefficients for the zeroth-order wave function in terms of the CMS determinants, since it satisfies the equation

$$\hat{H}^{\text{eff}}\left|\Psi_\alpha^P\right\rangle = \hat{P}\hat{H}\left|\Psi_\alpha\right\rangle = E_\alpha\left|\Psi_\alpha^P\right\rangle. \tag{12}$$

2.3.1 STATE-UNIVERSAL MRCC

The state-universal approach of Jeziorski and Monkhorst[12] (JM) relies on the following representation of the wave operator:

$$\hat{\Omega} = \sum_\mu e^{\hat{T}^\mu}\left|\Phi_\mu\right\rangle\left\langle\Phi_\mu\right|, \tag{13}$$

where the cluster operator $\hat{T}^\mu$ is constructed from the particle-hole creation operators relative to the reference determinant $\left|\Phi_\mu\right\rangle$ and is expanded to excitation level n

$$\hat{T}^\mu = \hat{T}_1^\mu + \hat{T}_2^\mu + \ldots + \hat{T}_n^\mu. \tag{14}$$

In all the MRCC methods based on the wave operator formalism, the t-amplitude conditions are obtained by left-projection of the CC equations onto the complement space $M_n^\perp$ corresponding to excitation level n. Specifically,

$$M_n^\perp = \left\{\left|\Phi_{ij\ldots}^{ab\ldots}(\mu)\right\rangle \notin M_0; \mu = 1,2,\ldots,d; \ (i,j,\ldots)\in\mu_{\text{occ}}, (a,b,\ldots)\in\mu_{\text{vir}}\right\}, \tag{15}$$

where for each reference μ, $(i,j,\ldots)$ and $(a,b,\ldots)$ denote all sets of m orbitals $(m=1,2,\ldots,n)$ from the occupied and virtual space of μ, respectively. All excited determinants $\left|\Phi_{ij\ldots}^{ab\ldots}(\mu)\right\rangle$ which already appear in the model space M_0 are excluded from $M_n^\perp$ to maintain intermediate normalization of the correlated wave function.

Introducing the JM *ansatz* for the wave operator into the time-independent Bloch equations

$$\hat{H}\hat{\Omega} = \hat{\Omega}\hat{H}\hat{\Omega},\qquad\qquad(16)$$

followed by projection onto $\mathsf{M}_n^{\perp}$ yields the equations for the t-amplitudes

$$\left\langle \Phi_{ij\cdots}^{ab\cdots}(\mu) \middle| \overline{H}_{\mu} \middle| \Phi_{\mu} \right\rangle = \sum_{\nu(\neq\mu)} \left\langle \Phi_{ij\cdots}^{ab\cdots}(\mu) \middle| e^{-\hat{T}^{\mu}} e^{\hat{T}^{\nu}} \middle| \Phi_{\nu} \right\rangle \mathrm{H}_{\nu\mu}^{\mathrm{eff}} \qquad (\mu = 1,2,\ldots,d)\qquad(17)$$

where we have introduced the similarity-transformed Hamiltonian with respect to the $\hat{\mathrm{T}}^{\mu}$ operator

$$\overline{\mathrm{H}}_{\mu} = e^{-\hat{\mathrm{T}}^{\mu}} \hat{H} e^{\hat{\mathrm{T}}^{\mu}}.\qquad\qquad(18)$$

Note that the SUMRCC $\hat{\mathrm{T}}^{\mu}$ and $\hat{\mathrm{T}}^{\nu}$ equations are coupled through the t-amplitudes of *all* the reference determinants, as well as the off-diagonal matrix elements of the effective Hamiltonian.

2.3.2 STATE-SPECIFIC MRCC

State-specific theories are recovered when one assumes that the wave operator lifts only one specific state from the model space to the exact wave function. Therefore the wave operator is indicated with a label, for example $\hat{\Omega}_{\alpha}$, and is defined as

$$\left| \Psi_{\alpha} \right\rangle = \hat{\Omega}_{\alpha} \left| \Psi_{\alpha}^{P} \right\rangle.\qquad\qquad(19)$$

The SS simplification introduces the problem of sufficiency conditions, because the number of equations that can be derived by introducing the state-specific wave operator into the Schrödinger equation is lower than the number of t-amplitudes contained in the $\hat{\mathrm{T}}^{\mu}$ operators. This problem arises only for the redundant amplitudes that generate the same excited determinant starting from two different reference determinants. Since the t-amplitudes are

27

underdetermined, one must introduce supplementary conditions. In SSMRCC this choice is not univocal, and various theories adopt different sufficiency conditions.

State-specific Brillouin-Wigner coupled cluster is obtained by introducing the SSJM wave operator in the SSBW form of the Bloch equation

$$\hat{\Omega}_\alpha = 1 + \hat{B}_\alpha \hat{V} \hat{\Omega}_\alpha , \tag{20}$$

where $\hat{B}_\alpha$ is the BW resolvent

$$\hat{B}_\alpha = \frac{\hat{Q}}{E_\alpha - \hat{H}_0} , \tag{21}$$

and the Hamiltonian operator is partitioned into two components, $\hat{H} = \hat{H}_0 + \hat{V}$. The equations that determine the t-amplitudes are

$$E_\alpha \left\langle \Phi_{ij\ldots}^{ab\ldots}(\mu) \middle| e^{\hat{T}^\mu} \middle| \Phi_\mu \right\rangle = \left\langle \Phi_{ij\ldots}^{ab\ldots}(\mu) \middle| \hat{H} e^{\hat{T}^\mu} \middle| \Phi_\mu \right\rangle \qquad (\mu = 1, 2, \ldots, d) , \tag{22}$$

which are coupled only through the exact energy of the state under consideration – a computational advantage emphasized by Hubač and co-workers.[26-31] A drawback to the choice of sufficiency conditions leading to Eq. (22) is that BWMRCC is not rigorously size extensive.

Size-extensivity corrections for BWMRCC are obtained from the generalized Bloch equation derived by Pittner[28] in terms of a variable parameter λ,

$$\lambda E_\alpha \hat{\Omega}_\alpha \hat{P} + (1-\lambda)\hat{\Omega}_\alpha \hat{H}_0 \hat{P} = \hat{H} \hat{\Omega}_\alpha \hat{P} - (1-\lambda)\hat{\Omega}_\alpha \hat{P} \hat{V} \hat{\Omega}_\alpha \hat{P} . \tag{23}$$

The corresponding explicit expression for the generalized t-amplitude equation is then

$$\begin{aligned}
\lambda E_\alpha \left\langle \Phi_{ij\ldots}^{ab\ldots}(\mu) \middle| e^{\hat{T}^\mu} \middle| \Phi_\mu \right\rangle &= \left\langle \Phi_{ij\ldots}^{ab\ldots}(\mu) \middle| \left(\hat{H} e^{\hat{T}^\mu} \right)_C \middle| \Phi_\mu \right\rangle + \lambda \left\langle \Phi_{ij\ldots}^{ab\ldots}(\mu) \middle| \left(\hat{H} e^{\hat{T}^\mu} \right)_{\text{DCL+UL}} \middle| \Phi_\mu \right\rangle \\
&= \lambda \left\langle \Phi_{ij\ldots}^{ab\ldots}(\mu) \middle| \hat{H} e^{\hat{T}^\mu} \middle| \Phi_\mu \right\rangle + (1-\lambda) \left\langle \Phi_{ij\ldots}^{ab\ldots}(\mu) \middle| \overline{H}_\mu \middle| \Phi_\mu \right\rangle
\end{aligned} \tag{24}$$

In the above formula the subscript C refers to the connected diagrams, whereas DCL and UL refer, respectively, to the disconnected linked diagrams and the unlinked diagrams. If we set $\lambda = 1$ we recover the BWMRCC method, while for $\lambda = 0$ we recover the Rayleigh-Schrödinger (RS) Bloch equation CC. In the *a posteriori* size-extensivity correction (apBWCC), the MRCC equations are solved for $\lambda = 1$, and following convergence a final iteration is performed with $\lambda = 0$. The iterative size-extensivity correction (iBWCC) is performed by decreasing continuously the parameter λ to zero while converging the cluster amplitudes. In the *a posteriori* correction, size extensivity is achieved only approximately, while in the iterative correction the final energy is size extensive and equal to the RS Bloch equation energy. However, the intruder problem is thus reintroduced in the iBWCC scheme. We assess the effectiveness of these size-extensivity corrections in this paper.

The derivation of the state-specific multireference coupled cluster formalism of Mukherjee and co-workers[20,21] starts by inserting the state-specific JM wave operator into the expansion for the exact wave function

$$\left| \Psi_\alpha \right\rangle = \hat{\Omega}_\alpha \left| \Psi_\alpha^P \right\rangle = \sum_\mu e^{\hat{T}^\mu} \left| \Phi_\mu \right\rangle \left\langle \Phi_\mu \middle| \Psi_\alpha^P \right\rangle = \sum_\mu e^{\hat{T}^\mu} \left| \Phi_\mu \right\rangle c_{\mu\alpha} . \tag{25}$$

From the Schrödinger equation, one thus has

$$\sum_\mu \left[\hat{H} e^{\hat{T}^\mu} \left| \Phi_\mu \right\rangle c_{\mu\alpha} - E_\alpha e^{\hat{T}^\mu} \left| \Phi_\mu \right\rangle c_{\mu\alpha} \right] = 0 . \tag{26}$$

If we multiply on the left side by the identity

$$1 = e^{\hat{T}^\mu} e^{-\hat{T}^\mu} = e^{\hat{T}^\mu} (\hat{P} + \hat{Q}) e^{-\hat{T}^\mu} = \sum_\nu e^{\hat{T}^\mu} \left| \Phi_\nu \right\rangle \left\langle \Phi_\nu \middle| e^{-\hat{T}^\mu} + e^{\hat{T}^\mu} \hat{Q} e^{-\hat{T}^\mu} = \hat{P}_\mu + \hat{Q}_\mu , \tag{27}$$

we get

$$\sum_{\mu,\nu} e^{\hat{T}^\mu} |\Phi_\nu\rangle H^{\text{eff}}_{\nu\mu} c_{\mu\alpha} + \sum_\mu e^{\hat{T}^\mu} \hat{Q}\overline{H}_\mu |\Phi_\mu\rangle c_{\mu\alpha} - E_\alpha \sum_\mu e^{\hat{T}^\mu} |\Phi_\mu\rangle c_{\mu\alpha} = 0, \qquad (28)$$

after noting that $H^{\text{eff}}_{\nu\mu} = \langle \Phi_\nu | \overline{H}_\mu | \Phi_\mu \rangle$. Upon interchanging the dummy indices μ and ν in the double summation of Eq. (28) and collecting the individual terms, we obtain

$$\sum_\mu \left[\sum_\nu e^{\hat{T}^\nu} |\Phi_\mu\rangle H^{\text{eff}}_{\mu\nu} c_{\nu\alpha} + e^{\hat{T}^\mu} \hat{Q}\overline{H}_\mu |\Phi_\mu\rangle c_{\mu\alpha} - E_\alpha e^{\hat{T}^\mu} |\Phi_\mu\rangle c_{\mu\alpha} \right] = 0. \qquad (29)$$

Equation (29) can be satisfied by setting the individual terms in the μ summation to zero. This sufficiency condition implies, after multiplication by $e^{-\hat{T}^\mu}$ and left projection on the excited determinants $\langle \Phi^{ab\ldots}_{ij\ldots}(\mu) |$, that the t-amplitudes satisfy

$$\langle \Phi^{ab\ldots}_{ij\ldots}(\mu) | \overline{H}_\mu | \Phi_\mu \rangle c_{\mu\alpha} + \sum_{\nu(\neq\mu)} \langle \Phi^{ab\ldots}_{ij\ldots}(\mu) | e^{-\hat{T}^\mu} e^{\hat{T}^\nu} | \Phi_\mu \rangle H^{\text{eff}}_{\mu\nu} c_{\nu\alpha} = 0 \quad (\mu = 1,\ldots,d). \qquad (30)$$

It is worth noticing the difference in the sufficiency conditions of BWCC and MkCC. First, the BWCC equations obtained through the state-specific BW form of the Bloch equation are equivalently derived by assuming a sufficiency condition in which individual μ terms in Eq. (26) are identically zero. On the contrary, Mukherjee's sufficiency conditions are derived by first rearranging the CC equations before equating individual μ terms. In BWCC the equations naturally decouple (in the amplitudes) for each reference and are explicitly dependent on the correlation energy only. Therefore, in BWCC theory the sufficiency conditions on the redundant amplitudes for reference μ depend only on the $\hat{T}^\mu$ amplitudes. In the case of MkCC, the redundant amplitudes for reference μ are dependent on the amplitudes of *the entire* model space through the renormalization factor $e^{-\hat{T}^\mu} e^{\hat{T}^\nu}$. Last, we recall that BWCC and MkCC have an advantage over SUCC because they are devoid of the intruder state problem.

2.4 IMPLEMENTATION OF ARBITRARY-ORDER MRCC

Here we give a brief description of our string-based coupled cluster code written to study model systems and to facilitate further development of MRCC theory. All the methods were implemented at the University of Georgia with a new program called **DETC++**, interfaced to the Psi 3.2.3[94] package. **DETC++** is a string-based code. Therefore a generic state vector is expanded in terms of Slater determinants times a coefficient

$$\left|\Psi\right\rangle = \sum_{I} C_{I}\left|\Phi_{I}\right\rangle, \tag{31}$$

where the Slater determinants are expressed in terms of Handy's alpha and beta strings[92]

$$\left|\Phi_{I}\right\rangle = \left|I_{\alpha}I_{\beta}\right\rangle. \tag{32}$$

The wave function expansion is limited to only those determinants with the requested symmetry and excitation level limitations. **DETC++** is capable of manipulating general strings of creation-annihilation operators

$$\hat{a}_{a}^{+}\hat{a}_{b}^{+}\ldots\hat{a}_{i}\,\hat{a}_{j}\ldots, \tag{33}$$

and to apply a generic operator defined as

$$\hat{O} = \sum_{ab\ldots ij\ldots} O_{ij\ldots}^{ab\ldots}\,\hat{a}_{a}^{+}\hat{a}_{b}^{+}\ldots\hat{a}_{i}\,\hat{a}_{j}\ldots, \tag{34}$$

to any state vector through the rules of second quantization

$$\begin{aligned} a_{i}^{\dagger}\left|\Phi_{\mu}\right\rangle &= \delta_{0,n_{i}^{(\mu)}}(-1)^{\Gamma(\Phi_{\mu},i)}\left|\ldots 1_{i}\ldots\right\rangle \\ a_{i}\left|\Phi_{\mu}\right\rangle &= \delta_{1,n_{i}^{(\mu)}}(-1)^{\Gamma(\Phi_{\mu},i)}\left|\ldots 0_{i}\ldots\right\rangle \end{aligned}, \tag{35}$$

where the delta factors and the sign factor $(-1)^{\Gamma(\Phi_\mu, i)}$ ensure that Fermi-Dirac statistics are satisfied. In **DETC++** we avoid the recomputation of the effect of the second quantization operators by pre-computing single replacement lists of strings.

The generic operator expansion includes only the non-vanishing matrix elements limited to the desired irreducible representation. Therefore operators like $\hat{H}$ and $\hat{T}^\mu$ contain only the operator strings that belong to the totally symmetric representation. The present program was tested (1) against the FCI energies of several first-row atoms, computed with Sherrill's determinantal CI code **DETCI**[95] (contained in the Psi 3.2.3[94] package) to validate the code relative to the $\hat{H}$ operator, and (2) with arbitrary-order coupled cluster results of Hirata[86] to verify the code relative to the $e^{\hat{T}^\mu}$ operator. Moreover the SUCC, BWCC and MkCC codes were validated at the singles and doubles excitation level with results previously published in the literature.[22,93,96,97] Finally computations of the Full SUCC, Full BWCC and Full MkCC energies were executed to demonstrate complete numerical equivalency to FCI. The detailed benchmarks used to validate **DETC++** are reported in the Supplementary Material.[98]

The wave operator MRCC methods described in Section 2 are implemented in **DETC++** by defining an appropriate residual vector $\left|\Delta_\mu\right\rangle$ that vanishes when the respective coupled cluster equations are converged. The residual vector for the three methods can be derived from Eqs. (17), (22), and (30):

$$\left\langle\Phi_{ij\cdots}^{ab\cdots}(\mu)\left|\Delta_\mu\right\rangle_{\mathrm{MRCC}} = \begin{cases} \left\langle\Phi_{ij\cdots}^{ab\cdots}(\mu)\left|\overline{H}_\mu\right|\Phi_\mu\right\rangle - \sum_{\nu(\neq\mu)}\left\langle\Phi_{ij\cdots}^{ab\cdots}(\mu)\left|e^{-\hat{T}^\mu}e^{\hat{T}^\nu}\right|\Phi_\nu\right\rangle \mathrm{H}_{\nu\mu}^{\mathrm{eff}} & \mathrm{SUCC} \\ \left\langle\Phi_{ij\cdots}^{ab\cdots}(\mu)\left|\hat{H}e^{\hat{T}^\mu}\right|\Phi_\mu\right\rangle - E_\alpha\left\langle\Phi_{ij\cdots}^{ab\cdots}(\mu)\left|e^{\hat{T}^\mu}\right|\Phi_\mu\right\rangle & \mathrm{BWCC} \\ \left\langle\Phi_{ij\cdots}^{ab\cdots}(\mu)\left|\overline{H}_\mu\right|\Phi_\mu\right\rangle c_{\mu\alpha} + \sum_{\nu(\neq\mu)}\left\langle\Phi_{ij\cdots}^{ab\cdots}(\mu)\left|e^{-\hat{T}^\mu}e^{\hat{T}^\nu}\right|\Phi_\mu\right\rangle \mathrm{H}_{\mu\nu}^{\mathrm{eff}} c_{\nu\alpha} & \mathrm{MkCC} \end{cases} . \quad (36)$$

The update equations that we have implemented are similar to those used by Hirata and Bartlett,[86] but shifted by the standard BW term $E_\alpha - H^{\text{eff}}_{\mu\mu}$. Specifically,

$$t^{ab\cdots}_{ij\cdots}(\mu, \text{new}) = t^{ab\cdots}_{ij\cdots}(\mu, \text{old}) + \frac{\text{sgn}(ij\ldots; ab\ldots)\left\langle \Phi^{ab\cdots}_{ij\cdots}(\mu) \middle| \Delta_\mu \right\rangle}{E_\alpha - H^{\text{eff}}_{\mu\mu} + \varepsilon^{ab\cdots}_{ij\cdots}(\mu)}, \tag{37}$$

where the function $\text{sgn}(ij\ldots; ab\ldots)$ is the sign associated with the action of one cluster operator on the vacuum $\left| \Phi_\mu \right\rangle$

$$\left(\ldots \hat{a}^+_b \hat{a}_j \hat{a}^+_a \hat{a}_i \ldots\right) \left| \Phi_\mu \right\rangle = \text{sgn}(ij\ldots; ab\ldots)\left| \Phi^{ab\cdots}_{ij\cdots}(\mu) \right\rangle. \tag{38}$$

The standard Raleigh-Schrödinger denominators terms are computed with respect to the vacuum μ

$$\varepsilon^{abc\cdots}_{ijk\cdots}(\mu) = f^\mu_{ii} + f^\mu_{jj} + f^\mu_{kk} + \ldots - f^\mu_{aa} - f^\mu_{bb} - f^\mu_{cc} - \ldots, \tag{39}$$

as

$$f^\mu_{pp} = h_{pp} + \sum_{k \in \left| \Phi_\mu \right\rangle} \left(pp \mid kk\right) - \left(pk \mid pk\right), \tag{40}$$

where the sum runs over all the occupied orbitals of Slater determinant μ. Eq. (37) resembles the ordinary SRCC update equation. The BW term $E_\alpha - H^{\text{eff}}_{\mu\mu}$ helps improve convergence and does not vanish even in the case of degenerate orbitals. Since the residual vector is null when convergence is reached, we can shift the denominator by an arbitrary value to improve convergence of the ground state wave function without affecting the final results. This shift technique was necessitated here for some geometries of the BeH_2 model system. All computations were carried out without convergence acceleration algorithms like the direct inversion in the iterative subspace (DIIS)[99,100] or the reduced linear equation (RLE)[101] method.

2.5 MODEL SYSTEM MRCC RESULTS

In this section we analyze the results from MRCC computations on the H4, P4, BeH$_2$, and H8 model systems. The basis sets used in this work are described in each subsection below and are fully specified in the Supplementary Material (see Ref. 98). Most of the plots will report the deviation of the total electronic energy from the FCI value at a given molecular geometry $\mathbf{R}$ and for a given method X

$$\Delta E_X(\mathbf{R}) = E_X(\mathbf{R}) - E_{FCI}(\mathbf{R}). \tag{41}$$

We prefer to adopt this quantity, as a measure the accuracy of a certain method, rather than the percent of the correlation energy recovered

$$\%E_{corr} = 100 \cdot \frac{E_X(\mathbf{R}) - E_{Ref.}(\mathbf{R})}{E_{FCI}(\mathbf{R}) - E_{Ref.}(\mathbf{R})}, \tag{42}$$

since the former is independent of the definition of the uncorrelated reference wave function energy, $E_{Ref.}(\mathbf{R})$. We also use the non-parallelism error (NPE) as a measure of the relative deviation from the FCI potential energy surface (PES). The NPE is defined as

$$NPE = \max_{\mathbf{R}}[\Delta E_X(\mathbf{R})] - \min_{\mathbf{R}}[\Delta E_X(\mathbf{R})], \tag{43}$$

and provides an indication of the degree of parallelism of the potential energy surface computed with a given method X with respect to the FCI potential energy surface. Tables 1.1-1.4 report the NPE values computed for the four models studied here.

The effect of different choices of molecular orbitals in SRCC and MRCC (at both the valence-universal and state-universal level) were studied by Jankowski et al.[102-104] on the H4 model. For SUCC the orbital choice affected mainly the states dominated by a single configuration; in the multireference region the energy was less sensitive to orbital choice. For the

H4 system, complete-active-space self-consistent-field (CASSCF, here abbreviated CAS) orbitals performed better than the Hartree-Fock orbitals.

The H4, P4, BeH$_2$, and H8 models investigated here all involve only two closed-shell reference determinants. All electron correlation methods (including SRCC) were applied with a uniform set of CAS(2,2) orbitals, either optimized on the ground state or state-averaged on the lowest two states. These orbitals were generated by the **DETCAS** code of Sherrill, contained in the Psi 3.2.3 package.[94] As in the SRCC case, the MRCC methods applied here are rigorously invariant to all (occ,occ) and (vir,vir) orbital rotations completely *outside the active space*. In contrast, orbital rotations within the active space do change the MRCC energy for all methods studied here, as demonstrated numerically by Pittner *et al*. in the BW case.[28,30] Therefore a canonicalization scheme must be specified for the active space orbitals in MRCC theory. In all computations performed here, the two active-space orbitals have different point-group symmetry, a condition that defines them uniquely.

2.5.1 THE H4 MODEL

The H4 model consists of four hydrogen atoms arranged in an isosceles trapezoidal configuration with all the nearest-neighbor distances (r) fixed to exactly 2 bohr. At this geometry the bonds between the hydrogen atoms are considerably stretched when compared to the H$_2$ bond length of 1.4 bohr. The trapezoid can be deformed by varying the angle θ in Scheme 2.1 from 90°

r = 2 bohr
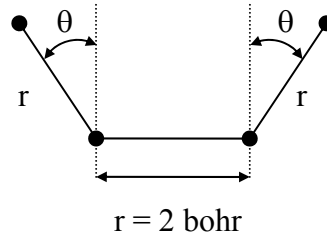
Scheme 2.1. The H4 Model.

(square configuration) to 180° (linear configuration). The angle θ, expressed in radians, is related to a continuous parameter $\alpha \in \left[0, \frac{1}{2}\right]$ by the formula $\theta = \pi(\alpha + \frac{1}{2})$. This model system was first introduced by Jankowski and Paldus[105] for testing coupled-pair theory for quasi-degenerate systems. Subsequently, the H4 model has been studied using the SUCC,[13,96,106] BWCC,[93] MkCC[22], MRexpT[81] and MRPT[21] methods.

When the parameter α is equal to zero the system possesses D_{4h} symmetry, and the zeroth-order wave function is described by a single electronic configuration $(1a_{1g})^2 (1e_u)^2$ that involves the two degenerate determinants

$$\begin{aligned} |\Phi_1\rangle &= \left|(1a_{1g})^2 (1e_{ua})^2\right\rangle \\ |\Phi_2\rangle &= \left|(1a_{1g})^2 (1e_{ub})^2\right\rangle \end{aligned} \qquad (44)$$

For trapezoidal configurations ($0 < \alpha < 1/2$, C_{2v} symmetry) and the linear configuration ($\alpha = 1/2$, $D_{\infty h}$ symmetry) the degeneracy is lifted. In C_{2v} symmetry the zeroth-order wave function is mapped into the two determinants

$$\begin{aligned} |\Phi_1\rangle &= \left|(1a_1)^2 (1b_2)^2\right\rangle \\ |\Phi_2\rangle &= \left|(1a_1)^2 (2a_1)^2\right\rangle \end{aligned} \qquad (45)$$

while for the linear geometry ($D_{\infty h}$)

36

$$\left|\Phi_1\right\rangle = \left|(1\sigma_g^+)^2(1\sigma_u^+)^2\right\rangle$$
$$\left|\Phi_2\right\rangle = \left|(1\sigma_g^+)^2(2\sigma_g^+)^2\right\rangle .$$

(46)

For both the trapezoidal and linear geometries $\left|\Phi_1\right\rangle$ is the dominant configuration.
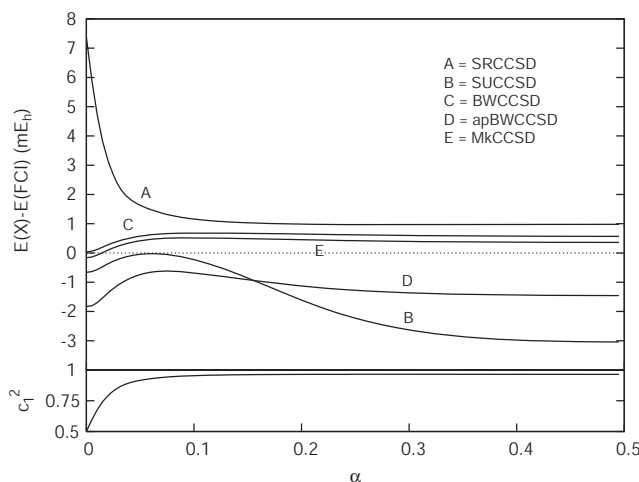
Figure 2.1. MRCCSD/DZP energy curves for the 1^1A_1 ground state of the H4 model system All computations (including single-reference CC) employed CAS(2,2) orbitals optimized for the 1^1A_1 state. The lower panel shows the square of the CAS(2,2) CI coefficient of $\left|\Phi_1\right\rangle$ versus the parameter α.

Fig. 2.1 shows the performance of the SRCC, SUCC, BWCC, apBWCC, and MkCC methods at the singles and doubles (SD) level for the ground state of the H4 model using a $(4s1p/2s1p)$ DZP[107,108] basis set with $\alpha_p(H) = 0.75$ bohr^{-2} (see Supplementary Material, Ref. 98). The molecular orbitals are obtained from a CAS(2,2) computation and are optimized for the ground state.

The SRCCSD method shows a strong deviation from the FCI curve in the multireference region of the potential energy curve, with a deviation of more that 7 mE$_h$ for the square configuration ($\alpha = 0$). However, in the single reference region ($\alpha > 0.1$) SRCCSD provides energies within 1 mE$_h$ of FCI. The SUCCSD multireference method tends to give energies too

negative, with a maximum error of ca. 3 mE$_h$, giving poorest performance in the single reference region. BWCCSD shows a deviation from the FCI energy that is less than 1 mE$_h$ along the entire plot, while apBWCCSD performs worse, with a maximum error of ca. 2 mE$_h$. MkCCSD provides energies that are within 0.5 mE$_h$ of the FCI curve. NPE values for the ground and excited states of the H4 model for the (SR and MR) coupled cluster methods are reported in Table 2.1. The BWCCSD and MkCCSD methods provide the best results in terms of NPE values: 0.64 and 0.68 mE$_h$, respectively, while for the SUCC and apBWCC methods the NPE is greater than 1 mE$_h$.

Table 2.1. Non-parallelism error (NPE) in microhartrees (μE$_h$) for the 1^1A_1 and 2^1A_1 states of the H4 model system computed with the DZP basis set.

1^1A_1 state CAS(2,2) orbitals	CC Theory				
Excitation level	SR	SU	BW	apBW	Mk
SD	6403	2998	644	1142	677
SDT	2135	2759	139	553	107
1^1A_1 state SA-CAS(2,2) orbitals	CC Theory				
Excitation level	SR	SU	BW	apBW	Mk
SD	6585	2356	787	2071	839
SDT	2105	2398	115	1904	106
2^1A_1 state SA-CAS(2,2) orbitals	CC Theory				
Excitation level	SU	BW	apBW	Mk	
SD	1643	2157	9008	2016	
SDT	4382	3707	4288	3843	
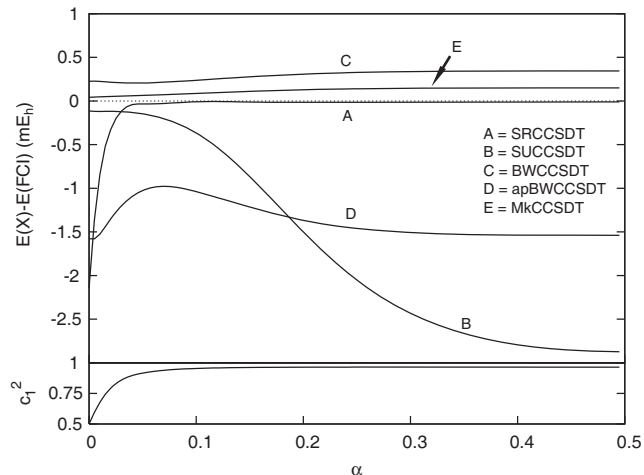
Figure 2.2. MRCCSDT/DZP energy curves for the 1^1A_1 ground state of the H4 model system. See Fig. 2.1 caption for details.

The inclusion of triple excitations in SRCC and MRCC yields the results in Fig. 2.2 SRCCSDT performs poorly only in the multireference region near $\alpha = 0$, while it exhibits minuscule deviations from the FCI curve for $\alpha > 0.05$. Curiously, the state-universal SUCCSDT curve starts in the multireference square configuration ($\alpha = 0$) with a small error (-0.11 mE$_h$) but deviates considerably (-2.87 mE$_h$) at the single-reference linear configuration ($\alpha = 1/2$). On the contrary, the BWCCSDT and MkCCSDT curves are nearly parallel to full CI along the entire potential energy curve, with NPE values of 0.14 and 0.11 mE$_h$, respectively. MkCC has an absolute error 1/2 as large as BWCC. The apBWCCSDT method provides a potential energy curve that lies more than 1 mE$_h$ below the FCI curve and that is not accurately parallel to FCI (NPE = 0.55 mE$_h$).
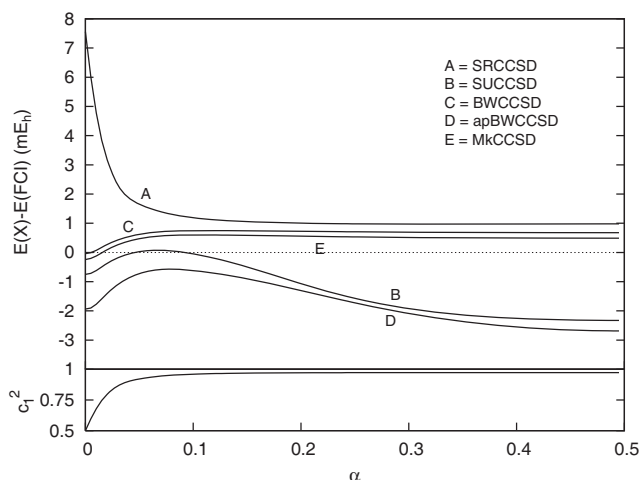
Figure 2.3. MRCCSD/DZP energy curves for the 1^1A_1 ground state of the H4 model system. All computations (including single-reference CC) employed state-averaged CAS(2,2) orbitals and weights: $0.5(1^1A_1)$ and $0.5(2^1A_1)$. The lower panel shows the square of the CAS(2,2) CI coefficient of $\left|\Phi_1\right\rangle$ versus the parameter α.

We have also investigated the $(1^1A_1, 2^1A_1)$ states of the H4 model jointly. For this purpose molecular orbitals were obtained from state-averaged (SA) CAS(2,2) computations with equal weights for the ground and excited states. The deviation from FCI for the ground state, computed now with SA-CAS orbitals, is depicted in Figs. 2.3 and 2.4. At both the SD and SDT levels these results show that the SUCC, BWCC, and MkCC methods are not substantially affected by the choice of the orbitals. The SUCC plots using SA-CAS orbitals exhibit a lower NPE (2.40 mE_h for SUCCSD, 2.44 mE_h for SUCCSDT) compared to the case in which ground-state CAS orbitals are used (3.00 mE_h for SUCCSD, 2.76 mE_h for SUCCSDT). In contrast, the quality of the apBWCC potential energy curve degrades, as apparent in the drastic increase of the NPE values (Table 2.1).
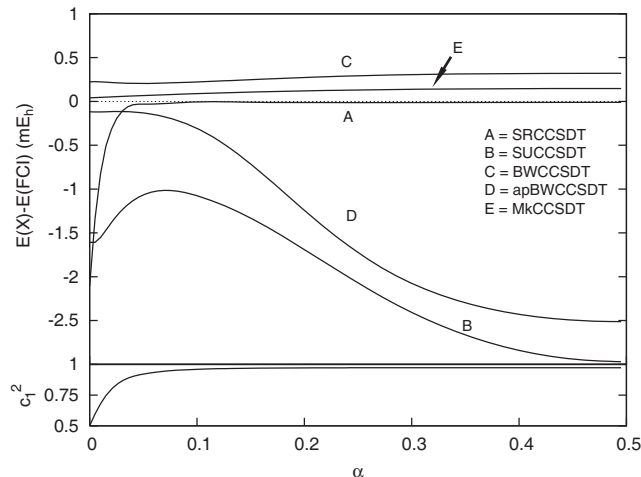
Figure 2.4. MRCCSDT/DZP energy curves for the 1^1A_1 ground state of the H4 model system. See Fig. 2.3 caption for details.

The deviation from FCI for the first excited state (2^1A_1) of the H4 model at the SD and SDT levels of theory, obtained by converging on the second root of the effective Hamiltonian, is shown in Figs. 2.5 and 2.6. For the SUCC method no extra computation is required since the effective Hamiltonian is state universal and built upon the lowest two determinants of A_1 symmetry. At the SD level the SUCC, BWCC, and MkCC methods show a significant deviation (3-6 mE_h) from the FCI curve and a NPE greater than for the ground state. The apBWCC curve shows even larger deviations (5-14 mE_h) from FCI, particularly in the single reference region ($\alpha > 0.1$). For the 2^1A_1 state, the inclusion of triple excitations in the cluster operator introduces several significant changes (Fig. 2.6). The SUCCSDT, BWCCSDT, and MkCCSDT potential energy curves deviate from FCI curve by no more than 0.35 mE_h for $\alpha < 0.1$, but the errors grow to about -4 mE_h as the linear configuration is approached. The apBWCC curve continues to show significant deviation from FCI, but less pronounced than observed in the corresponding SD computation.
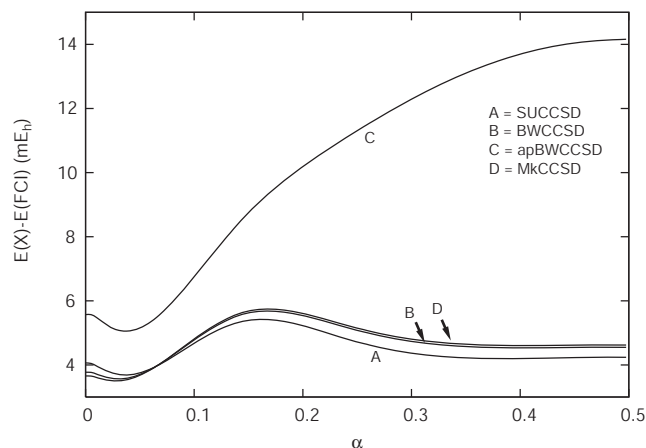
Figure 2.5. MRCCSD/DZP energy curves for the 2^1A_1 excited state of the H4 model system. All computations employed state-averaged CAS(2,2) orbitals and weights: $0.5(1^1A_1)$ and $0.5(2^1A_1)$.
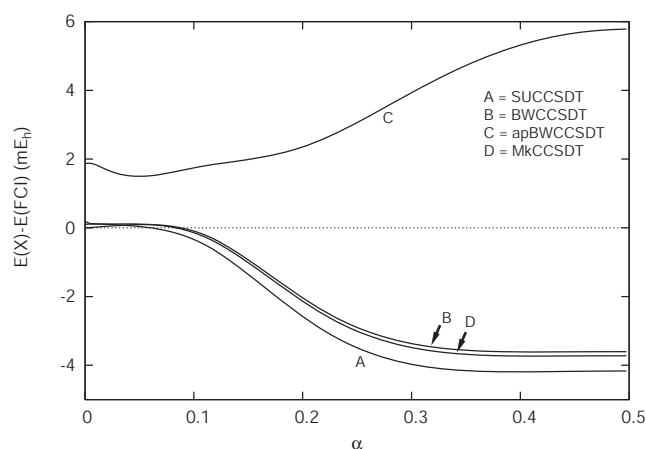
Figure 2.6. MRCCSDT/DZP energy curves for the 2^1A_1 state of the H4 model system. See Fig. 2.5 caption for details.

2.5.2 THE P4 MODEL

The P4 model consists of four hydrogen atoms arranged in a rectangular configuration with fixed height of 2 bohr and variable length, as measured by the parameter α in bohr. This model system was first introduced by Jankowski and Paldus[105] and has been tested with SUCC[13,106] and MkCC theories.[22] Varying the parameter α, the P4 model gives three different

types of geometrical configurations: (A) compressed, $\alpha < 2$; (B) square, $\alpha = 2$; and (C) elongated, $\alpha > 2$.
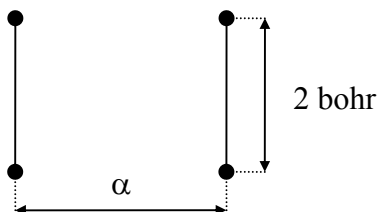
Scheme 2.2. The P4 Model.

For the square configuration (D_{4h}) the zeroth-order wave function is described by a linear combination of the two degenerate determinants

$$
\begin{aligned}
\left|\Phi_1\right\rangle &= \left|(1a_{1g})^2(1e_{ua})^2\right\rangle \\
\left|\Phi_2\right\rangle &= \left|(1a_{1g})^2(1e_{ub})^2\right\rangle
\end{aligned}
\tag{47}
$$

which map into the non-degenerate (D_{2h}) set

$$
\begin{aligned}
\left|\Phi_1\right\rangle &= \left|(1a_1)^2(1b_{3u})^2\right\rangle \\
\left|\Phi_2\right\rangle &= \left|(1a_1)^2(1b_{2u})^2\right\rangle
\end{aligned}
\tag{48}
$$

for both compression or elongation. This feature makes the P4 model a good complement to the H4 model, because the P4 zeroth-order wave function becomes multireference in character in the middle of the potential energy curve and not just at one extreme.

Figs 2.7 and 2.8 show the deviation from FCI for the ground state of the P4 model using the DZP basis set already employed for the H4 model and CAS(2,2) molecular orbitals optimized for the ground state. The plot of the square of the largest CI coefficient of the zeroth-order wave function (lower panel of Fig. 2.7 and 2.8) clearly indicates that the multireference region of the problem is centered at $\alpha = 2$ and extends roughly from 1.75 to 2.25 bohr.
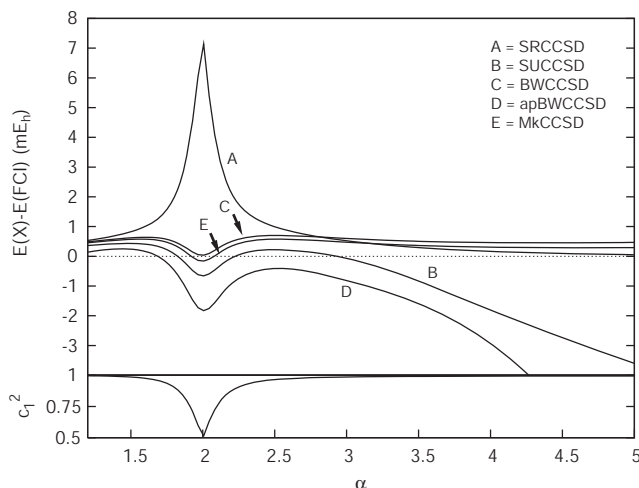
Figure 2.7. MRCCSD/DZP energy curves for the 1^1A_1 ground state of the P4 model system. All computations (including single-reference CC) employed CAS(2,2) orbitals optimized for the 1^1A_1 state. The lower panel shows the square of the CAS(2,2) CI coefficient of $|\Phi_1\rangle$ versus the parameter α.
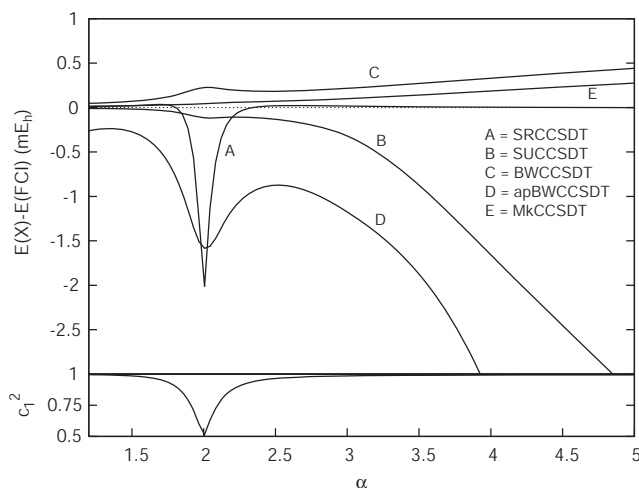
Figure 2.8. MRCCSDT/DZP energy curves for the 1^1A_1 ground state of the P4 model system See Fig. 2.7 caption for details.

Single-reference SRCCSD gives a pronounced cusp at the square configuration ($\alpha = 2$); nevertheless, it provides an accurate potential energy curve outside the multireference zone. State-universal SUCCSD is capable of describing the system in the multireference zone, but it shows increasing deviations of 1-3 mE_h from FCI for large values of the parameter α. BWCCSD

and MkCCSD provide the best results, with absolute errors always less than 1 mE_h and NPEs of 0.66 and 0.74 mE_h, respectively. The *a posteriori* correction to BWCCSD degrades the results, as shown by an NPE of ca. 8.0 mE_h, a value even larger than the NPE of SRCC (7.3 mE_h).

The inclusion of triple excitations reduces the height of the cusp for SRCC and, in general, slightly reduces the NPE for all the MRCC methods, except for apBWCC. Among all the methods, MkCCSDT is the only one in Figs. 2.7 and 2.8 that does not exhibit a "hump" in the curve near $\alpha = 2$. MkCCSDT also has the smallest NPE, ca. 0.2 mE_h. As previously noticed for the H4 system, none of the MRCC methods are able to match the accuracy to SRCC in the single-reference regions. For example, in P4, when $\alpha = 5$ bohr, SRCCSDT has an error of less than 0.001 mE_h, while for BWCCSDT and MkCCSDT the error is, respectively, 0.44 and 0.28 mE_h.

Table 2.2. Non-parallelism error (NPE) in microhartrees (μE_h) for the 1^1A_1 state of the P4 model system in the range $\alpha \in [1.2,5.0]$, computed with DZP basis set.

	CC Theory				
Excitation level	SR	SU	BW	apBW	Mk
SD	7319	4036	665	8016	739
SDT	2178	3222	394	8434	259

2.5.3 THE BEH2 MODEL

The dissociation of beryllium hydride was studied in the context of single-reference coupled cluster theory by Purvis, Shepard, Brown and Bartlett.[109] These authors examined BeH_2 at selected points along a C_{2v} path from the linear molecule toward dissociated products Be + H_2. Later, several authors investigated the performance of multireference methods using the BeH_2

model.[20,22,37,110-118] Here we introduce a revision of this model, with the following motivation: (1) increase the number of sample points along the potential energy curve, limited only to nine in the original model;[109] and (2) include the effects of core-core correlation for the beryllium atom. Our model is obtained by constraining the path of each hydrogen atom to a particular line, as defined in Scheme 2.3. The beryllium atom is placed at the origin of the axis, while the two hydrogen atoms move along the dashed lines described by the equations

$$y(x) = \pm(2.54 - 0.46x), \tag{49}$$

where x lies in the range 0 - 4 bohr. This set of configurations interpolates the path between points A-H of the original model.[109]
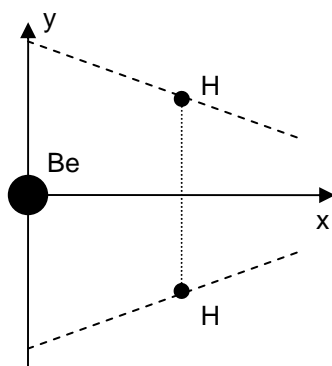
Scheme 2.3. The BeH$_2$ Model.

The basis set employed here for BeH$_2$ (and detailed in the Supplementary Material, Ref. 98) is a more loosely contracted variant of the double-ζ basis adopted in previous benchmark studies.[20,22,37,109-118] In particular, we used a Be($10s3p/3s2p$), H($4s/2s$)[107,108] contraction with a tight beryllium p primitive function to describe core-core correlation. The hydrogen basis is identical to the s manifold of the DZP basis set utilized above for the H4 and P4 models.

Molecular BeH_2 at its linear ($D_{\infty h}$) equilibrium geometry has the dominant configuration

$$\left|\Phi_1\right\rangle = \left|(1\sigma_g)^2(2\sigma_g)^2(1\sigma_u)^2\right\rangle, \tag{50}$$

which correlates to

$$\left|\Phi_1\right\rangle = \left|(1a_1)^2(2a_1)^2(1b_2)^2\right\rangle \tag{51}$$

in C_{2v} symmetry. In contrast, the dissociated $Be + H_2$ system is dominated by

$$\left|\Phi_2\right\rangle = \left|(1a_1)^2(2a_1)^2(3a_1)^2\right\rangle. \tag{52}$$

Therefore, a change of electronic configuration occurs along the dissociation path, with an intervening region in which $\left|\Phi_1\right\rangle$ and $\left|\Phi_2\right\rangle$ are quasidegenerate. SRCC methods are thus inherently flawed for the BeH_2 model. Within a SRCC formalism, $\left|\Phi_1\right\rangle$ can be used as a reference in the molecular region, and switching to reference $\left|\Phi_2\right\rangle$ allows description of the fragments. But in the vicinity of the transition state there is a discontinuity between the two energy curves, neither giving an accurate result. There is an additional pitfall for the BeH_2 model. In the linear configuration, the Hartree-Fock orbital energy of the unoccupied 1π orbital is lower than that of the $3\sigma_g^*$ antibonding orbital. For a proper description of the dissociation process, any multireference computation should continuously follow the $(1\sigma_u)^2 \leftrightarrow (3\sigma_g^*)^2$ zeroth-order wave function solution.[119] We were careful to ensure that this solution was obtained for both the CAS(2,2) orbitals and the multireference coupled cluster wave functions at all points along the BeH_2 dissociation path.

Figs. 2.9-2.12 display our results for the BeH_2 model for exciatation levels 2-5 (SD through SDTQP). SRCC curves are shown using $\left|\Phi_1\right\rangle$ as a Fermi vacuum in the range

$0 < x < 3.0$ and $\left|\Phi_2\right\rangle$ for the range $2.5 < x < 4.0$. We have found that the SUCC method presents

several issues of convergence for low ($0 < x < 0.5$) and high ($3.5 < x < 4$) values of x, and

denominator shifting in Eq. (37) was required to converge most of the points on the potential

energy curve. BWCC and MkCC converged without need of a denominator shift.

As the plots indicate, SRCC is unable to describe accurately the potential energy curve in

the multireference regime ($2.5 < x < 3.0$ bohr). The BWCCSD and MkCCSD methods perform

better than SUCCSD, with maximum errors below 2 mE$_h$. The NPE values for the SSMRCCSD

methods are lower than for SUMRCCSD. For example, the NPE is 2.2 mE$_h$ for MkCCSD but

5.7 mE$_h$ for SUCCSD. The inclusion of triples does not correct the misbehavior of the SRCC

solutions, while it reduces the absolute error for the BWCC and MkCC methods below 0.5 mE$_h$

and the corresponding NPEs by an order of magnitude (Table 2.3). At this level of truncation,

SUCC performs satisfactorily in the multireference region, but it strongly deviates from the FCI

curve when the zeroth-order wave function has single-reference character (absolute error

ca. 5 mE$_h$, NPE = 5.4 mE$_h$).

Table 2.3. Non-parallelism error (NPE) in microhartrees (μE_h) for the 1^1A_1 state of the BeH$_2$ model system, computed with [Be($3s2p$)/H($2s$)] basis set.

Excitation level	CC Theory				
	SR (Φ_1) $x\in[0,3]$	SR (Φ_2) $x\in[2.5,4]$	SU $x\in[0.15,3.5]$	BW $x\in[0,4]$	Mk $x\in[0,4]$
SD	15768	8082	5727	1922	2238
SDT	10700	9977	5449	443	198
SDTQ	14.1	37.4	3.2	0.7	0.6
SDTQP	0.3	37.2	6.8	0.3	0.0

With the inclusion of quadruples, the SSMRCC methods give absolute errors around 0.5 μE_h, three orders of magnitude better than the CCSDT approximation. The SUCCSDTQ method can deviate by more that 1 μE_h, while the SRCCSDTQ curves show divergence in the multireference regime. All the MRCC methods display oscillatory error curves in the multireference regime. However, the MRCC energy curves and their derivatives remain perfectly smooth. To illustrate this point we have also included in Fig. 2.11 a smaller plot of the total energy of a section of the multireference regime. Further details regarding this point are given in the Supplementary Information, where we report numerical gradients computed at the MRCCSDTQ level. Finally, at the SDTQP level the CC energies deviate from FCI by less than 1 μE_h for the MkCC and BWCC methods, but the SRCC and SUCC errors can be much larger. Indeed, MkCC provides results that are virtually indistinguishable from the FCI curve. MkCC is superior to BWCC with a NPE of 0.0 μE_h and an absolute error less than 10^{-8} E_h.
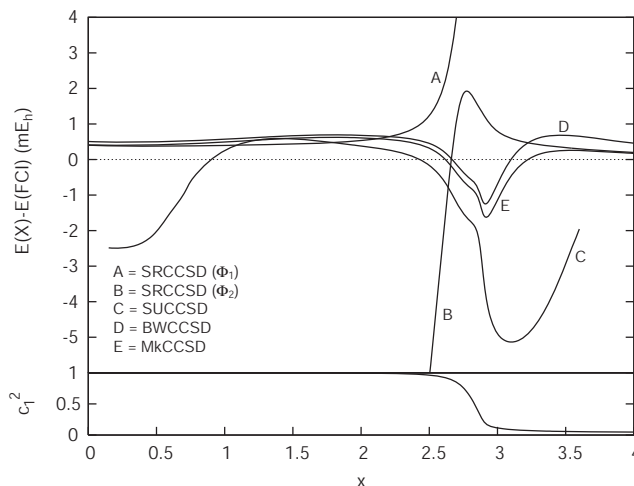
Figure 2.9. MRCCSD/[Be($3s2p$)/H($2s$)] energy curves for the 1^1A_1 ground state of the BeH$_2$ model system. All computations (including single-reference CC) employed CAS(2,2) orbitals optimized for the 1^1A_1 state. The lower panel shows the square of the CAS(2,2) CI coefficient of $\left|\Phi_1\right\rangle$ versus the parameter x. The SUCC curve is shown only in the range of convergence.
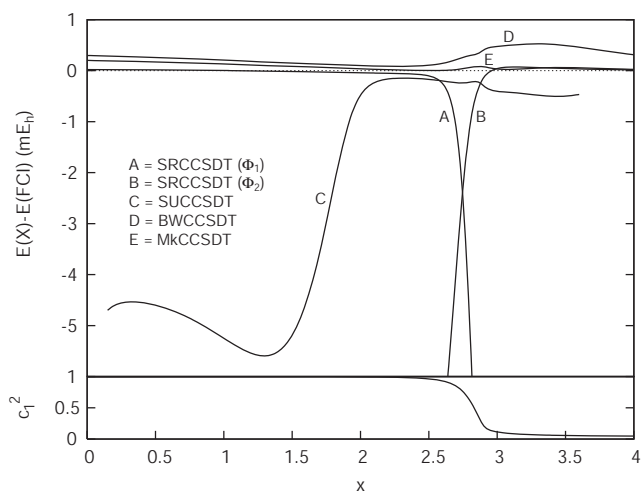
Figure 2.10. MRCCSDT/[Be($3s2p$)/H($2s$)] energy curves for the 1^1A_1 ground state of the BeH$_2$ model system. See Fig. 2.9 caption for details.
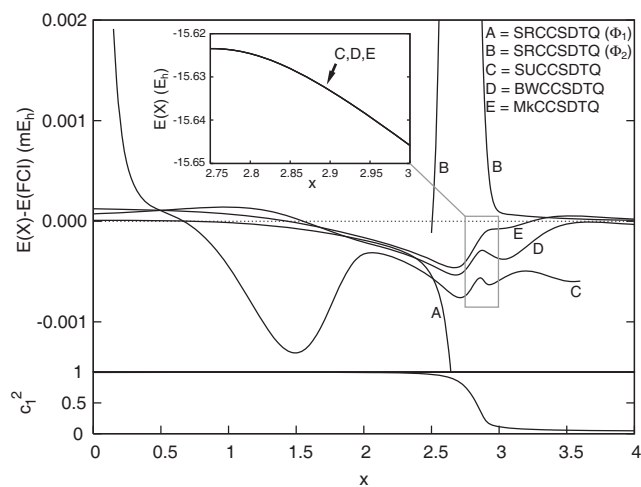
Figure 2.11. MRCCSDTQ/[Be($3s2p$)/H($2s$)] energy curves for the 1^1A_1 ground state of the BeH$_2$ model system. See Fig. 2.9 caption for details.
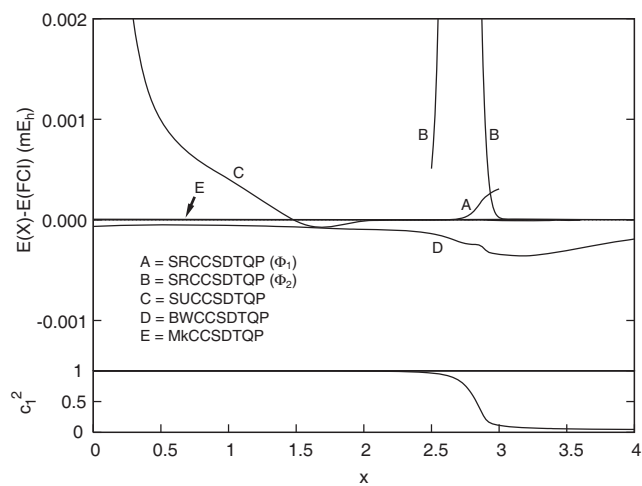
Figure 2.12. MRCCSDTQP/[Be($3s2p$)/H($2s$)] energy curves for the 1^1A_1 ground state of the BeH$_2$ model system. See Fig. 2.9 caption for details.

2.5.4 THE H8 MODEL

The H8 model consists of eight hydrogen atoms arranged in an octagonal configuration with four bond lengths fixed to exactly 2 bohr. A variable parameter α (measured in bohr) determines the deviation from the D_{8h} configuration due to the displacement of a pair of parallel H_2 molecules. Scheme 2.4 depicts the H8 model and gives the definition of the parameter α. This model system was introduced in the 1980s by Jankowski, Meissner and Wasilewski[120] and later has been studied intensively by several authors with CASCCSD,[47,48] SUCC,[13,106,121] BWCC,[97] MRCEPA,[24] MkCC[122], and MRexpT[81] theories. As in the P4 model, upon varying the parameter α, the H8 model gives three different types of geometrical configurations: (A) compressed, $\alpha < 0$; (B) octagonal, $\alpha = 0$; and (C) elongated, $\alpha > 0$.
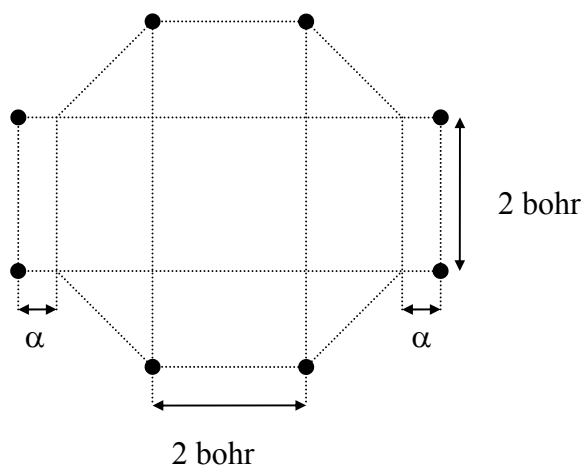
Scheme 2.4. The H8 Model.

The H8 system is described by a two-dimensional model space defined by the two electronic configurations (in D_{2h} symmetry)

$$\begin{aligned}
\left|\Phi_1\right\rangle &= \left|(1a_g)^2(1b_{3u})^2(1b_{2u})^2(1b_{1g})^2\right\rangle \\
\left|\Phi_2\right\rangle &= \left|(1a_g)^2(1b_{3u})^2(1b_{2u})^2(2a_g)^2\right\rangle
\end{aligned}.$$

(53)

For the compressed geometry the $|\Phi_1\rangle$ configuration is the restricted Hartree-Fock ground state, while for the elongated geometry, $|\Phi_2\rangle$ becomes lower in energy than $|\Phi_1\rangle$. The zeroth-order wave function for the D_{8h} geometry is well described by the electronic configuration

$$(1a_{1g})^2(1e_{1g})^4(1e_{1u})^2, \tag{54}$$

comprising two degenerate determinants.

Single and multireference coupled cluster results for excitation levels 2-6 (SD through SDTQPH) are plotted for the H8 model in Figs. 2.13-2.17. The SRCC computations used reference $|\Phi_1\rangle$ as a Fermi vacuum for $\alpha < 0$ and $|\Phi_2\rangle$ for $\alpha > 0$. All computations employed ground-state CAS(2,2) orbitals and the s manifold of the DZP basis set utilized above for the H4 and P4 models.[107,108]
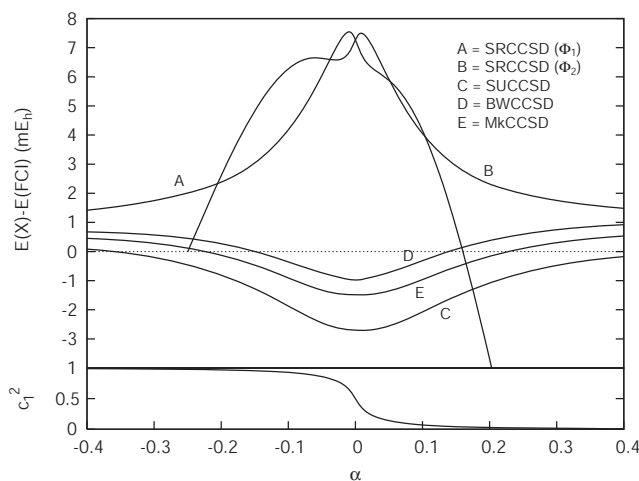
Figure 2.13. MRCCSD/DZ energy curves for the 1^1A_1 ground state of the H8 model system. All computations (including single-reference CC) employed CAS(2,2) orbitals optimized for the 1^1A_1 state. The lower panel shows the square of the CAS(2,2) CI coefficient of $|\Phi_1\rangle$ versus the parameter α.
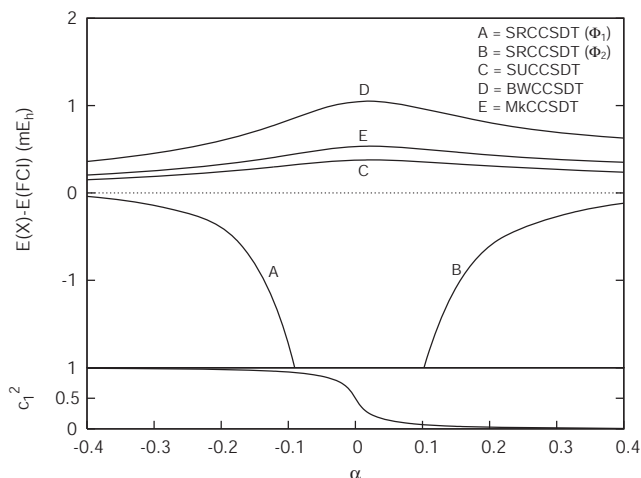
Figure 2.14. MRCCSDT/DZ energy curves for the 1^1A_1 ground state of the H8 model system. See Fig. 2.13 caption for details.

Table 2.4. Non-parallelism error (NPE) in microhartrees (μE_h) for the 1^1A_1 state of the H8 model system, computed with DZ basis set.

	CC Theory				
Excitation level	SR (Φ_1) $\alpha \in [-0.4,0]$	SR (Φ_2) $\alpha \in [0,0.4]$	SU $\alpha \in [-0.4,0.4]$	BW $\alpha \in [-0.4,0.4]$	Mk $\alpha \in [-0.4,0.4]$
SD	6102	5995	2768	1906	2019
SDT	8580	8500	226	716	330
SDTQ	77.7	77.0	6.3	10.0	6.1
SDTQP	79.3	79.3	1.0	5.5	2.0
SDTQPH	0.1	0.1	0.0	0.0	0.0

The two SRCC curves exhibit discontinuities in the multireference regime and large errors, most manifestly at the triples level, where the NPE is ca. 8.6 mE_h and 8.4 mE_h when using, respectively, $|\Phi_1\rangle$ and $|\Phi_2\rangle$ as the reference. The MRCCSD methods show NPE values smaller than 3 mE_h, and the error is further reduced by the inclusion of triple excitations, most

significantly in the case of SUCCSDT (NPE = 0.2 mE$_h$) and MkCCSDT (NPE = 0.3 mE$_h$) (Table 2.4). The MRCC methods have the largest absolute errors in the multireference region. For example, at $\alpha = 0$, BWCCSD is more accurate than MkCCSD and SUCCSD, with absolute errors of −1, −1.5, and −2.7 mE$_h$, respectively. This ordering is reversed by the inclusion of triples. Thus, at $\alpha = 0$, SUCCSDT is more accurate than MkCCSDT and BWCCSDT, with absolute errors of 0.4, 0.5, and 1.0 mE$_h$, respectively. In the single-reference region ($|\alpha| > 0.2$) the MRCC curves are more accurate than SRCC only for the SD level. Once higher-order excitations ($n > 2$) are included, the MRCC methods again fail to match the accuracy of SRCC, when the Hartree-Fock reference predominates. For example, for $\alpha = 0.4$, where the zeroth-order wave function is dominated by $\left| \Phi_2 \right\rangle$, the energy error of SRCCSDT with respect to FCI is −0.1 mE$_h$, while for SUCCSDT, BWCCSDT and MkCCSDT it is 0.2, 0.4, and 0.6 mE$_h$, respectively.
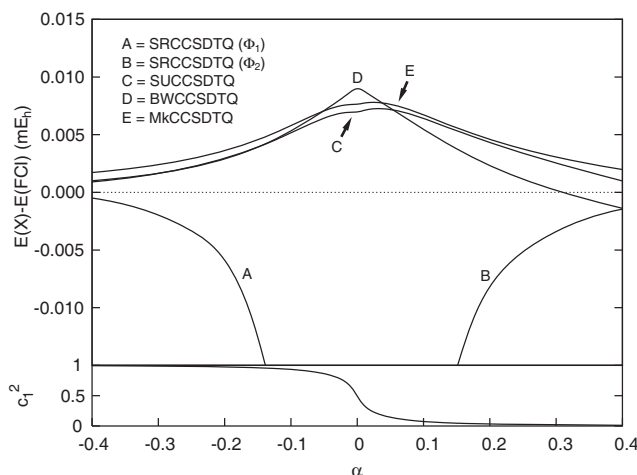
Figure 2.15. MRCCSDTQ/DZ energy curves for the 1^1A_1 ground state of the H8 model system. See Fig. 2.13 caption for details.

Quadruple excitations reduce the NPE below 0.01 mE_h for all MRCC methods. For SRCCSDTQ the NPE is around 0.08 mE_h (Table 2.4). All MRCCSDTQ methods outperform SRCCSDTQ in the multireference region. The absolute errors at the octagonal geometry ($\alpha = 0$) for the MRCCSDTQ methods are below 9 μE_h, with little difference in performance. In the single-reference region ($|\alpha| > 0.2$) the MRCC curves show maximum deviations from FCI of ca. 6 μE_h, comparable to the deviation observed for SRCC (ca. 10 μE_h). In conclusion, at this level of excitations the performance of the various MRCC methods is approximately the same.
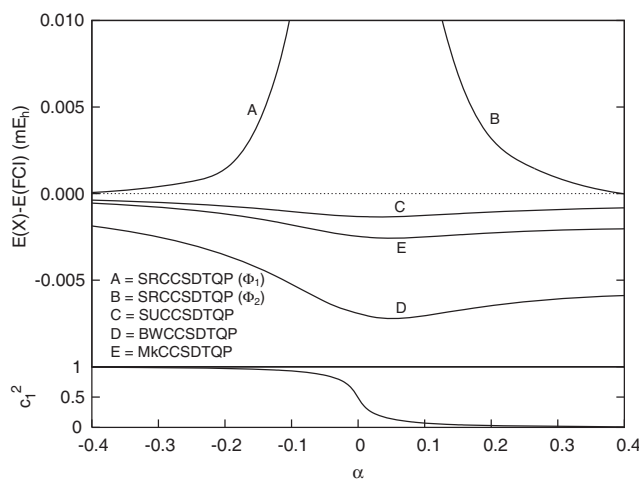
Figure 2.16. MRCCSDTQP/DZ energy curves for the 1^1A_1 ground state of the H8 model system. See Fig. 2.13 caption for details.

The CCSDTQP schemes are extremely accurate for all the MRCC methods. However, SRCCSDTQP still has a pronounced discontinuity in the multireference region. The best performance at $\alpha = 0$ is provided by SUCCSDTQP (NPE = 1.0 μE_h, absolute error -1.3 μE_h) and MkCCSDTQP (NPE = 2.0 μE_h, absolute error -2.5 μE_h) with BWCCSDTQP about three times less accurate. Inclusion of all excitations through hextuples gives potential energy curves with

errors less than 0.02 μE_h for all MRCC methods. The SRCCSDTQPH error peaks at about 0.14 μE_h near $\alpha = 0$ and shows only a small cusp when the reference changes from $|\Phi_1\rangle$ to $|\Phi_2\rangle$.
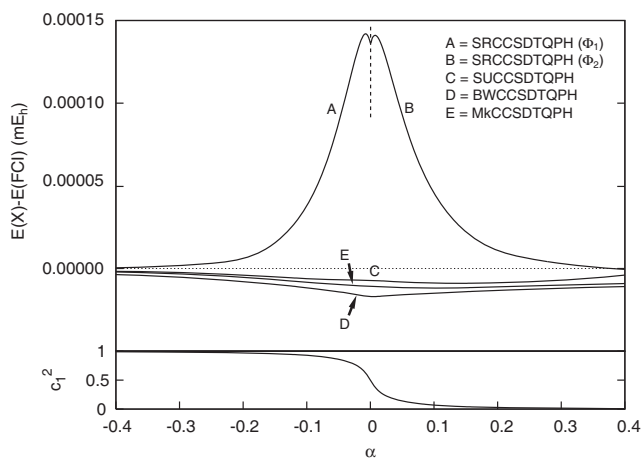
Figure 2.17. MRCCSDTQPH/DZ energy curves for the 1^1A_1 ground state of the H8 model system. See Fig. 2.13 caption for details.

2.6 SUMMARY

A new, arbitrary-order string-based code has been used to compute multireference coupled cluster (MRCC) energies with excitation levels ranging from doubles to hextuples for the H4, P4, BeH$_2$ and H8 models. Extensive tests were executed for genuine multireference coupled cluster theories based on the wave operator formalism: (a) the state universal (SU) method of Jeziorski and Monkhorst;[12] (b) the state-specific Brillouin-Wigner (BW) approach, including *a posteriori* corrections for lack of size extensivity;[26-31] and (c) the state-specific and rigorously size extensive method of Mukherjee (Mk).[20-25] Companion full CI (FCI) and single-reference coupled cluster (SRCC) computations facilitated rigorous assessments of the MRCC methods.

The error curves (with respect to FCI) in Figs. 2.1-2.17 demonstrate that for ground electronic states MkCC is clearly superior to SUCC at all levels of truncation of the cluster operator. The only exception to this statement for the systems studied here is the H8 model in the case of triple and higher excitations. The ground-state error curves show that MkCC is also generally better than BWCC, but as measured by the non-parallelism error (NPE) index of Tables 2.1-2.4, MkCC and BWCC are quite competitive. For the one excited state examined here (2^1A_1 for the H4 model), MkCC and BWCC perform just as well as SUCC.

One qualitative measure of the performance of the MRCC methods is the degree to which the error curves remain flat throughout the single and multireference regions of the geometric configuration space. For the H4, P4, BeH_2, and H8 models, none of the MRCC methods completely achieves this goal at the single and double excitation level. However, in the ground-state computations, MkCCSDT meets this criterion exceedingly well, certainly better than BWCCSDT and SUCCSDT in general. A disappointing feature of SUCC is its pronounced tendency to deteriorate in accuracy outside the immediate vicinity of quasidegeneracy in the electronic structure, thus enhancing the curvature of the SUCC error functions.

The NPE indices in Tables 2.1-2.4 provide quantitative information on the degree to which the various coupled cluster curves parallel the FCI results. The average ground-state NPE values for SUCCSD, BWCCSD, and MkCCSD are 3.9, 1.3, and 1.4 mE_h, respectively. The inclusion of triple excitations yields significant improvements, the average ground-state NPE values for SUCCSDT, BWCSDT, and MkCCSDT being reduced to 2.91, 0.42 and 0.22 mE_h, respectively.

A final measure of the performance is given in Table 2.5, where absolute errors with respect to FCI are listed for each coupled cluster method, as computed at the points of maximum

multireference character. At these points [H4($\alpha = 0$), P4($\alpha = 2$), BeH$_2$($x = 2.85$), H8($\alpha = 0$)] the

CI coefficients in the CAS(2,2) zeroth-order wave functions are equivalent ($c_1^2 = c_2^2 = 1/2$).

Once again the superiority of the MkCC method is demonstrated. Also note the dramatic

improvement when quadruple excitations are included. Among the MRCCSDTQ entries, the

absolute errors are all less than 10 μE_h, or 2 cm^{-1}.

Table 2.5. Errors in microhartrees (μE_h) for the 1^1A_1 ground state of the H4, P4, BeH$_2$, and H8 models computed at the maximum multireference point using ground-state CAS(2,2) orbitals.

H4 and P4	CC Theory				
Excitation level	SR	SU	BW	apBW	Mk
SD	7372	−661	35	−1826	−162
SDT	−2143	−114	226	−1578	43
BeH$_2$	CC Theory				
Excitation level	SR (Φ_1)	SR (Φ_2)	SU	BW	Mk
SD	10041	1563	−2032	−762	−1016
SDT	−8253	−442	−214	327	80
SDTQ	−12.7	4.0	−0.6	−0.3	−0.2
SDTQP	0.1	3.9	−0.001	−0.2	−0.003
H8	CC Theory				
Excitation level	SR (Φ_1)	SR (Φ_2)	SU	BW	Mk
SD	7272	7272	−2699	−984	−1483
SDT	−8618	−8618	374	1041	530
SDTQ	−70.7	−70.7	7.0	9.0	7.6
SDTQP	79.3	79.3	−1.3	−6.9	−2.5
SDTQPH	0.1	0.1	−0.008	−0.017	−0.011

In summary, the MkCC approach is shown to be the method of choice among the MRCC formalisms investigated here for the H4, P4, BeH$_2$, and H8 models. Of course, caution is warranted in extrapolating this conclusion to more realistic chemical systems. More definitive conclusions will become apparent after the development of production-level MkCC codes capable of treating larger molecules with extensive basis sets. For the model systems, multireference BWCC often provides results of comparable accuracy to MkCC. However, the lack of size extensivity of BWCC poses real limitations to its broad application. In our tests of the proposed *a posteriori* (ap) size-extensivity correction to BWCC,[28] we found a serious degradation of results in all cases. For example, in the P4 system, both apBWCCSD and apBWCCSDT have non-parallelism errors more than one order of magnitude greater than their BWCC and MkCC counterparts. Our investigation also found that the corresponding iterative size-extensivity correction (iBWCC) fails even more severely than apBWCC, so we do not report explicit data here.

Despite the success of the MkCC method, there are still directions for further improvements. First, it is disappointing that all the wave operator MRCC methods investigated here were often unable to match the accuracy of SRCC theory in the single-reference regions of the H4, P4, BeH$_2$, and H8 models. This deficiency was not observed at the SD excitation level but was seen in all cases after triple excitations were included. While this deficiency was only 0.5 mE$_h$ in magnitude or smaller, one nonetheless wonders what subtle flaw might exist in MkCCSDT that makes it less accurate than SRCCSDT when the system has little multireference character. Second, the inclusion of triple excitations in a perturbative fashion [(T) approximations] should be a valuable development for the application of MkCC theory to larger systems. Work in this direction has been undertaken recently both by Li and Paldus[19] for

SUCC and Demel and Pittner[123] for BWCC. Finally, the general application of MkCC theory

must deal with the $\left\langle \Phi_{ij\cdots}^{ab\cdots}(\mu)\middle|e^{-\hat{T}^{\mu}}e^{\hat{T}^{\nu}}\middle|\Phi_{\mu}\right\rangle$ coupling terms in Eq. (30). However, for the very

important and widely applicable CCSD, and CCSDT cases, the exact evaluation of these terms

presents no difficulties. Indeed, we plan to report on a new production-level MkCCSD code for

CAS(2,2) model spaces in the near future. This achievement will bring numerous chemical

applications within the reach of genuine, fully size extensive, wave operator MRCC methods for

the first time.

2.7 ACKNOWLEDGMENTS

REFERENCES

[1]   J. Čížek, J. Chem. Phys. **45**, 4256 (1966).

[2]   D. Yarkony, *Modern Electronic Structure Theory*. (World Scientific, Singapore ; River
         Edge, NJ, 1995).

[3]   T. D. Crawford and H. F. Schaefer, Rev. Comp. Chem. **14**, 33 (2000).

[4]   R. J. Bartlett, in *Theory and Applications of Computational Chemistry*, edited by C. E.
         Dykstra, G. Frenking, K. S. Kim, and G. E. Scuseria (Elsevier, 2005).

[5]   J. Paldus, in *Theory and Applications of Computational Chemistry*, edited by C. E. Dykstra, G. Frenking, K. S. Kim, and G. E. Scuseria (Elsevier, 2005).

[6]   J. Gauss, in *The Encyclopedia of Computational Chemistry*, edited by N. L. A. P.v. R. Schleyer, T. Clark, J. Gasteiger, P. A. Kollman, H. F.Schaefer III, and P. R. Scheiner (Wiley, Chichester, 1998), pp. 615.

[7]   R. J. Bartlett, *Recent Advances in Coupled-Cluster Methods*. (World Scientific, Singapore, 1997).

[8]   D. Mukherjee, R. K. Moitra, and A. Mukhopadhyay, Mol. Phys. **33**, 955 (1977).

[9]   M. A. Haque and D. Mukherjee, J. Chem. Phys. **80**, 5058 (1984).

[10]   N. D. K. Petraco, L. Horný, H. F. Schaefer, and I. Hubač, J. Chem. Phys. **117**, 9580 (2002).

[11]   L. Horný, H. F. Schaefer, I. Hubač, and S. Pal, Chem. Phys. **315**, 240 (2005).

[12]   B. Jeziorski and H. J. Monkhorst, Phys. Rev. A **24**, 1668 (1981).

[13]   J. Paldus, P. Piecuch, L. Pylypow, and B. Jeziorski, Phys. Rev. A **47**, 2738 (1993).

[14]   P. Piecuch and J. Paldus, Phys. Rev. A **49**, 3479 (1994).

[15]   X. Li and J. Paldus, J. Chem. Phys. **119**, 5320 (2003).

[16]   X. Li and J. Paldus, J. Chem. Phys. **119**, 5346 (2003).

[17]   X. Li and J. Paldus, J. Chem. Phys. **120**, 5890 (2004).

[18]   X. Li and J. Paldus, Int. J. Quantum Chem. **99**, 914 (2004).

[19]   X. Li and J. Paldus, J. Chem. Phys. **124**, 034112 (2006).

[20]   U. S. Mahapatra, B. Datta, B. Bandyopadhyay, and D. Mukherjee, Adv. Quantum Chem. **30**, 163 (1998).

[21]   U. S. Mahapatra, B. Datta, and D. Mukherjee, J. Phys. Chem. A **103**, 1822 (1999).

22 U. S. Mahapatra, B. Datta, and D. Mukherjee, J. Chem. Phys. **110**, 6171 (1999).

23 S. Chattopadhyay, U. S. Mahapatra, and D. Mukherjee, J. Chem. Phys. **112**, 7939 (2000).

24 S. Chattopadhyay, D. Pahari, D. Mukherjee, and U. S. Mahapatra, J. Chem. Phys. **120**, 5968 (2004).

25 S. Chattopadhyay, P. Ghosh, and U. S. Mahapatra, J. Phys. B-At. Mol. Opt. **37**, 495 (2004).

26 I. Hubač and P. Neogrady, Phys. Rev. A **50**, 4558 (1994).

27 J. Masik, I. Hubač, and P. Mach, J. Chem. Phys. **108**, 6571 (1998).

28 J. Pittner, J. Chem. Phys. **118**, 10876 (2003).

29 J. Pittner and O. Demel, J. Chem. Phys. **122**, 181101 (2005).

30 J. Pittner, P. Nachtigall, P. Carsky, J. Masik, and I. Hubač, J. Chem. Phys. **110**, 10275 (1999).

31 I. Hubač and S. Wilson, J. Phys. B-At. Mol. Opt. **34**, 4259 (2001).

32 I. Hubač, J. Pittner, and P. Carsky, J. Chem. Phys. **112**, 8779 (2000).

33 J. Pittner, X. Z. Li, and J. Paldus, Mol. Phys. **103**, 2239 (2005).

34 L. Adamowicz, J. P. Malrieu, and V. V. Ivanov, J. Chem. Phys. **112**, 10075 (2000).

35 D. I. Lyakh, V. V. Ivanov, and L. Adamowicz, J. Chem. Phys. **122**, 024108 (2005).

36 J. Olsen, J. Chem. Phys. **113**, 7140 (2000).

37 M. Kallay, P. G. Szalay, and P. R. Surjan, J. Chem. Phys. **117**, 980 (2002).

38 X. Z. Li, I. Grabowski, K. Jankowski, and J. Paldus, Adv Quantum Chem **36**, 231 (2000).

39 X. Z. Li and J. Paldus, J. Chem. Phys. **107**, 6257 (1997).

40 X. Z. Li and J. Paldus, Collect. Czech. Chem. C. **63**, 1381 (1998).

41 X. Z. Li and J. Paldus, Chem. Phys. Lett. **286**, 145 (1998).

42   X. Z. Li and J. Paldus, J. Chem. Phys. **108**, 637 (1998).

43   X. Z. Li and J. Paldus, J. Chem. Phys. **110**, 2844 (1999).

44   X. Z. Li and J. Paldus, J. Chem. Phys. **113**, 9966 (2000).

45   X. Z. Li and J. Paldus, Int. J. Quantum Chem. **80**, 743 (2000).

46   X. Z. Li and J. Paldus, Mol. Phys. **98**, 1185 (2000).

47   P. Piecuch and L. Adamowicz, J. Chem. Phys. **100**, 5792 (1994).

48   P. Piecuch and L. Adamowicz, Chem. Phys. Lett. **221**, 121 (1994).

49   K. Kowalski, S. Hirata, M. Wloch, P. Piecuch, and T. L. Windus, J. Chem. Phys. **123** (2005).

50   K. Kowalski and P. Piecuch, J. Chem. Phys. **113**, 8490 (2000).

51   K. Kowalski and P. Piecuch, Chem. Phys. Lett. **344**, 165 (2001).

52   K. Kowalski and P. Piecuch, J. Chem. Phys. **115**, 643 (2001).

53   P. Piecuch, S. Hirata, K. Kowalski, P. D. Fan, and T. L. Windus, Int. J. Quantum Chem. **106**, 79 (2006).

54   A. I. Krylov, C. D. Sherrill, E. F. C. Byrd, and M. Head-Gordon, J. Chem. Phys. **109**, 10669 (1998).

55   A. I. Krylov, C. D. Sherrill, and M. Head-Gordon, J. Chem. Phys. **113**, 6509 (2000).

56   C. D. Sherrill, A. I. Krylov, E. F. C. Byrd, and M. Head-Gordon, J. Chem. Phys. **109**, 4171 (1998).

57   S. R. Gwaltney, E. F. C. Byrd, T. Van Voorhis, and M. Head-Gordon, Chem. Phys. Lett. **353**, 359 (2002).

58   S. R. Gwaltney and M. Head-Gordon, Abstr Pap Am Chem S **219**, U338 (2000).

59   S. R. Gwaltney and M. Head-Gordon, Chem. Phys. Lett. **323**, 21 (2000).

[60] S. R. Gwaltney and M. Head-Gordon, J. Chem. Phys. **115**, 2014 (2001).

[61] S. R. Gwaltney, C. D. Sherrill, M. Head-Gordon, and A. I. Krylov, J. Chem. Phys. **113**, 3548 (2000).

[62] P. D. Fan, K. Kowalski, and P. Piecuch, Mol. Phys. **103**, 2191 (2005).

[63] K. Jankowski, J. Paldus, and P. Piecuch, Theor. Chim. Acta **80**, 223 (1991).

[64] K. Kowalski and P. Piecuch, J. Chem. Phys. **113**, 18 (2000).

[65] K. Kowalski and P. Piecuch, J. Chem. Phys. **116**, 7411 (2002).

[66] P. Piecuch, K. Kowalski, I. S. O. Pimienta, P. D. Fan, M. Lodriguito, M. J. McGuire, S. A. Kucharski, T. Kus, and M. Musial, Theor Chem Acc **112**, 349 (2004).

[67] I. S. O. Pimienta, K. Kowalski, and P. Piecuch, J. Chem. Phys. **119**, 2951 (2003).

[68] K. Kowalski and P. Piecuch, J. Chem. Phys. **113**, 5644 (2000).

[69] K. Kowalski and P. Piecuch, J. Chem. Phys. **122** (2005).

[70] P. Piecuch, K. Kowalski, I. S. O. Pimienta, and M. J. McGuire, Int Rev Phys Chem **21**, 527 (2002).

[71] P. Piecuch, S. A. Kucharski, and K. Kowalski, Chem. Phys. Lett. **344**, 176 (2001).

[72] P. Piecuch, S. A. Kucharski, V. Spirko, and K. Kowalski, J. Chem. Phys. **115**, 5796 (2001).

[73] P. Piecuch and M. Wloch, J. Chem. Phys. **123** (2005).

[74] M. J. McGuire and P. Piecuch, J Am Chem Soc **127**, 2608 (2005).

[75] R. L. DeKock, M. J. McGuire, P. Piecuch, W. D. Allen, H. F. Schaefer, K. Kowalski, S. A. Kucharski, M. Musial, A. R. Bonner, S. A. Spronk, D. B. Lawson, and S. L. Laursen, J. Phys. Chem. A **108**, 2893 (2004).

76   S. Coussan, Y. Ferro, A. Trivella, M. Rajzmann, P. Roubin, R. Wieczorek, C. Manca, P. Piecuch, K. Kowalski, M. Wloch, S. A. Kucharski, and M. Musial, J. Phys. Chem. A **110**, 3920 (2006).

77   A. Kinal and P. Piecuch, J. Phys. Chem. A **110**, 367 (2006).

78   M. J. McGuire, P. Piecuch, K. Kowalski, S. A. Kucharski, and M. Musial, J. Phys. Chem. A **108**, 8878 (2004).

79   C. D. Sherrill and P. Piecuch, J. Chem. Phys. **122** (2005).

80   M. Hanrath, J. Chem. Phys. **123**, 084102 (2005).

81   M. Hanrath, Chem. Phys. Lett. **420**, 426 (2006).

82   J. Paldus and H. C. Wong, Comput Phys Commun **6**, 1 (1973).

83   H. C. Wong and J. Paldus, Comput Phys Commun **6**, 9 (1973).

84   C. L. Janssen and H. F. Schaefer, Theor. Chim. Acta **79**, 1 (1991).

85   X. Z. Li and J. Paldus, J. Chem. Phys. **101**, 8812 (1994).

86   S. Hirata and R. J. Bartlett, Chem. Phys. Lett. **321**, 216 (2000).

87   S. Hirata, P. D. Fan, A. A. Auer, M. Nooijen, and P. Piecuch, J. Chem. Phys. **121**, 12197 (2004).

88   S. Hirata, J. Phys. Chem. A **107**, 9887 (2003).

89   M. Kallay, J. Gauss, and P. G. Szalay, J. Chem. Phys. **119**, 2991 (2003).

90   M. Kallay and J. Gauss, J. Chem. Phys. **120**, 6841 (2004).

91   M. L. Abrams and C. D. Sherrill, Chem. Phys. Lett. **404**, 284 (2005).

92   P. J. Knowles and N. C. Handy, Chem. Phys. Lett. **111**, 315 (1984).

93   J. Masik and I. Hubač, Adv. Quantum. Chem. **31**, 75 (1999).

[94] T. D. Crawford, C. D. Sherrill, E. F. Valeev, J. T. Fermann, R. A. King, M. L. Leininger, S. T. Brown, C. L. Janssen, E. T. Seidl, J. P. Kenny, and W. D. Allen, PSI 3.2.3 (2005).

[95] C. D. Sherrill and H. F. Schaefer, Adv. Quantum. Chem. **34**, 143 (1999).

[96] P. Piecuch and J. Paldus, J. Chem. Phys. **101**, 5875 (1994).

[97] I. Hubač, P. Mach, and S. Wilson, Int. J. Quantum Chem. **104**, 387 (2005).

[98] See EPAPS Document No. ___ for pdf file containing the gaussian basis sets, benchmarks, numerical gradients and energy points. This document can be reached via a direct link in the online article's HTML reference section or via the EPAPS homepage (http://www.aip.org/pubservs/epaps.html).

[99] T. P. Hamilton and P. Pulay, J. Chem. Phys. **84**, 5728 (1986).

[100] G. E. Scuseria, T. J. Lee, and H. F. Schaefer, Chem. Phys. Lett. **130**, 236 (1986).

[101] G. D. Purvis and R. J. Bartlett, J. Chem. Phys. **75**, 1284 (1981).

[102] K. Jankowski, J. Gryniakow, and K. Rubiniec, Int. J. Quantum Chem. **67**, 221 (1998).

[103] K. Jankowski, K. Kowalski, K. Rubiniec, and J. Wasilewski, Int. J. Quantum Chem. **67**, 205 (1998).

[104] K. Jankowski, L. Meissner, and K. Rubiniec, Int. J. Quantum Chem. **67**, 239 (1998).

[105] K. Jankowski and J. Paldus, Int. J. Quantum Chem. **18**, 1243 (1980).

[106] P. Piecuch and J. Paldus, J. Phys. Chem. **99**, 15354 (1995).

[107] T. H. Dunning, J. Chem. Phys. **53**, 2823 (1970).

[108] S. Huzinaga, J. Chem. Phys. **42**, 1293 (1965).

[109] G. D. Purvis, R. Shepard, F. B. Brown, and R. J. Bartlett, Int. J. Quantum Chem. **23**, 835 (1983).

[110] R. K. Chaudhuri, J. P. Finley, and K. F. Freed, J. Chem. Phys. **106**, 4067 (1997).

[111] S. B. Sharp and G. I. Gellene, J. Phys. Chem. A **104**, 10951 (2000).

[112] J. Ma, S. H. Li, and W. Li, J. Comp. Chem. **27**, 39 (2006).

[113] P. J. A. Ruttink, J. H. van Lenthe, and P. Todorov, Mol. Phys. **103**, 2497 (2005).

[114] S. Chattopadhyay and U. S. Mahapatra, J. Phys. Chem. A **108**, 11664 (2004).

[115] J. Pittner, H. V. Gonzalez, R. J. Gdanitz, and P. Carsky, Chem. Phys. Lett. **386**, 211 (2004).

[116] A. Banerjee and J. Simons, Chem. Phys. **81**, 297 (1983).

[117] R. J. Gdanitz and R. Ahlrichs, Chem. Phys. Lett. **143**, 413 (1988).

[118] R. J. Gdanitz, Int. J. Quantum Chem. **85**, 281 (2001).

[119] While benchmarking our code, we found that in Ref. 22 the 1π rather than the $3\sigma_g^*$ orbital was mistakenly correlated in the zeroth-order wave function of BeH_2 at the linear geometry.

[120] K. Jankowski, L. Meissner, and J. Wasilewski, Int. J. Quantum Chem. **28**, 931 (1985).

[121] X. Li and J. Paldus, J. Chem. Phys. **103**, 1024 (1995).

[122] U. S. Mahapatra, B. Datta, and D. Mukherjee, Mol. Phys. **94**, 157 (1998).

[123] O. Demel and J. Pittner, J. Chem. Phys. **124**, 144112 (2006).

CHAPTER 3

COUPLING TERM DERIVATION AND GENERAL IMPLEMENTATION OF STATE-SPECIFIC

MULTIREFERENCE COUPLED CLUSTER THEORIES[‡]

3.1 Abstract

Simple closed-form expressions are derived for the "same vacuum" renormalization terms that arise in state-specific multireference coupled cluster (MRCC) theories. Explicit equations are provided for these coupling terms through the triple excitation level of MRCC theory, and a general expression is included for arbitrary-order excitations. The first production-level code (PSIMRCC) for state-specific and rigorously size-extensive Mukherjee multireference coupled cluster singles and doubles (MkCCSD) computations has been written. This code is also capable of evaluating analogous Brillouin-Wigner multireference energies (BWCCSD), including *a posteriori* size-extensivity corrections. Using correlation-consistent basis sets (cc-pVXZ, X = D, T, Q), MkCCSD and BWCCSD were tested and compared on two classic multireference problems: (1) the dissociation potential curve of molecular fluorine (F_2), and (2) the structure and vibrational frequencies of ozone. Comparison with experimental data shows that the Mukherjee method is generally superior to Brillouin-Wigner theory in predicting energies, structures, and vibrational frequencies. Particularly accurate results for F_2 are obtained by applying the MkCCSD method with localized molecular orbitals. Although MkCCSD theory greatly improves upon single-reference CCSD for the geometric parameters and a_1 vibrational frequencies of ozone, the antisymmetric stretching frequency $\omega_3(b_2)$ remains pathological and cannot be properly treated without the inclusion of connected triple excitations. Finally, we report preliminary multireference MkCCSD results for the singlet-triplet splittings in *ortho*-, *meta*-, and *para*-benzyne, coming within 1.5 kcal mol^{-1} of experiment in all cases.

For the first time high-order

3.2 INTRODUCTION

State-universal[1] (SU) and state-specific[2,3] (SS) multireference coupled cluster theories (MRCC), in the Hilbert space formulation, are perhaps the most sound methods for computing accurate energies of quasi-degenerate molecular systems that require a multiconfigurational zeroth-order wave function. However, the technical difficulties of true MRCC formalisms have led to a number of alternative theories built on a single-reference framework, including the CASCC[4-7] approach, the reduced multireference (RM-RCCSD) method,[8-16] active-space CC approaches,[17-23] orbital-optimized CC schemes,[24-26] spin-flip methods,[27-34] higher-order, noniterative corrections derived from the similarity-transformed Hamiltonian,[35-39] and a broad class of method-of-moments CC (MM-CC)[40-45] and renormalized CC methods.[46-51] Notwithstanding these advances, renewed research on genuine multireference coupled cluster methods has given promising results,[3,52-62] and our interest in this paper is the development of rigorous, robust, SS-MRCC methods for practical chemical problems.

The state-universal MRCC approach was developed by Jeziorski and Monkhorst[1] (JM) and relies on a wave operator formalism. The wave operator ($\hat{\Omega}$) ansatz is

$$\hat{\Omega} = \sum_{\mu=1}^{d} e^{\hat{T}^{\mu}} \left| \Phi_{\mu} \right\rangle \left\langle \Phi_{\mu} \right|, \tag{1}$$

where $\left| \Phi_{\mu} \right\rangle$ belongs to the reference space (or model space) of d Slater determinants used to describe the zeroth-order wave function, and $\hat{T}^{\mu}$ incorporates dynamical correlation by exciting electrons from the occupied orbitals ($i, j, \ldots$) to the virtual orbitals ($a, b, \ldots$) of reference μ. A complete model space (CMS) is generally assumed, containing all possible distributions of m electrons in n orbitals [CAS(m, n)], but SUCC theory can also be formulated for an incomplete

71

model space.[52] Within this partition of the space of determinants, a projection operator onto the model space is defined as

$$\hat{P} = \sum_{\mu=1}^{d} \left| \Phi_{\mu} \right\rangle \left\langle \Phi_{\mu} \right| \tag{2}$$

as well as its orthogonal complement, $\hat{Q} = 1 - \hat{P}$. The JM wave operator is used to "lift" an approximate zeroth-order wave function for state α, written as a linear combination of reference determinants weighted by coefficients $c_{\mu}^{(\alpha)}$,

$$\left| \Psi_{\alpha}^{P} \right\rangle = \sum_{\mu} \left| \Phi_{\mu} \right\rangle c_{\mu}^{(\alpha)}, \tag{3}$$

to the corresponding exact wave function $\left| \Psi_{\alpha} \right\rangle$, which has the final form

$$\left| \Psi_{\alpha} \right\rangle = \hat{\Omega} \left| \Psi_{\alpha}^{P} \right\rangle = \sum_{\mu} e^{\hat{T}^{\mu}} \left| \Phi_{\mu} \right\rangle c_{\mu}^{(\alpha)}. \tag{4}$$

An effective Hamiltonian matrix

$$H_{\mu\nu}^{\mathrm{eff}} = \left\langle \Phi_{\mu} \left| \hat{H} e^{\hat{T}^{\nu}} \right| \Phi_{\nu} \right\rangle, \tag{5}$$

is diagonalized to obtain the energies $E^{(\alpha)}$ and weighting coefficients $c_{\mu}^{(\alpha)}$ from the eigenequation

$$\sum_{\nu=1}^{d} H_{\mu\nu}^{\mathrm{eff}} c_{\nu}^{(\alpha)} = E^{(\alpha)} c_{\mu}^{(\alpha)} \quad (\mu = 1, 2, \ldots, d). \tag{6}$$

The Bloch equation[1] for the wave operator gives the SUCC t-amplitude equations

$$\left\langle \Phi_{ij\cdots}^{ab\cdots}(\mu) \left| \bar{H}_{\mu} \right| \Phi_{\mu} \right\rangle = \sum_{\nu(\neq\mu)} \left\langle \Phi_{ij\cdots}^{ab\cdots}(\mu) \left| e^{-\hat{T}^{\mu}} e^{\hat{T}^{\nu}} \right| \Phi_{\nu} \right\rangle H_{\nu\mu}^{\mathrm{eff}} \quad (\mu = 1, 2, \ldots, d), \tag{7}$$

72

where $\bar{H}_\mu = e^{-\hat{T}^\mu} \hat{H} e^{\hat{T}^\mu}$ is the usual similarity-transformed Hamiltonian, and the determinants $\Phi^{ab\cdots}_{ij\cdots}(\mu)$ span all excitations contained in $\hat{T}^\mu$. The matrix elements of $\bar{H}_\mu$ are already present in single reference CC theory (SRCC), and thus may be easily coded using well know formulas reported more than ten years ago.[63-65] Jeziorski and Monkhorst proved that Eq. (7) leads to a size-extensive theory, by showing that all terms therein are connected quantities. In particular, the effective Hamiltonian matrix is a connected quantity for a CMS, because in this case

$$H^{\text{eff}}_{\nu\mu} = \left\langle \Phi_\nu \left| \hat{H} e^{\hat{T}^\mu} \right| \Phi_\mu \right\rangle = \left\langle \Phi_\nu \left| \bar{H}_\mu \right| \Phi_\mu \right\rangle, \tag{8}$$

and the similarity-transformed Hamiltonian contains only connected terms.

Perturbation theory was used by JM to prove the connected nature of the coupling terms $\left\langle \Phi^{ab\cdots}_{ij\cdots}(\mu) \left| e^{-\hat{T}^\mu} e^{\hat{T}^\nu} \right| \Phi_\nu \right\rangle$, also called "renormalization" terms.[1] The derivation of closed-form expressions for these terms is rather involved, and was a hindrance to the development of the SUCC method. The coupling terms take on numerous expressions, since they depend explicitly on the two references μ and ν, on the excitation level of the determinant used to left-project the SUCC equations, and the truncation scheme adopted for the cluster operator. Thus, the earlier derivations of the SUCC coupling terms were exclusively limited to model spaces formed by two closed-shell determinants and single and double (SD) excitation levels.[66-69] The most recent derivations are those by Li and Paldus[52] based on the algebraic approach, and by Paldus, Li, and Petraco[70] using diagrammatic procedures. These papers extended the coupling term treatment to the case of two generic determinants $\left| \Phi_\mu \right\rangle$ and $\left| \Phi_\nu \right\rangle$, while still assuming a cluster operator truncated at the SD level. Although the work of Paldus and co-workers,[52,70] in principle, solves the problem of finding closed expressions for the SUCC coupling terms, the final formulas are very generic and still require explicit simplification for all the possible cases.

A major difficulty with SUCC theory is the *intruder state problem*, which significantly limits its applicability. Intruder problems arise when an excited electronic state outside the model space drops into the energy regime of the chosen zeroth-order manifold in some region of the potential energy surface.[52,71,72] Li and Paldus[52-55,73] have recently revised the original SUCC formulation of JM, giving explicit "*C*-conditions" on the *t*-amplitudes that preserve size extensivity in the case of general model spaces. In this manner one can carefully select the reference determinants in the zeroth-order wave function to help avoid the intruder problem.

State-specific (SS) theories aim at treating one state at a time through a wave operator that lifts only one state

$$\left| \Psi_\alpha \right\rangle = \hat{\Omega}_\alpha \left| \Psi_\alpha^P \right\rangle. \tag{9}$$

By focusing on only one state, SS theories achieve two major improvements with respect to SUCC. First, they naturally avoid the intruder state problem, and second, they maximize accuracy for the state of interest.

The SS simplification introduces the problem of sufficiency conditions, because the number of equations that can be derived by introducing a state-specific wave operator into the Schrödinger equation is less than the number of *t*-amplitudes contained in the $\hat{T}^\mu$ operators. In particular, a redundancy exists among the *t*-amplitudes related to any determinant that can be generated from multiple references within the chosen excitation level cutoff. Since the *t*-amplitudes are underdetermined, one must introduce supplementary conditions. In SSMRCC this choice is not unequivocal, and various theories adopt different sufficiency conditions. Brillouin-Wigner[2,58,74-79] (BW) multireference coupled cluster and the MRCC approach of Mukherjee and co-workers[3,59-61,80-88] (here abbreviated as MkCC) are genuine state-specific

multireference CC theories based on the JM wave operator ansatz. These SS theories impose different sufficiency conditions on the t-amplitudes, with far-reaching consequences.

The BWCC method was first derived using the Brillouin-Wigner form of the Bloch equation.[2,58,74-79] A simpler derivation starts by inserting the JM expansion for the exact wave function [Eq. (4)] into the Schrödinger equation, yielding

$$\sum_{\mu} \left[\hat{H} e^{\hat{T}^{\mu}} \left| \Phi_{\mu} \right\rangle c_{\mu}^{(\alpha)} - E^{(\alpha)} e^{\hat{T}^{\mu}} \left| \Phi_{\mu} \right\rangle c_{\mu}^{(\alpha)} \right] = 0 . \tag{10}$$

The BWCC sufficiency conditions for the t-amplitudes consist in merely setting individual μ terms in Eq. (10) to be identically zero, leading to

$$\left\langle \Phi_{ij...}^{ab...}(\mu) \middle| \hat{H} e^{\hat{T}^{\mu}} \middle| \Phi_{\mu} \right\rangle = E^{(\alpha)} \left\langle \Phi_{ij...}^{ab...}(\mu) \middle| e^{\hat{T}^{\mu}} \middle| \Phi_{\mu} \right\rangle \quad (\mu = 1, 2, \ldots, d) . \tag{11}$$

Note that the amplitude equations for the various references are coupled only by the energy of the target state, a distinct computational advantage. BWCC solves the problem of intruder states but has one major deficiency – it is not size extensive. This is easily seen by expanding the first term in Eq. (11) as a sum of connected (C) diagrams, and disconnected linked (DCL) and unlinked (UL) diagrams

$$\hat{H} e^{\hat{T}^{\mu}} = \left(\hat{H} e^{\hat{T}^{\mu}} \right)_{C} + \left(\hat{H} e^{\hat{T}^{\mu}} \right)_{DCL+UL} . \tag{12}$$

The nonvanishing contribution of the DLC and UL diagrams leads to lack of size extensivity for the state-specific BWMRCC. In contrast, in the single reference[74,75] and Fock-Space multireference formulations of BWCC,[89,90] the disconnected contributions cancel at convergence, and therefore these methods are size extensive.

The solution of the size-extensivity problem in BWCC has been attempted by applying energy corrections after convergence of the BWCC t-amplitude equations. Both *a posteriori*

(apBWCC)[76] and the iterative (iBWCC)[77] correction schemes have been applied, as obtained

from a generalized Bloch equation[77] for the state-specific wave operator

$$\lambda E_\alpha \hat{\Omega}_\alpha \hat{P} + (1-\lambda)\hat{\Omega}_\alpha \hat{H}_0 \hat{P} = \hat{H}\hat{\Omega}_\alpha \hat{P} - (1-\lambda)\hat{\Omega}_\alpha \hat{P}\hat{V}\hat{\Omega}_\alpha \hat{P}, \tag{13}$$

where $\hat{H}_0$ and $\hat{V}$ derive from a well defined partition of the Hamiltonian, $\hat{H} = \hat{H}_0 + \hat{V}$. Setting

the parameter $\lambda = 1$ in Eq. (13) recovers the BWCC method, while $\lambda = 0$ yields the

Rayleigh-Schrödinger (RS) Bloch equation CC. In the *a posteriori* size-extensivity correction,

the MRCC equations are solved for $\lambda = 1$, and after convergence a final iteration is performed

with $\lambda = 0$. The iterative size-extensivity correction (iBWCC) is performed by continuously

decreasing the parameter λ to zero while converging the cluster amplitudes. In the *a posteriori*

correction, size extensivity is achieved only approximately, while in the iterative correction the

final energy is size extensive and equal to the RS Bloch equation energy. However, the intruder

problem is thus reintroduced in the iBWCC scheme.

The state specific MRCC method of Mukherjee (MkCC)[3,59-61,80-88] is obtained assuming

the JM ansatz for the wave operator and using a well defined set of sufficiency conditions. If we

multiply Eq. (10) by the identity

$$1 = e^{\hat{T}^\mu}e^{-\hat{T}^\mu} = e^{\hat{T}^\mu}(\hat{P}+\hat{Q})e^{-\hat{T}^\mu} = \sum_\nu e^{\hat{T}^\mu}\left|\Phi_\nu\right\rangle\left\langle\Phi_\nu\right|e^{-\hat{T}^\mu} + e^{\hat{T}^\mu}\hat{Q}e^{-\hat{T}^\mu} = \hat{P}_\mu + \hat{Q}_\mu, \tag{14}$$

we get

$$\sum_{\mu,\nu} e^{\hat{T}^\mu}\left|\Phi_\nu\right\rangle H^{\text{eff}}_{\nu\mu}c^{(\alpha)}_\mu + \sum_\mu e^{\hat{T}^\mu}\hat{Q}\bar{H}_\mu\left|\Phi_\mu\right\rangle c^{(\alpha)}_\mu - E^{(\alpha)}\sum_\mu e^{\hat{T}^\mu}\left|\Phi_\mu\right\rangle c^{(\alpha)}_\mu = 0. \tag{15}$$

Upon interchanging the dummy indices μ and ν in the double summation of Eq. (15) and

collecting the individual terms, we obtain

$$\sum_{\mu}\left[\sum_{\nu}e^{\hat{T}^{\nu}}\left|\Phi_{\mu}\right\rangle H_{\mu\nu}^{\text{eff}}c_{\nu}^{(\alpha)}+e^{\hat{T}^{\mu}}\hat{Q}\bar{H}_{\mu}\left|\Phi_{\mu}\right\rangle c_{\mu}^{(\alpha)}-E^{(\alpha)}e^{\hat{T}^{\mu}}\left|\Phi_{\mu}\right\rangle c_{\mu}^{(\alpha)}\right]=0. \tag{16}$$

The MkCC sufficiency conditions are chosen such that Eq. (16) is satisfied by setting the individual terms in the μ summation to zero. After multiplication by $e^{-\hat{T}^{\mu}}$ and left projection on the excited determinants $\Phi_{ij\ldots}^{ab\cdots}(\mu)$, the final t-amplitude equations become

$$\left\langle\Phi_{ij\ldots}^{ab\cdots}(\mu)\left|\bar{H}_{\mu}\right|\Phi_{\mu}\right\rangle c_{\mu}^{(\alpha)}+\sum_{\nu(\neq\mu)}\left\langle\Phi_{ij\ldots}^{ab\cdots}(\mu)\left|e^{-\hat{T}^{\mu}}e^{\hat{T}^{\nu}}\right|\Phi_{\mu}\right\rangle H_{\mu\nu}^{\text{eff}}c_{\nu}^{(\alpha)}=0\quad(\mu=1,2,\ldots,d). \tag{17}$$

Mukherjee and co-workers[3] proved the connected nature of the coupling terms $\left\langle\Phi_{ij\ldots}^{ab\cdots}(\mu)\left|e^{-\hat{T}^{\mu}}e^{\hat{T}^{\nu}}\right|\Phi_{\mu}\right\rangle$ and thus showed that MkCC is rigorously size extensive. These coupling terms resemble those present in SUCC theory, but with the key difference that both the bra and ket refer to the same reference μ. Expressions for these coupling terms were not reported by Mukherjee and co-workers. The idea that such terms would somehow be difficult to express has been stated in the literature,[77] and probably the apparently slight difference between the SUCC and MkCC coupling terms was not considered relevant.

The Mukherjee multireference approach has been investigated both at the CCSD and CEPA (coupled electron pair approximation) levels, and applied to the H4, P4, and BeH$_2$ model systems, as well as Li$_2$, F$_2$,[87] and several other diatomic molecules.[61] A perturbative scheme (MkPT) has also been developed.[83,84] While the MkCC method has given encouraging results in these tests, it has not been used in conjunction with large basis sets, and it is not currently implemented into a production-level code.

In our earlier paper[62] we investigated the effect of high order excitations (trough hextuple level) in SUCC, BWCC, apBWCC, and MkCC. The results obtained from the H4, P4, BeH$_2$, and H8 model systems indicated that MkCC and BWCC are competitive theories and provide more

accurate potential energy curves than SUCC and apBWCC. Moreover, when we analyzed the effect of the truncation of the excitation level, we found that MkCC shows a faster convergence to the FCI limit than BWCC. We thus concluded that even at the singles and doubles level, MkCC may provide accurate potential energy curves and that the inclusion of full triples promises to deliver energetics accurate to better than 1 kcal mol^{-1}.

In the present paper we derive explicit formulas for the MkCC coupling terms and then describe our new production-level implementation. Two derivations of the coupling terms are presented. The first involves the use of the resolution of the identity[52] and is worked out in the body of this article for the CCSD approximation. Appendix I reports a more general derivation using the properties of the "common amplitudes". Appendix II provides the explicit expressions for the coupling terms in the MkCCSDT approximation. Computations of the potential energy curve of F_2, vibrational frequencies of ozone, and preliminary results on the singlet-triplet splittings for the three isomers of benzyne are then presented as representative applications of our production-level MRCC code.

3.3 DERIVATION OF THE COUPLING TERMS

It is convenient, when dealing with state specific MRCC theories, to partition the space of spin orbitals into five subsets: 1) frozen core (**FC**), doubly occupied in all the determinants; 2) doubly occupied (**DO**), specifically doubly occupied in all the reference determinants; 3) active (**A**), partially occupied in the reference space; orbitals **A** contain K active electrons; 4) external (**E**), unoccupied in all the reference determinants, and 5) frozen external (**FE**), unoccupied in all determinants. For a generic determinant, $\left| \Phi_\mu \right\rangle$, we define the *active occupied*

orbitals (occupied orbitals in the $\mathbf{DO} + \mathbf{A}$ space) $\mathrm{occ}(\mu)$, and the *active virtual* orbitals (unoccupied orbitals in the $\mathbf{A} + \mathbf{E}$ space) $\mathrm{vir}(\mu)$.

In the case of single and double excitations the cluster operators are the sum of two contributions

$$\hat{T}^{\mu} = \hat{T}_1^{\mu} + \hat{T}_2^{\mu}, \tag{18}$$

with the individual components expressed as

$$\hat{T}_1^{\mu} = \sum_i^{\mathrm{occ}(\mu)} \sum_a^{\mathrm{vir}(\mu)} t_i^a(\mu) \hat{a}_a^+ \hat{a}_i, \tag{19}$$

and

$$\hat{T}_2^{\mu} = \frac{1}{4} \sum_{i,j}^{\mathrm{occ}(\mu)} \sum_{a,b}^{\mathrm{vir}(\mu)} t_{ij}^{ab}(\mu) \hat{a}_b^+ \hat{a}_j \hat{a}_a^+ \hat{a}_i. \tag{20}$$

Here, we have been careful to note that the *t*-amplitudes in Eqs. (19) and (20) belong to reference μ by adding the symbol in parentheses (μ). Assuming the model space used to build the zeroth-order wave function to be a complete active space (CAS), we can require the wave operator to satisfy intermediate normalization

$$\hat{P}\hat{\Omega}\hat{P} = \hat{P}. \tag{21}$$

This condition implies that the so called *internal amplitudes* corresponding to excitations that transform a reference determinant Φ_{μ} into another reference determinant Φ_{ν} are set to zero:[1,77]

$$\cdots \hat{a}_b^{\dagger} \hat{a}_j \hat{a}_a^{\dagger} \hat{a}_i \left| \Phi_{\mu} \right\rangle = \pm \left| \Phi_{\nu} \right\rangle \quad \Rightarrow \quad t_{ij\cdots}^{ab\cdots}(\mu) = 0. \tag{22}$$

In the MkCCSD approximation, the set of determinants used to project the MRCC equation is limited to the singly and doubly excited determinants obtained from the Fermi vacuum $\left|\Phi_\mu\right\rangle$

$$\left\{\left|\Phi_i^a(\mu)\right\rangle, \left|\Phi_{ij}^{ab}(\mu)\right\rangle\right\}. \tag{23}$$

To derive the coupling coefficients, we use the resolution of the identity written with respect to the vacuum μ as

$$\hat{I} = \left|\Phi_\mu\right\rangle\left\langle\Phi_\mu\right| + \sum_m^{occ(\mu)} \sum_e^{vir(\mu)} \left|\Phi_m^e(\mu)\right\rangle\left\langle\Phi_m^e(\mu)\right| + \sum_{m<n}^{occ(\mu)} \sum_{e<f}^{vir(\mu)} \left|\Phi_{mn}^{ef}(\mu)\right\rangle\left\langle\Phi_{mn}^{ef}(\mu)\right| + \ldots \tag{24}$$

where we have explicitly separated contributions from the single, double, and higher excitations with respect to reference $\left|\Phi_\mu\right\rangle$.

3.3.1 SINGLE EXCITATIONS

Introducing the resolution of the identity in the coupling term

$$\left\langle\Phi_i^a(\mu)\left|e^{-\hat{T}^\mu}e^{\hat{T}^\nu}\right|\Phi_\mu\right\rangle \tag{25}$$

we obtain only two non-zero terms. The first term arises from the projection onto $\left|\Phi_\mu\right\rangle$ and is

$$\left\langle\Phi_i^a(\mu)\left|e^{-\hat{T}^\mu}\right|\Phi_\mu\right\rangle\left\langle\Phi_\mu\left|e^{\hat{T}^\nu}\right|\Phi_\mu\right\rangle = -t_i^a(\mu). \tag{26}$$

The second term arises from the singly excited determinants $\left|\Phi_m^e(\mu)\right\rangle$ and is

$$\sum_m^{occ(\mu)} \sum_e^{vir(\mu)} \left\langle\Phi_i^a(\mu)\left|e^{-\hat{T}^\mu}\right|\Phi_m^e(\mu)\right\rangle\left\langle\Phi_m^e(\mu)\left|e^{\hat{T}^\nu}\right|\Phi_\mu\right\rangle = \left\langle\Phi_i^a(\mu)\left|e^{\hat{T}^\nu}\right|\Phi_\mu\right\rangle. \tag{27}$$

Noticing that the exponential can contribute only with terms linear in $\hat{T}_1^{\nu}$ we find that the coupling terms may be expressed as

$$\left\langle \Phi_i^a(\mu) \middle| e^{-\hat{T}^{\mu}} e^{\hat{T}^{\nu}} \middle| \Phi_{\mu} \right\rangle = \left\langle \Phi_i^a(\mu) \middle| \hat{T}_1^{\nu} \middle| \Phi_{\mu} \right\rangle - t_i^a(\mu). \tag{28}$$

Of the t-amplitudes $t_m^e(\nu)$ belonging to $\hat{T}_1^{\nu}$, those that contribute to the first term of Eq. (28) need to satisfy $m \in \mathrm{occ}(\mu)$ and $e \in \mathrm{vir}(\mu)$; otherwise the sequence of operators $\hat{a}_e^+ \hat{a}_m$ would annihilate $\left| \Phi_{\mu} \right\rangle$. Therefore if we introduce the "common" amplitudes of operator $\hat{T}^{\nu}$ with respect to $\hat{T}^{\mu}$

$$t_{ij\ldots}^{ab\ldots}(\nu/\mu) = \begin{cases} t_{ij\ldots}^{ab\ldots}(\nu) & \begin{array}{l} \text{if } i,j,\ldots \in \mathrm{occ}(\mu) \\ \text{and } a,b,\ldots \in \mathrm{vir}(\mu), \end{array} \\ 0 & \text{else} \end{cases} \tag{29}$$

we can write the coupling term for singly excited determinants as

$$\left\langle \Phi_i^a(\mu) \middle| e^{-\hat{T}^{\mu}} e^{\hat{T}^{\nu}} \middle| \Phi_{\mu} \right\rangle = t_i^a(\nu/\mu) - t_i^a(\mu). \tag{30}$$

In the case $\nu = \mu$, the common amplitudes $t_i^a(\nu/\mu)$ correspond to $t_i^a(\mu)$, and the coupling terms are equal to zero.

As mentioned above, the terms arising from the projection onto doubly and higher excited determinants, like $\left\langle \Phi_i^a(\mu) \middle| e^{-\hat{T}^{\mu}} \middle| \Phi_{mn\ldots}^{ef\ldots}(\mu) \right\rangle$, are null. This can be seen easily by realizing that the quantity $e^{-\hat{T}^{\mu}} \middle| \Phi_{mn\ldots}^{ef\ldots}(\mu) \right\rangle$ does not have contributions from singly excited determinants.

3.3.2 DOUBLE EXCITATIONS

After introducing the resolution of the identity in the double excitations coupling element

$$\left\langle \Phi_{ij}^{ab}(\mu) \middle| e^{-\hat{T}^{\mu}} e^{\hat{T}^{\nu}} \middle| \Phi_{\mu} \right\rangle, \tag{31}$$

we get three terms deriving from the reference and the singly and doubly excited determinants. The first term contains contributions only from reference $|\Phi_{\mu}\rangle$

$$\left\langle \Phi_{ij}^{ab}(\mu) \middle| e^{-\hat{T}^{\mu}} \middle| \Phi_{\mu} \right\rangle \left\langle \Phi_{\mu} \middle| e^{\hat{T}^{\nu}} \middle| \Phi_{\mu} \right\rangle = -t_{ij}^{ab}(\mu) + P(ij) t_i^a(\mu) t_j^b(\mu), \tag{32}$$

where we have introduced the permutation operator $P(ij)$ defined as $P(ij)f(i,j) = f(i,j) - f(j,i)$.

The second term derives from singly excited determinants

$$\sum_{m}^{\text{occ}(\mu)} \sum_{e}^{\text{vir}(\mu)} \left\langle \Phi_{ij}^{ab}(\mu) \middle| e^{-\hat{T}^{\mu}} \middle| \Phi_m^e(\mu) \right\rangle \left\langle \Phi_m^e(\mu) \middle| e^{\hat{T}^{\nu}} \middle| \Phi_{\mu} \right\rangle$$
$$= -\sum_{m}^{\text{occ}(\mu)} \sum_{e}^{\text{vir}(\mu)} \left\langle \Phi_{ij}^{ab}(\mu) \middle| \hat{T}_1^{\mu} \middle| \Phi_m^e(\mu) \right\rangle \left\langle \Phi_m^e(\mu) \middle| \hat{T}_1^{\nu} \middle| \Phi_{\mu} \right\rangle, \tag{33}$$

and, after some algebra, it may be simplified to

$$-P(ij)P(ab) t_i^a(\mu) t_j^b(\nu/\mu). \tag{34}$$

The third term arises from doubly excited determinants and may be compactly written as

$$\sum_{m<n}^{\text{occ}(\mu)} \sum_{e<f}^{\text{vir}(\mu)} \left\langle \Phi_{ij}^{ab}(\mu) \middle| e^{-\hat{T}^{\mu}} \middle| \Phi_{mn}^{ef}(\mu) \right\rangle \left\langle \Phi_{mn}^{ef}(\mu) \middle| e^{\hat{T}^{\nu}} \middle| \Phi_{\mu} \right\rangle = \left\langle \Phi_{ij}^{ab}(\mu) \middle| \hat{T}_2^{\nu} + \frac{1}{2}\left(\hat{T}_1^{\nu}\right)^2 \middle| \Phi_{\mu} \right\rangle. \tag{35}$$

Using the "common" amplitudes as introduced above, Eq. (35) may be cast in closed form. The final expression for the double excitation coupling terms is then

$$\left\langle \Phi_{ij}^{ab}(\mu) \middle| e^{-\hat{T}^\mu} e^{\hat{T}^\nu} \middle| \Phi_\mu \right\rangle = -t_{ij}^{ab}(\mu) + P(ij)t_i^a(\mu)t_j^b(\mu)$$
$$-P(ij)P(ab)t_i^a(\mu)t_j^b(\nu/\mu)$$
$$+t_{ij}^{ab}(\nu/\mu) + P(ij)t_i^a(\nu/\mu)t_j^b(\nu/\mu) \qquad (36)$$
$$= C_{ij}^{ab}(\mu,\nu) - t_{ij}^{ab}(\mu).$$

To compact the equations in the next section, we have introduced the $C_{ij}^{ab}(\mu,\nu)$ tensors composed of all terms on the right side of Eq. (36) except $-t_{ij}^{ab}(\mu)$. In the actual computational scheme, the $C_{ij}^{ab}(\mu,\nu)$ *are not required to be formed or stored at all.*

3.3.3 AMPLITUDE EQUATIONS

Using the coupling terms derived in the previous two sections, it is possible to write the MkCCSD *t*-amplitude equations [Eq. (17)] in a more suitable form for implementation in a computer program. The single excitation *t*-amplitudes then satisfy

$$\Delta_i^a(\mu) = \left\langle \Phi_i^a(\mu) \middle| \bar{H}_\mu \middle| \Phi_\mu \right\rangle c_\mu^{(\alpha)} + \sum_{\nu(\neq\mu)} \left[t_i^a(\nu/\mu) - t_i^a(\mu) \right] H_{\mu\nu}^{\mathrm{eff}} c_\nu^{(\alpha)} = 0 \quad (\mu = 1,2,\ldots,d), \qquad (37)$$

while the double excitations equation can be written using the $C_{ij}^{ab}(\mu,\nu)$ tensors introduced above as

$$\Delta_{ij}^{ab}(\mu) = \left\langle \Phi_{ij}^{ab}(\mu) \middle| \bar{H}_\mu \middle| \Phi_\mu \right\rangle c_\mu^{(\alpha)} + \sum_{\nu(\neq\mu)} \left[C_{ij}^{ab}(\mu,\nu) - t_{ij}^{ab}(\mu) \right] H_{\mu\nu}^{\mathrm{eff}} c_\nu^{(\alpha)} = 0 \quad (\mu = 1,2,\ldots,d). \qquad (38)$$

The *t*-amplitude residuals $\Delta_i^a(\mu)$ and $\Delta_{ij}^{ab}(\mu)$ introduced in Eqs. (37) and (38) vanish only at convergence. The quantities $\left\langle \Phi_i^a(\mu) \middle| \bar{H}_\mu \middle| \Phi(\mu) \right\rangle$ and $\left\langle \Phi_{ij}^{ab}(\mu) \middle| \bar{H}_\mu \middle| \Phi(\mu) \right\rangle$ are projections of the similarity-transformed Hamiltonian for the CCSD case and are already available from SRCCSD theory (see Supplementary Material).[91] Eqs. (37) and (38) can be used in an iterative procedure to obtain the converged *t*-amplitudes, using the formulas

$$t_i^a(\mu, \text{new}) = t_i^a(\mu, \text{old}) + \frac{\Delta_i^a(\mu)}{f_{ii}(\mu) - f_{aa}(\mu) + E^{(\alpha)} - H_{\mu\mu}^{\text{eff}}}, \tag{39}$$

and

$$t_{ij}^{ab}(\mu, \text{new}) = t_{ij}^{ab}(\mu, \text{old}) + \frac{\Delta_{ij}^{ab}(\mu)}{f_{ii}(\mu) + f_{jj}(\mu) - f_{aa}(\mu) - f_{bb}(\mu) + E^{(\alpha)} - H_{\mu\mu}^{\text{eff}}}. \tag{40}$$

In these expressions the Fock matrix elements $[f_{pq}(\mu)]$ are computed with respect to vacuum $|\Phi_\mu\rangle$ as

$$f_{pq}(\mu) = h_{pq} + \sum_{k}^{\text{occ}(\mu)} \left[(pq \mid kk) - (pk \mid qk)\right] \tag{41}$$

from the one electron integrals h_{pq} and the standard two electron integrals $(pq \mid rs)$.

We have observed very robust convergence, although at times slow, using Eqs. (39) and (40). In cases where the coefficients $c_\mu^{(\alpha)}$ do not approach zero, convergence is often accelerated by making the substitutions $\Delta_i^a(\mu) \rightarrow \Delta_i^a(\mu)/c_\mu^{(\alpha)}$ and $\Delta_{ij}^{ab}(\mu) \rightarrow \Delta_{ij}^{ab}(\mu)/c_\mu^{(\alpha)}$ in Eqs. (39) and (40). Moreover, since the residuals vanish at convergence, the denominators in these update equations may be arbitrarily shifted to damp large variations in the t-amplitudes, especially in the first few iterations. Denominator shifting was not required in any of our examples, however it was previously found to be necessary to converge calculations on model systems.[62]

3.4 IMPLEMENTATION

We have implemented the multireference MkCC equations within a new coupled cluster program PSIMRCC developed at the University of Georgia and interfaced to the package Psi 3.2.3.[92] Molecular orbitals were generated using the code DETCAS by Sherrill,[93] and the integral transformation was performed by the routine TRANSQT, by Crawford, Sherrill, and Fermann.[92] The similarity-transformed Hamiltonian matrix elements were coded from spin-factored CCSD equations for an unrestricted reference. These matrix elements were derived from the corresponding spin-orbital equations,[64] as given in the Supplementary Material.[91] The coupling terms for the Mukherjee equations were coded according to Eqs. (30) and (36).

One of the advantages of using an unrestricted formulation is that it allows open-shell configurations to be treated. Thus, the present implementation is not restricted to the simplified case of a zeroth-order wave function composed of two closed-shell determinants. Currently, we can treat wave functions with references of the type CAS(1, m) and CAS(2, m) ($m = 2$, 3, …), where the first integer represents the number of electrons, while the second indicates the number of active orbitals.

The treatment of CAS(n, m) zeroth-order wave functions with $n > 2$ requires the computation of matrix elements of the effective Hamiltonian

$$H_{\nu\mu}^{\text{eff}} = \left\langle \Phi_\nu \left| \hat{H} e^{\hat{T}_1^\mu + \hat{T}_2^\mu} \right| \Phi_\mu \right\rangle, \tag{42}$$

that for certain references μ and ν requires projections of the SRCCSD equations on excitations higher than double. For a generic number of electrons in a CAS space, the connected nature of $H_{\nu\mu}^{\text{eff}}$ dictates that sextuple excitations are the highest projection of the SRCCSD equations required to construct $H_{\nu\mu}^{\text{eff}}$.[94] The coding of these higher terms (T, Q, P, and H) is very involved,

and the automatic derivation and implementation would represent a better solution.[95] Perhaps the use of an incomplete model space in conjunction with the *C*-conditions of Li and Paldus,[52-55,73] or the formulation of MkCC for incomplete model spaces by Pahari *et al*.[86] would be acceptable compromises. In any case the solution of this problem is beyond the scope of this research.

The computational scaling of Eqs. (37) and (38) has a leading term identical to the case of SRCCSD (O^2V^4) multiplied by the number of reference determinants d. The computation of the coupling terms does not alter the scaling since these require only $d(d-1)\left(OV + 9O^2V^2\right)$ operations approximately. Our program does take advantage of symmetry, although only through restrictions on the loops.

Our implementation of MkCCSD, BWCCSD, and apBWCCSD was benchmarked against our earlier reported arbitrary-order program DETC++,[62] based on a string expansion of the wave function. DETC++ is a pilot code limited to computations on systems containing few electrons and small basis sets. However, DETC++ proved to be a powerful tool for understanding of the effect of higher-excitations in multireference theories,[62] and also for debugging purposes. To further validate our production-level PSIMRCC code, we tested it against independent numerical results available in the literature.[57,75,87,96]

3.5 ORBITAL ROTATION ISSUES

Orbital rotation issues add intricacies to multireference coupled cluster computations. In the simple case of an active space involving two electrons in two orbitals, *three* reference configurations must be carefully considered,

$$\left|\Phi_1\right\rangle = \left|(\text{core})^2(\text{valence})^2 x\bar{x}\right\rangle$$

$$\left|\Phi_2\right\rangle = \left|(\text{core})^2(\text{valence})^2 y\bar{y}\right\rangle \qquad (43)$$

$$\left|\Phi_3\right\rangle = \frac{1}{\sqrt{2}}\left|(\text{core})^2(\text{valence})^2\left(x\bar{y}-\bar{x}y\right)\right\rangle,$$

where $(\text{core})^2$ and $(\text{valence})^2$ denote the doubly occupied core and valence orbitals, respectively, while (x, y) is the (HOMO, LUMO) orbital pair involved in the CAS(2,2) computations. A normalized zeroth-order wave function

$$\left|\Psi_0\right\rangle = c_1'\left|\Phi_1\right\rangle + c_2'\left|\Phi_2\right\rangle + c_3'\left|\Phi_3\right\rangle, \qquad (44)$$

can always be cast in the mathematically equivalent form

$$\left|\Psi_0\right\rangle = c_1\left|(\text{core})^2(\text{valence})^2 u\bar{u}\right\rangle + c_2\left|(\text{core})^2(\text{valence})^2 v\bar{v}\right\rangle, \qquad (45)$$

by the orbital rotation

$$\begin{pmatrix} u \\ v \end{pmatrix} = \begin{pmatrix} \cos\theta & \sin\theta \\ \sin\theta & -\cos\theta \end{pmatrix}\begin{pmatrix} x \\ y \end{pmatrix}, \qquad (46)$$

where

$$\tan 2\theta = \frac{\sqrt{2}c_3'}{c_1'-c_2'}, \qquad (47)$$

without changing the zeroth-order energy.[97,98] In other words, the open-shell singlet configuration $\left|\Phi_3\right\rangle$ can be removed from $\left|\Psi_0\right\rangle$ by an orbital rotation that leaves the zeroth-order energy invariant. The CI coefficients of the two forms of $\left|\Psi_0\right\rangle$ are related by

$$c_1 = \frac{S+1}{\sqrt{2\left(1+S^2\right)}}, \quad \text{and} \quad c_2 = \frac{S-1}{\sqrt{2\left(1+S^2\right)}}, \qquad (48)$$

where

$$S = \pm \frac{c_1' + c_2'}{\sqrt{\left(c_1' - c_2'\right)^2 + 2c_3'^2}} \, . \tag{49}$$

While MRCC wave functions of the JM form of Eq. (4) are invariant to orbital rotations within the **FC**, **DO**, and **E** spaces, the active-space rotations (**A**) given by Eq. (46) do change the MRCC wave function and energy. Thus, the open-shell singlet configuration $|\Phi_3\rangle$ cannot generally be neglected as a reference in MRCC computations of dynamical electron correlation. If (x, y) are of different symmetry, then $|\Phi_3\rangle$ has a coefficient $c_3^{(\alpha)} = 0$ in Eq. (4); accordingly, all determinants generated by $e^{\hat{T}^3} |\Phi_3\rangle$ do not contribute to the MRCC wave function. However, this situation does not persist if orbitals x and y take the same symmetry, either by means of a geometric distortion to a lower point group or by an orbital rotation which localizes the active space orbitals. Under such circumstances even if the orbitals are rotated so that $|\Phi_3\rangle$ does not contribute to the CASSCF wave function from which the orbitals are derived, the solutions of the MRCC equations will generally have a nonzero coefficient $c_3^{(\alpha)}$ in the final wave function, as well as contributions from excited determinants generated by $e^{\hat{T}^3} |\Phi_3\rangle$. Therefore, the most consistent MRCC treatment for general canonicalizations of the CASSCF orbitals or for the computation of vibrational frequencies for symmetry-lowering normal modes would include all three configurations (four determinants) of Eq. (43) in the model space.

Two common approaches for uniquely defining the active-space orbitals, and hence the MRCC wave function, are (1) diagonalizing the CASSCF one-particle density matrix to obtain natural orbitals and (2) diagonalizing the average Fock matrix

$$\varepsilon_{ij}' = h_{ij} + \sum_k^{occ} f_k \left[2(ij \mid kk) - (ik \mid jk) \right], \tag{50}$$

within the active space.[99,100] In Eq. (50) f_k is the fractional occupation of each molecular orbital

k, *i.e.*, $f_k = 1$ in the **FC** and **DO** spaces, whereas $f_k = c_1^2$ or c_2^2 for active orbitals u and v in Eq.

(45). The other quantities in Eq. (50) are standard one-electron (h_{ij}) and two-electron repulsion

$[(ij\,|\,kk),\ (ik\,|\,jk)]$ integrals. In the case of a two-electron / two-orbital active space, the use of

CASSCF natural orbitals always eliminates the open-shell singlet configuration in $|\Psi_0\rangle$ and

casts the reference wave function into the form of Eq. (45). This choice of orbitals (u, v) provides

a convenient starting point for specifying more general choices of active-space orbitals (x, y) by

means of a single rotation angle θ, according to Eq. (46). In the F_2 and O_3 applications to follow,

we investigate the important question of the dependence of MRCC total energies and molecular

properties on the orbital rotation angle θ.

3.6 APPLICATIONS

3.6.1 F_2

The computation of the entire potential energy curve of ground-state molecular fluorine

represents a very challenging problem for *ab initio* theories. The multireference character of the

system at large distances and the presence of low-lying intruder states are known to be the major

causes of incorrect or inaccurate theoretical predictions.[96] Numerous many-body theories have

been applied to F_2. A nice tabulation of spectroscopic constants of F_2 obtained from a plethora of

earlier *ab initio* studies appears in a 2001 paper by Pittner and co-workers.[57] Focusing here only

on multireference methods, the most recent investigations have employed BWCC,[57,77,96] various

CC-corrections to MRCI,[101] MkPT,[82] MkCC,[3] CAS(2,2)CCSD[102] and SS-MRCEPA.[103]

Both the F_2 molecule at its equilibrium geometry (r_e = 1.412 Å)[104] and the open-shell fluorine atom are single-reference problems. However, when F_2 is stretched, the highest occupied molecular orbital (HOMO) $3\sigma_g$ and the lowest unoccupied molecular orbital (LUMO) $3\sigma_u$ become quasidegenerate. Therefore, a correct description at intermediate geometries ($r_e < r < \infty$) requires a zeroth-order wave function that is a linear combination of two closed-shell determinants,

$$\left|\Phi_1\right\rangle = \left|(core)2\sigma_g^2 2\sigma_u^2 1\pi_u^4 1\pi_g^4 3\sigma_g^2\right\rangle, \tag{51}$$

and

$$\left|\Phi_2\right\rangle = \left|(core)2\sigma_g^2 2\sigma_u^2 1\pi_u^4 1\pi_g^4 3\sigma_u^2\right\rangle. \tag{52}$$

Table 3.1 shows the ground-state properties of F_2 computed at the SRCCSD, SRCCSDT, MkCCSD, BWCCSD, and apBWCCSD levels using the series of correlation-consistent basis sets of Dunning[105] (cc-pVXZ, X = D, T, Q) together with values extrapolated to the complete basis set limit. For the extrapolation, the total electronic energy was partitioned into two terms. The first one corresponds to the total SCF or CASSCF energy and was fitted to the functional form[106]

$$E_{SCF/CASSCF}(X) = A + Be^{-CX}, \tag{53}$$

where X is the cardinal number corresponding to the maximum angular momentum of the basis set. The correlation energy was extrapolated using the formulas[107]

$$E_{SRCC}(X) - E_{SCF}(X) = A + BX^{-3}, \tag{54}$$

and

$$E_{MRCC}(X) - E_{CASSCF}(X) = A + BX^{-3}. \tag{55}$$

Table 3.1. Single- and multireference coupled cluster results for the electronic ground state of F_2.[a]

Theory	Basis Set	r_e (Å)	D_e (kcal mol^{-1})[b,c]	ω_e (cm^{-1})
Single Reference	cc-pVDZ	1.4320	22.2 [52.8]	885
CCSD	cc-pVTZ	1.3946	28.2 [68.4]	1012
	cc-pVQZ	1.3906	29.7 [72.6]	1016
	∞	1.3868	30.7 [75.0]	1026
Single Reference	cc-pVDZ	1.4577	27.3 [27.8]	787
CCSDT	cc-pVTZ	1.4154	34.6 [35.9]	923
	cc-pVQZ	1.4124	36.5 [38.1]	925
	∞	1.4089	37.7 [38.5]	935
Mukherjee	cc-pVDZ	1.4548	31.7 (28.2)	793
CCSD	cc-pVTZ	1.4127	39.4 (35.1)	925
	cc-pVQZ	1.4093	41.2 (37.1)	926
	∞	1.4057	42.6 (38.5)	934
Brillouin-Wigner	cc-pVDZ	1.4469	37.6 (18.9)	821
CCSD	cc-pVTZ	1.4060	46.8 (22.3)	953
	cc-pVQZ	1.4024	49.0 (23.4)	955
	∞	1.3988	50.8 (24.1)	963
A Posteriori BW	cc-pVDZ	1.4681	25.0 (38.4)	749
CCSD	cc-pVTZ	1.4236	30.2 (49.4)	880
	cc-pVQZ	1.4206	31.2 (52.7)	881
	∞	1.4172	31.8 (55.0)	888
Experiment		1.41193[d]	38.3[e]	917[d]

[a] Single-reference coupled cluster results computed with canonical ($D_{\infty h}$) Hartree-Fock orbitals; multireference coupled cluster results computed with CAS(2,2) orbitals. Core orbitals frozen in all computations.

[b] Single-reference coupled cluster dissociation energies used twice the energy of an individual F atom as the endpoint. Supermolecule results obtained by continuous elongation of the internuclear distance in F_2 are listed in brackets. In the supermolecule approach an internuclear separation of only (25 bohr, 8 bohr) was used for (SRCCSD, SRCCSDT) to avert convergence difficulties, but these distances are sufficient to recover the dissociation limit to within 0.1 kcal mol^{-c}.

[c] For the multireference methods, the dissociation energy computations employed a supermolecule with an internuclear separation of 100 bohr as the endpoint. Values obtained from ($D_{\infty h}$, delocalized) CAS(2,2) natural orbitals at the listed optimum bond distances are listed first, whereas values in parentheses were determined from single-point computations with ($C_{\infty v}$, localized) CAS(2,2) orbitals and with inclusion of the third, open-shell singlet reference.

[d] Reference 104.

[e] Derived from Reference 110. See text for details.

The primary SRCCSD and SRCCSDT dissociation energies reported in Table 3.1 were computed with respect to the fragments as

$$D_e = 2E(\text{F}) - E(\text{F}_2),$$ (56)

using the ACES2 program suite.[108,109] The experimental value of D_e was determined from the spectroscopic constants tabulated by Herzberg[104] and the D_0 measured by Yang *et. al.*[110] The zero-point vibrational energy (ZPVE) was computed as

$$\text{ZPVE} = G_0 + \frac{\omega_e}{2} - \frac{\omega_e x_e}{4},$$ (57)

where the G_0 term[104,111] is given by

$$G_0 = \frac{B_e}{4} + \frac{\alpha_e \omega_e}{12 B_e} + \frac{\alpha_e^2 \omega_e^2}{12 B_e^3} - \frac{\omega_e x_e}{4}.$$ (58)

The largest basis set (cc-pVQZ) and the complete basis set extrapolated values show that SRCCSD, SRCCSDT, MkCCSD and BWCCSD intrinsically underestimate the F-F bond length while apBWCCSD overestimates it. Among the MRCC methods, the MkCCSD prediction for the bond length is the closest to the experimental value, with an error of −0.0062 Å. By comparison, BWCCSD predicts a bond length with an error of −0.0131 Å. The SRCCSDT results indicate that triple excitations are essential for accurate prediction of the molecular geometry.

In the complete basis set (CBS) limit, SRCCSD overestimates the harmonic frequency by more than 100 cm^{-1}. BWCCSD and apBWCCSD respectively overestimate and underestimate the frequency by 46 cm^{-1} and 29 cm^{-1}, while MkCCSD is within 17 cm^{-1} of the experimental value. Triple excitations correct the problem in SRCCSD and in the CBS limit deliver a

SRCCSDT result within $20\ cm^{-1}$ of experiment, and virtually identical to MkCCSD. The vibrational frequencies show similar behavior to the dissociation energy.

The dissociation potential curves of F_2 computed with SRCCSD, MkCCSD, BWCCSD, and apBWCCSD using the triple-zeta correlation-consistent basis set (cc-pVTZ) of Dunning,[105] delocalized ($D_{\infty h}$) CAS(2,2) natural orbitals, and freezing the fluorine core are depicted in Fig. 3.1. The SRCCSD curve was computed using $|\Phi_1\rangle$ as the reference, while for all the MRCC methods
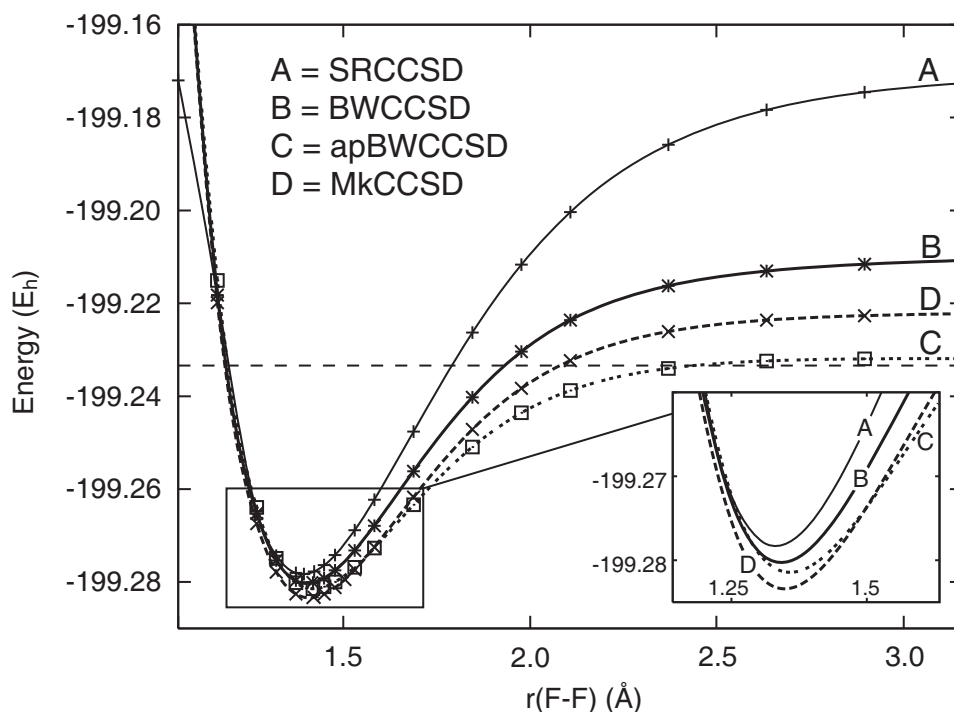
Figure 3.1. Dissociation curve of F_2 computed with the SRCCSD, MkCCSD, BWCCSD, and apBWCCSD methods using the cc-pVTZ basis set and delocalized ($D_{\infty h}$) CAS(2,2) natural orbitals. Twice the corresponding ROHF-SRCCSD energy of the F atom is shown as a dotted line at $-199.233339\ E_h$.

the zeroth-order wave function contains $|\Phi_1\rangle$ and $|\Phi_2\rangle$. None of the curves shows any divergence or singularities, but the quantitative results are considerably different. For example, SRCCSD overestimates the dissociation energy of F_2 almost by a factor of two. For the MRCC

methods, there are no unphysical barriers in the dissociation curves such as that encountered with CASPT2 theory near r(F-F) = 3 Å.[96] However, MkCCSD is the only multireference theory to predict an accurate dissociation energy with the cc-pVTZ basis set (39.4 kcal mol^{-1}) as compared to experiment (38.3 kcal mol^{-1}). The cc-pVTZ BWCCSD and apBWCCSD results are more than 8 kcal mol^{-1} too large and small, respectively. The failure of BWCCSD to represent the dissociation curve as accurately as MkCCSD is likely due to the lack of size extensivity in BWCC. In this regard, apBWCCSD apparently overestimates the size-extensivity correction to BWCCSD.

We performed a more detailed examination of the dissociation energy of F_2, obtaining the collection of D_e entries in Table 3.1. Single-reference CCSD is seen to have an enormous size-consistency (not size-extensivity) error.[112-114] Focusing on the complete basis set CCSD extrapolations, continuous elongation of the F-F distance yields D_e = 75.0 kcal mol^{-1} as the supermolecule limit, as compared to 30.7 kcal mol^{-1} from twice the energy of an individual F atom. Full inclusion of triple excitations reduces the size-consistency error to only 0.8 kcal mol^{-1}, and CBS single-reference CCSDT theory gives a dissociation energy within 1 kcal mol^{-1} of experiment. Of the multireference methods of concern in Table 3.1, only MkCCSD is rigorously size extensive. However, MkCCSD only becomes size consistent if the orbitals are localized on the fragments in the separated atom limit, in which case the MkCCSD energy obtained from localized CAS(2,2) orbitals is twice the single-reference CCSD energy of the F atom using ROHF orbitals. To investigate the effect of orbital localization and size-consistency errors on the predicted dissociation energies, all MkCCSD, BWCCSD, and apBWCCSD values were computed both with delocalized ($D_{\infty h}$) CAS(2,2) natural orbitals (u, v) and with corresponding fragment-localized ($C_{\infty v}$) orbitals (x, y) obtained by a $\theta = 45°$ rotation in Eq. (46).

Because the localization removes the inversion symmetry of the active-space orbitals (but not of the overall wave function), all computations with $\theta = 45°$ canonicalization were executed in C_{2v} symmetry with the inclusion of the open-shell singlet reference $|\Phi_3\rangle$ in Eq. (43). Since all of our MRCC methods are invariant to orbital rotations within the **FC**, **DO**, and **E** spaces, it is not necessary to explicitly localize the orbitals outside the active space.

The importance of using large basis sets and extrapolations to the CBS limit to assess the accuracy of the MRCC dissociation energies is abundantly clear in Table 3.1. For example, the BWCCSD D_e value (with $D_{\infty h}$ orbitals) of 37.6 kcal mol^{-1} with the cc-pVDZ basis set is within 1 kcal mol^{-1} of experiment, but the corresponding CBS limit of $D_e = 50.8$ kcal mol^{-1} is over 12 kcal mol^{-1} too large. An appealing characteristic of MkCCSD theory is that D_e changes only about 4 kcal mol^{-1} with orbital localization. With delocalized orbitals, CBS MkCCSD gives $D_e = 42.6$ kcal mol^{-1}, which is 4.3 kcal mol^{-1} above experiment. However, if the size consistency error is removed by localizing the active-space orbitals, then CBS MkCCSD yields a dissociation energy remarkably close (within 0.2 kcal mol^{-1}) of experiment. To demonstrate that this high accuracy is not a fluke, we re-computed r_e and ω_e at the CBS MkCCSD level with localized orbitals and obtained 1.4134 Å and 915 cm^{-1}, respectively, again in almost perfect agreement with the experimental values of 1.41193 Å and 917 cm^{-1}. In contrast to MkCCSD, the CBS (BWCCSD, apBWCCSD) dissociation energies are (decreased, increased) by more than 20 kcal mol^{-1} if the size consistency errors are removed by localizing the active-space orbitals.[115] Moreover, neither of the Brillouin-Wigner methods yields a satisfactory dissociation energy in the CBS limit, regardless of whether the active-space orbitals are localized or not. The best performance of these methods is delivered by CBS apBWCCSD with delocalized orbitals (31.8 kcal mol^{-1} vs. 38.3 kcal mol^{-1} from expt.). The only way to achieve good agreement with

experiment for the BW methods would be to artificially vary the orbital rotation angle θ as a function of bond distance.

In summary, MkCCSD provides excellent results for r_e, D_e, and ω_e of F_2 and is superior to the other multireference coupled cluster methods tested here. In particular, our complete basis set results show that MkCCSD is the only theory among the MRCC methods to deliver accurate energetics for the dissociation of F_2. If localized orbitals are employed to remove size-consistency errors, CBS MkCCSD predicts an extremely accurate dissociation energy. While this success does not appear to be fortuitous, more studies are required to determine if such agreement is a general occurrence.

3.6.2 OZONE

Over the years, ozone has become a graveyard for electronic structure theories, in large part because it requires a multireference zeroth-order wave function *and* rigorous accounting of dynamical electron correlation for the accurate prediction of molecular properties. A recent paper by Hino and co-workers[116] provides an excellent summary of the long saga[12,76,99,117-143] of *ab initio* methods applied to the ozone problem. Notably, the ordering of the fundamental vibrational frequencies for the two stretching modes is incorrectly predicted by many theoretical methods. Unrestricted Hartree-Fock (UHF),[129] two-configuration self-consistent-field (TCSCF),[123] CASSCF,[120,126] second- and third-order restricted Møller-Plesset perturbation theory,[129] configuration interaction with single and double excitations (CISD), and multireference CISD (MRCISD),[99] all incorrectly predict the antisymmetric stretch (ω_3, expt. 1089 cm^{-1}) to be higher in frequency than the symmetric stretch (ω_1, expt. 1135 cm^{-1}).[122]

Single-reference coupled cluster methods yield accurate predictions of the molecular geometry and vibrational frequencies of ozone only when iterative or perturbative triple excitations are included.[128,131,134] It is also maintained that the inclusion of quadruple excitations is essential for quantitative agreement with experiment. When quadruples are accounted for via the approximate CCSDT(Q$_f$) method, ω_1 and ω_3 are reduced by ca. 30 cm^{-1} and 5 cm^{-1}, respectively, relative to the CCSDT results, bringing all the frequencies within 22 cm^{-1} of the experimental values.[135] Other approaches applied to ozone and based on the coupled cluster ansatz include the Bruckner-orbital B-CCD and B-CCD(T) approximations,[136-138] equation-of-motion coupled cluster (EOM-CC),[141,142] reduced MRCC methods,[12] and tailored coupled cluster.[116]

Ozone was also the subject of a previous apBWCCSD study by Hubač, Pittner, and Čársky.[76] These authors computed the structure and vibrational frequencies at the apBWCCSD/cc-pVTZ level of theory using RHF orbitals. Quite satisfactory results were obtained for the O-O distance (1.280 Å), the O-O-O angle (116.3°), ω_1 (1095 cm^{-1}), and ω_2 (703 cm^{-1}), all of which we were able to confirm with our independent computer codes. However, Hubač *et al.*[76] also reported an anomalously large antisymmetric stretching frequency of ω_3 = 1505 cm^{-1} at the same level of theory. The vibrational frequencies were computed numerically, and for the C_s displacements the open-shell configuration $\left| \Phi_3 \right\rangle$ of Eq. (43) was not included in the zeroth-order wave function. This omission has a large effect on the predicted value of ω_3. In particular when we execute an apBWCCSD/cc-pVTZ computation of ω_3 using RHF orbitals and including $\left| \Phi_3 \right\rangle$ as a reference, we find ω_3 = 386 i cm^{-1}.

In one of the most recent theoretical papers on ozone,[116] the tailored CCSD method (TCCSD) of Bartlett and co-workers[144] was used to compute the molecular structure and

harmonic vibrational frequencies of this troublesome species. The TCCSD scheme employs a single-reference framework but explicitly divides the cluster operator ($\hat{T}$) into a dynamic ($\hat{T}^{\text{ext}} = \hat{T}_1^{\text{ext}} + \hat{T}_2^{\text{ext}}$) and a nondynamic part ($\hat{T}^{\text{CAS}}$). The smallest $\hat{T}^{\text{CAS}}$ giving a correct description of the electronic ground state employed a CAS(12,9) space involving the $2p$ orbitals of each oxygen atom. Using this CAS(12,9) space for both orbital optimization and for fixing $\hat{T}^{\text{CAS}}$, the TCCSD method gave the stretching frequencies (ω_1, ω_3) = (1089, 1030) cm^{-1} and (1137, 1098) cm^{-1} with the cc-pVDZ and cc-pVTZ basis sets, respectively. The latter results are removed from experiment by only (+2, +9) cm^{-1}; however, this excellent agreement would diminish somewhat if a larger basis set were used.

The problematic ozone system provides a valuable benchmark for the performance of the MRCC methods we have implemented. The zeroth-order wave function we have used in our MRCC computations to describe the ground state of ozone in C_{2v} symmetry is composed of the two closed-shell determinants

$$
\begin{aligned}
\left|\Phi_1\right\rangle &= \left|(\text{core})^2 3a_1^2 2b_2^2 4a_1^2 5a_1^2 3b_2^2 1b_1^2 4b_2^2 6a_1^2 1a_2^2\right\rangle \\
\left|\Phi_2\right\rangle &= \left|(\text{core})^2 3a_1^2 2b_2^2 4a_1^2 5a_1^2 3b_2^2 1b_1^2 4b_2^2 6a_1^2 2b_1^2\right\rangle,
\end{aligned}
\tag{59}
$$

which contribute to the wave function ca. 90% ($\left|\Phi_1\right\rangle$) and 10% ($\left|\Phi_2\right\rangle$), respectively, at the equilibrium geometry. In Table 3.2 we report the geometry and harmonic vibrational frequencies of the ground state of ozone computed with SRCCSD, SRCCSD(T), SRCCSDT, MkCCSD, BWCCSD, and apBWCCSD using the cc-pVXZ (X = D, T, Q) basis sets and freezing the oxygen $1s$ orbitals. With the largest basis (cc-pVQZ), single-reference coupled cluster with singles and doubles underestimates the O-O bond length by 0.034 Å. This result is improved by inclusion of perturbative and iterative triples, reducing the error to −0.009 Å for the case of CCSD(T). The

cc-pVQZ MkCCSD method predicts the O-O distance with an error of −0.019 Å, while for BWCCSD the error is larger, −0.024 Å. The *a posteriori* BWCCSD correction causes the O-O bond to elongate, giving an error of −0.012 Å. For the bond angle of ozone, the cc-pVQZ CCSD(T), CCSDT, MkCCSD, and BWCCSD values are all within 0.3° of experiment. The corresponding CCSD and apBWCCSD angles are 0.8° and 0.9° too large and small, respectively.

The vibrational frequency data in Table 3.2 show again the necessity of using large basis sets in assessing intrinsic errors for theoretical methods. For all coupled cluster methods, the ω_1 values increase significantly in going from the cc-pVDZ to the cc-pVQZ basis set, revealing larger inherent errors with respect to the experimental harmonic frequencies. For example, the cc-pVDZ MkCCSD ω_1 prediction is only 11 cm^{-1} larger than experiment, but the corresponding cc-pVQZ frequency is 63 cm^{-1} too large. For the symmetric O-O stretch and O-O-O bend, all multireference methods substantially improve upon the CCSD predictions. Specifically, with the cc-pVQZ basis set, the CCSD (ω_1, ω_2) errors of (14.0%, 7.7%) are reduced to (8.9%, 5.7%) with BWCCSD, to (5.6%, 4.5%) with MkCCSD, and finally to (1.3%, 3.2%) with apBWCCSD. In this comparison MkCCSD is superior to BWCCSD, but apBWCCSD is the best of the three MRCC methods, approaching SRCCSD(T) in accuracy.

In C_{2v} symmetry, the HOMO ($1a_2$) and LUMO ($2b_1$) belong to different irreducible representations (irreps), and the open-shell singlet configuration $|\Phi_3\rangle$ of Eq. (43) does not contribute to the electronic wave function. However, displacements along the antisymmetric stretching mode lower the point group to C_s, and the irrep of both the HOMO and LUMO becomes a''. In order to compute ω_3 properly, $|\Phi_3\rangle$ must be added as a reference, and orbital canonicalization becomes an issue, as discussed in Section IV.
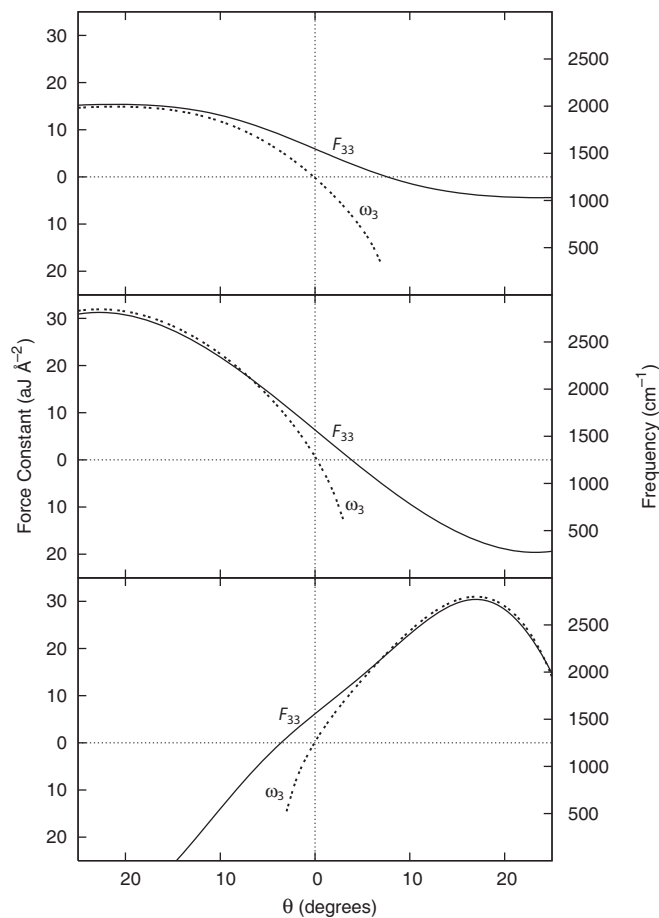
Figure 3.2. Ozone harmonic vibrational frequency (ω_3) and diagonal force constant (F_{33}) for the antisymmetric stretching coordinate [$S_3 = \frac{1}{\sqrt{2}}\left(r_{OO} - r'_{OO}\right)$] computed using the cc-pVDZ basis set and with CAS(2,2) natural orbitals rotated according to Eq. (46).

We investigated the sensitivity of the antisymmetric stretching frequency of ozone to orbital canonicalization by computing MkCCSD, BWCCSD, and apBWCCSD values for ω_3 and F_{33} [the quadratic force constant for internal coordinate $S_3 = \frac{1}{\sqrt{2}}\left(r_{OO} - r'_{OO}\right)$] as a function of the orbital rotation angle θ in Eq. (46). All three references in Eq. (43) were employed for all MRCC methods uniformly as a function of S_3. To clarify the θ dependence, the orbital rotation angle was fixed, independent of the value of S_3, and all computations were thus executed in C_s symmetry. The plots in Fig. 3.2 reveal a surprisingly strong dependence of ω_3 and F_{33} on θ, one that is most

100

pronounced in the BWCCSD and apBWCCSD cases but is still substantial with the MkCCSD method. It is striking that the experimental $\omega_3 = 1089 \text{ cm}^{-1}$ value can be reproduced with cc-pVDZ (BWCCSD, apBWCCSD, MkCCSD) computations merely by selecting $\theta = (1.0°, -1.0°, 1.6°)$ in the orbital canonicalization. More disturbing is the onset of imaginary ω_3 values at $\theta = (3.9°, -3.6°, 7.6°)$ for the cc-pVDZ (BWCCSD, apBWCCSD, MkCCSD) methods.
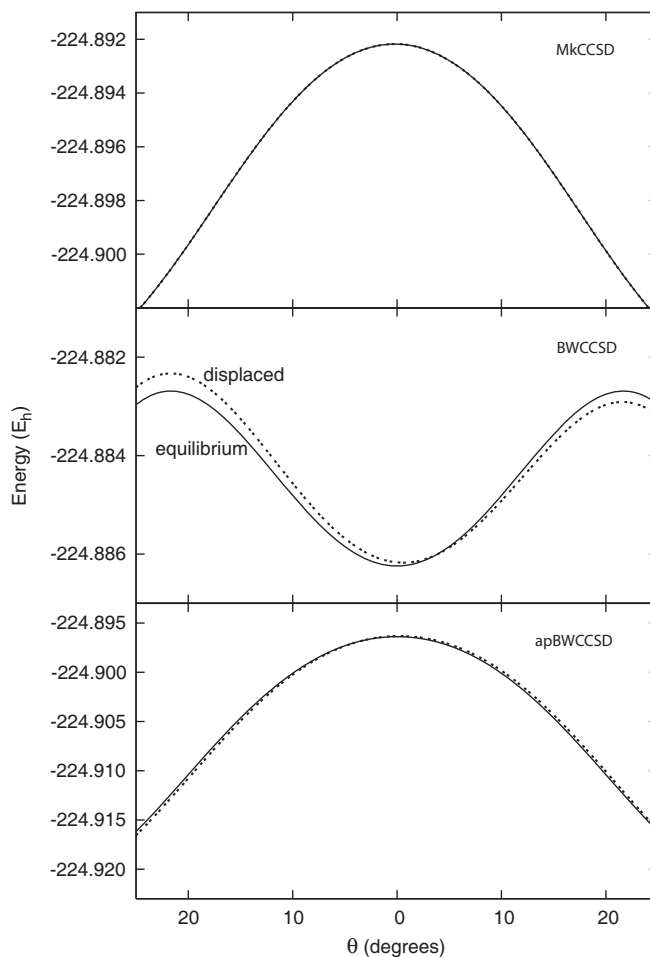
Figure 3.3. Effect of orbital rotation on the total MRCC energies of equilibrium and antisymmetrically displaced $[\, S_3 = \frac{1}{\sqrt{2}}(r_{OO} - r'_{OO}) = 0.01 \text{Å}\,]$ ozone computed using the cc-pVDZ basis set and with CAS(2,2) natural orbitals rotated according to Eq. (46).

In Fig. 3.3 the effect of θ on the total MRCC energies is shown for both the equilibrium structure and the geometry with S_3 displaced by 0.01 Å. All methods are approximately stationary with respect to orbital rotations near $\theta = 0$. Stationary values for the energy ($dE/d\theta = 0$) at the (equilibrium, displaced) geometries are found for MkCCSD when $\theta = (0°, -0.2°)$, $\theta = (0°, 0.6°)$ for BWCCSD, and $\theta = (0°, 0.2°)$ for apBWCCSD. However, small deviations of θ from zero substantially (raise, lower, lower) the total energies at the cc-pVDZ (BWCCSD, apBWCCSD, MkCCSD) levels. The sensitivity of the MRCC predictions to active-space orbital rotations is rather unsatisfactory and makes the computed values of ω_3 somewhat arbitrary. The inclusion of triple excitations in these MRCC wave functions is apparently necessary to stabilize the curvature of the potential energy surface along the antisymmetric stretching mode of ozone.

In Table 3.2, MRCC values of ω_3 are given from computations with $|\Phi_3\rangle$ included as a reference configuration and with CASSCF natural orbitals. The properties of natural orbitals dictate that $c_3' = 0$ in Eq. (44) for all displacements into C_s symmetry.[145] Thus, the use of CASSCF natural orbitals is equivalent to a $\theta = 0°$ canonicalization in Eq. (46). We confirmed that the C_{2v} solutions for each MRCC wave function could be continuously followed upon finite, antisymmetric displacements of the O-O bonds. The cc-pVQZ entries for ω_3 in Table 3.2 exhibit errors of 20.3%, 24.0%, and 21.9% respectively, for MkCCSD, BWCCSD, and apBWCCSD. Not only are these discrepancies disappointingly large, but they also exceed the SRCCSD error of 17.7%, not to mention the SRCCSD(T) result which is accurate to better than 1%. Using orbitals canonicalized by the averaged Fock matrix [Eq. (50)] only changes the MkCCSD ω_3 prediction by +5 cm^{-1}, with the cc-pVDZ basis. In addition, with Hartree-Fock orbitals cc-pVDZ

MkCCSD gives $\omega_3 = 1259$ cm^{-1}, 20 cm^{-1} above the corresponding result with CASSCF natural orbitals.

In summary, the MRCCSD methods substantially improve upon SRCCSD for the geometric parameters and a_1 frequencies of ozone. However, for the $\omega_3(b_2)$ antisymmetric stretching frequency, there is some deterioration in accuracy when the MRCCSD schemes are used rather than SRCCSD, as well as a disturbing sensitivity to orbital canonicalization. The high accuracy of SRCCSD(T) is matched by MRCCSD results for none of the properties of ozone investigated here.

Table 3.2. Single- and multireference coupled cluster equilibrium geometries (r_e) and harmonic vibrational frequencies (ω_i) for ozone.[a]

Theory	Basis Set	r_{OO} (Å)	θ_{OOO} (deg)	$\omega_1(a_1)$ (cm^{-1})	$\omega_2(a_1)$ (cm^{-1})	$\omega_3(b_2)$ (cm^{-1})
Single Reference CCSD	cc-pVDZ	1.2590	117.3	1251	753	1237
	cc-pVTZ	1.2500	117.6	1278	763	1266
	cc-pVQZ	1.2438	117.7	1294	771	1282
Single Reference CCSD(T)	cc-pVDZ[b]	1.284	116.6	1118	704	977
	cc-pVTZ[b]	1.275	116.9	1153	716	1054
	cc-pVQZ[b]	1.269	117.1	1169	725	1081
Single Reference CCSDT	cc-pVDZ	1.2834	116.5	1127	706	1065
	cc-pVTZ[b]	1.274	116.8	1163	717	1117
Mukherjee Multireference CCSD	cc-pVDZ	1.2764	115.9	1146	728	1239
	cc-pVTZ	1.2663	116.3	1180	739	1289
	cc-pVQZ	1.2594	116.5	1198	748	1310
Brillouin-Wigner Multireference CCSD	cc-pVDZ	1.2703	116.2	1186	738	1284
	cc-pVTZ	1.2604	116.6	1218	748	1331
	cc-pVQZ	1.2537	116.8	1236	757	1350
A Posteriori BW Multireference CCSD	cc-pVDZ	1.2829	115.4	1098	720	1261
	cc-pVTZ	1.2726	115.8	1133	730	1313
	cc-pVQZ	1.2655	116.0	1150	739	1327
Experiment[c]		1.278	116.8	1135	716	1089

[a] Single-reference coupled cluster computations used canonical Hartree-Fock orbitals; multireference coupled cluster computations used CAS(2,2) natural orbitals. Core orbitals frozen in all computations.

[b] Reference 134.

[c] Reference 121 for r_e structure. The ω_i values are from Ref. 122 and were derived from a fit of harmonic frequencies, χ_{ij} anharmonicity constants, and a Darling-Dennison coupling parameter to 33 observed vibrational band origins of $^{16}O_3$ and $^{18}O_3$.

3.6.3 BENZYNES

Ortho, meta, and para-benzyne (Scheme 1) represent a well known class of compounds that show various degrees of diradical character.[146]
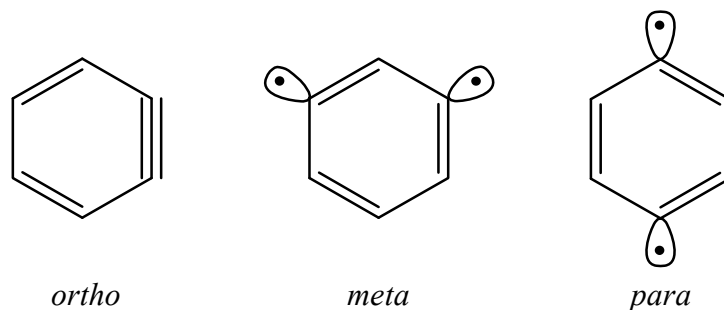
ortho   meta   para

Scheme 3.1. *Ortho-, meta-* and *para*-benzyne

For all three of these isomers the ground state is a singlet. Theoretical studies[147-149] on these compounds have revealed that the degree of diradical character for the benzynes follows the ordering

ortho < *meta* < *para*.

The singlet-triplet energy splittings (ΔE_{ST}) for *ortho*-, *meta*-, and *para*-benzyne were first measured in photoelectron spectroscopy experiments by Leopold, Miller, and Lineberger[150] and Wenthold, Squires, and Lineberger.[151] These authors found the following ordering for ΔE_{ST}:

ortho (37.5 kcal mol^{-1}) > *meta* (21.0 kcal mol^{-1}) > *para* (3.8 kcal mol^{-1}).

Wenthold, *et al.*[151] also reported an alternative value for ΔE_{ST} for *para*-benzyne, 2.1 kcal mol^{-1}.

Theoretical ΔE_{ST} predictions have been reported by several authors including Cramer, Nash, and Squires,[147] Lindh, Bernhardsson, and Schütz,[148] as well as de Visser, Filatov, and Shaik.[149] These findings support the ordering of diradical character of the benzynes given above.

Table 3.3 shows the singlet-triplet energy splittings predicted for *o*-, *m*-, and *p*-benzyne at the MkCCSD level using the cc-pVDZ basis set[105] (ΔE_{ST}^{MkCCSD}), ROHF molecular orbitals, and freezing the carbon 1*s* orbitals. The singlet zeroth-order wave function for the benzynes was chosen of the form

$$\left|\Psi_S^P\right\rangle = c_1\left|\Phi_{1,S}\right\rangle + c_2\left|\Phi_{2,S}\right\rangle, \tag{60}$$

with

$$\left|\Phi_{1,S}\right\rangle = \left|(core)^2(valence)^2(HOMO)^2\right\rangle$$
$$\left|\Phi_{2,S}\right\rangle = \left|(core)^2(valence)^2(LUMO)^2\right\rangle. \tag{61}$$

The triplet wave function was computed *within the same formalism* by converging on the $M_S = 0$ solution. Tests of this procedure indicated remarkable agreement (within 0.2 kcal mol^{-1}) with full configuration interaction (FCI) singlet-triplet splittings.[152] Therefore, the zeroth-order triplet wave function was taken as

$$\left|\Psi_T^P\right\rangle = \frac{1}{\sqrt{2}}\left(\left|\Phi_{1,T}\right\rangle + \left|\Phi_{2,T}\right\rangle\right), \tag{62}$$

with

$$\left|\Phi_{1,T}\right\rangle = \left|(core)^2(valence)^2(HOMO_\alpha)^1(LUMO_\beta)^1\right\rangle$$
$$\left|\Phi_{2,T}\right\rangle = \left|(core)^2(valence)^2(HOMO_\beta)^1(LUMO_\alpha)^1\right\rangle. \tag{63}$$

The (HOMO, LUMO) orbitals for *o*-, *m*-, and *p*-benzyne in C_{2v}, C_{2v}, and D_{2h} symmetry are (a_1, b_2), (a_1, b_1), and (b_{2u}, a_g), respectively.

The molecular geometries of singlet *ortho*- and *meta*-benzyne were optimized at the cc-pVDZ/RHF-CCSD(T) level of theory. For triplet *ortho*- and *meta*-benzyne, UHF-CCSD(T) wave functions were used. Singlet and triplet *para*-benzyne were optimized using spatial

symmetry-broken orbitals and cc-pVDZ/UHF-CCSD(T) wave functions. For singlet and triplet *para*-benzyne, the molecular orbitals break D_{2h} symmetry, but the final geometric structures retain D_{2h} symmetry. The geometrical parameters for the optimized structures of the singlet and triplet benzyne isomers are reported in the Supplementary Material.[91] Our procedures for obtaining geometric structures were chosen because previous studies have showed that perturbative triples are essential to avoid artifacts like a bicyclic structure for *meta*-benzyne, and a broken-symmetry UHF reference is needed for singlet *para*-benzyne to prevent the occurrence of imaginary vibrational frequencies for the D_{2h} structure.[153,154]

Table 3.3 also includes estimates for the complete basis set limit of the singlet-triplet splittings, as well as zero-point vibrational energy (ZPVE) corrections. The CBS correction ($\Delta E_{ST}^{\text{BasisSet}}$) was estimated as

$$\Delta E_{ST}^{\text{BasisSet}} = \Delta E_{ST}^{\text{CCSD}}(\text{CBS}) - \Delta E_{ST}^{\text{CCSD}}(\text{cc-pVDZ}). \tag{64}$$

The $\Delta E_{ST}^{\text{CCSD}}(\text{CBS})$ term was computed as the difference between the extrapolated singlet and triplet energies using RHF-CCSD and ROHF-CCSD. The extrapolation was performed according to Eqs. (53) and (54). ZPVE corrections ($\Delta E_{ST}^{\text{ZPVE}}$) were computed without scaling using the same levels of theory adopted for the geometry optimizations. The vibrational frequencies were all real, and are reported in the Supplementary Material.[91]

As shown in Table 3.3, the final MkCCSD singlet-triplet splittings for *o-*, *m-*, and *p*-benzyne are 38.5, 19.5 and 2.4 kcal mol^{-1}, respectively. The agreement with experimental data and previous theoretical investigations is quite good despite the fact that contributions from triple excitations are missing. Our final MkCCSD values are all within 1.5 kcal mol^{-1} of experiment.[151] Our value of ΔE_{ST} for *para*-benzyne, 2.4 kcal mol^{-1}, is in closer agreement with the alternative

value of ΔE_{ST} reported in Ref. 151 (2.1 kcal mol^{-1}) rather than the accepted one (3.8 kcal mol^{-1}). However, this result should not be considered definitive. From Table 3.3 one may observe that in the case of *meta*-benzyne the experimental ΔE_{ST} is underestimated by 1.5 kcal mol^{-1}. If we shift our prediction for by this same amount, we end up with ΔE_{ST} = 3.9 kcal mol^{-1}, very close to the conventional ΔE_{ST} given by Wenthold and co-workers.[151] The inclusion of triple excitations in the MkCC wave function would be able to provide a more definitive ΔE_{ST} for *para*-benzyne, and hence aid in the assignment of the experimental value.[155]

Table 3.3. Singlet-Triplet Splittings (in kcal mol^{-1}) for the Three Isomers of Benzyne.

Energetic Contribution	*o*-Benzyne	*m*-Benzyne	*p*-Benzyne
$\Delta E_{ST}^{\text{MkCCSD}}$	35.1	18.7	4.5
$\Delta E_{ST}^{\text{BasisSet}}$	3.6	0.1	−2.3
$\Delta E_{ST}^{\text{ZPVE}}$	−0.3	0.7	0.3
Total	38.5	19.5	2.4
CASPT2/aANO[a]	32.6	19.0	5.8
CCSD(T)/pVTZ[a]	35.3	20.7	2.3
CASRS3/CBL(4 : 3,4)[b]	36.5	18.6	2.2
REKS/6-31G(d)[c]	36.5	21.6	4.1
Experiment[d]	37.7 ± 0.7		
Experiment[e]	37.5 ± 0.3	21.0 ± 0.3	3.8 ± 0.3
Experiment[f]			2.1 ± 0.4

[a] Reference 147.

[b] Reference 148.

[c] Reference 149.

[d] Reference 150.

[e] Reference 151.

[f] Reference 151, alternative value.

3.7 SUMMARY

The matrix elements of the "same vacuum" multireference coupled cluster renormalization terms have been derived, and explicit formulas are given here for the state-specific MRCCSD and MRCCSDT cases. The MRCCSD couplings have been implemented in a new production-level code (PSIMRCC), capable of computing Mukherjee and Brillouin-Wigner state-specific multireference coupled cluster energies. Three rigorous and representative applications of our MRCC code are reported here: (1) the dissociation curve and spectroscopic constants of F_2, (2) the structure and vibrational frequencies of the ozone molecule, and (3) the singlet-triplet splittings in *ortho*-, *meta*-, and *para*-benzyne.

The results in Tables 3.1 and 3.2 support the accuracy and reliability of MkCCSD when compared to single-reference CCSD and Brillouin-Wigner multireference CCSD. The dissociation of F_2 clearly demonstrates that the lack of size extensivity in BWCCSD, even if approximately corrected by apBWCCSD, can cause large errors when these MRCC methods are applied to molecular fragmentation processes. In contrast, the rigorously size-extensive MkCCSD method with delocalized CAS(2,2) natural orbitals provides a dissociation energy in the CBS limit of D_e = 42.6 kcal mol^{-1}, as compared to 38.3 kcal mol^{-1} from experiment. Remarkably, if localized CAS(2,2) orbitals are utilized to eliminate size-consistency errors, CBS MkCCSD gives D_e within 0.2 kcal mol^{-1} of experiment.

Ozone is the most severe test for the MRCC theories investigated here. With the cc-pVQZ basis set, the [SRCCSD, BWCCSD, MkCCSD, SRCCSD(T)] methods underestimate the O-O bond length by (0.034, 0.024, 0.019, 0.009) Å, in order. Simultaneously, the same series of methods overestimates $\omega_1(a_1)$ by (159, 101, 63, 34) cm^{-1} and $\omega_2(a_1)$ by (55, 41, 32, 9) cm^{-1}. These trends demonstrate clear merit in the MkCCSD approach, although the pathological nature

of the O_3 system engenders larger errors than normal. However, the antisymmetric stretching frequency of ozone, $\omega_3(b_2)$, remains a problem, as none of the MRCCSD methods, when applied with CASSCF natural orbitals, is able to improve upon SRCCSD or place this frequency below $\omega_1(a_1)$, as observed experimentally. Significantly, we find that the value of ω_3 predicted by the MRCCSD methods is quite sensitive to orbital canonicalization, and rotations within the (HOMO, LUMO) active space of less than 2° can yield a fortuitous, exact reproduction of the empirical $\omega_3 = 1089$ cm^{-1}.

Finally, we tested MkCCSD on the singlet-triplet energy splittings (ΔE_{ST}) of the three isomers of benzyne. The triplet wave function was computed, *within the same MRCC formalism*, by converging on the two-determinant $M_S = 0$ solution. Our ΔE_{ST} results are in very good agreement (within 1.5 kcal mol^{-1}) with the experimental values, even without the inclusion of connected triple excitations.

As the ozone example demonstrates, a desirable improvement would be the inclusion of a perturbative treatment of triple excitations in MkCCSD. But a rather tedious problem hinders further progress. In SRCCSD(T) the use of a restricted reference or the canonicalization of the molecular orbitals may be used to form a diagonal Fock matrix. This in turn permits the evaluation of the (T) correction on-the-fly, without the need of storing the T_3 amplitudes. In the case of MRCC, it is generally impossible (except for some special cases) to find a set of orbitals that gives diagonal Fock matrices $[f_{pq}(\mu)]$ for all the references μ. Off-diagonal terms of the Fock matrix make the evaluation of the (T) correction an iterative process for which *all* the T_3 amplitudes must be stored. The implementation of an approximate (T) correction has been pursued by Li and Paldus for SUCC,[55] as well as Demel and Pittner for BWCC.[79] Research on a viable MkCCSD(T) method is clearly warranted.

Our work shows that MkCC theory, in the single and double excitation approximation, is a widely applicable tool for the study of real chemical problems with multireference character. The formulas that we have derived allow for a systematic improvement of this model by including higher excitations. Our earlier benchmark study[62] on the H4, P4, BeH_2, and H8 model systems revealed that MkCCSDT is a particularly robust theory, giving potential energy curves nearly coincident with and parallel to the FCI limit throughout the single and multireference regions of geometric configuration space. Therefore, MkCCSDT theory − a multireference coupled cluster method that is size extensive, intruder free and that can potentially achieve chemical accuracy − is a prominent target for future development.

3.8 ACKNOWLEDGMENTS

APPENDIX A. GENERAL EXPRESSION FOR THE MKCC COUPLING TERMS

Here we provide a derivation of a general-order expression for the MkCC coupling terms.

Let us first notice that by definition the action of the operator $\hat{T}^\nu$ on reference $\left|\Phi_\mu\right\rangle$ produces only contributions from the "common" amplitudes $t_{ij\cdots}^{ab\cdots}(\nu/\mu)$ (see Section II.A for the definition). Thus we may define a cluster operator $\hat{T}^{\nu/\mu}$ containing only the amplitudes that are common to operator $\hat{T}^\nu$ with respect to reference $\left|\Phi_\mu\right\rangle$. This allows us to write

$$\hat{T}^\nu\left|\Phi_\mu\right\rangle = \hat{T}^{\nu/\mu}\left|\Phi_\mu\right\rangle. \tag{65}$$

After noticing that $\hat{T}^{\nu/\mu}$ and $\hat{T}^\mu$ commute we can simplify the coupling terms

$$e^{-\hat{T}^\mu}e^{\hat{T}^\nu}\left|\Phi_\mu\right\rangle = e^{-\hat{T}^\mu}e^{\hat{T}^{\nu/\mu}}\left|\Phi_\mu\right\rangle = e^{-\hat{T}^\mu+\hat{T}^{\nu/\mu}}\left|\Phi_\mu\right\rangle \tag{66}$$

and introduce a new operator

$$
\begin{aligned}
\Delta\hat{T}^{(\nu/\mu,\mu)} &= \sum_{k=1}^{n}\frac{1}{k!}\sum_{i,j,\ldots}^{occ(\mu)}\sum_{a,b,\ldots}^{vir(\mu)}\left[t_{ij\cdots}^{ab\cdots}(\nu/\mu)-t_{ij\cdots}^{ab\cdots}(\mu)\right]\underbrace{\ldots\hat{a}_b^+\hat{a}_j\hat{a}_a^+\hat{a}_i}_{n-\text{tuple excitation}} \\
&= \sum_{k=1}^{n}\frac{1}{k!}\sum_{i,j,\ldots}^{occ(\mu)}\sum_{a,b,\ldots}^{vir(\mu)}\Delta t_{ij\cdots}^{ab\cdots}(\nu/\mu,\mu)\underbrace{\ldots\hat{a}_b^+\hat{a}_j\hat{a}_a^+\hat{a}_i}_{n-\text{tuple excitation}} \\
&= \sum_{k=1}^{n}\Delta\hat{T}_k^{(\nu/\mu,\mu)}
\end{aligned}
\tag{67}
$$

that allows us to rewrite the coupling terms as

$$\left\langle\Phi_{ij\cdots}^{ab\cdots}(\mu)\left|e^{-\hat{T}^\mu}e^{\hat{T}^\nu}\right|\Phi_\mu\right\rangle = \left\langle\Phi_{ij\cdots}^{ab\cdots}(\mu)\left|e^{\Delta\hat{T}^{(\nu/\mu,\mu)}}\right|\Phi_\mu\right\rangle. \tag{68}$$

We have thus expressed the MkCC coupling terms in terms of a standard coupled cluster expression that may be evaluated using algebraic or diagrammatic techniques.

Starting from Eq. (68) we can easily derive the coupling terms needed for MkCCSDT. The single and double excitations are identical to the MkCCSD case

$$\left\langle \Phi_i^a(\mu) \middle| e^{-\hat{T}^\mu} e^{\hat{T}^\nu} \middle| \Phi_\mu \right\rangle = \left\langle \Phi_i^a(\mu) \middle| \Delta\hat{T}_1^{(\nu/\mu,\mu)} \middle| \Phi_\mu \right\rangle$$
$$= t_i^a(\nu/\mu) - t_i^a(\mu), \tag{69}$$

$$\left\langle \Phi_{ij}^{ab}(\mu) \middle| e^{-\hat{T}^\mu} e^{\hat{T}^\nu} \middle| \Phi_\mu \right\rangle = \left\langle \Phi_{ij}^{ab}(\mu) \middle| \Delta\hat{T}_2^{(\nu/\mu,\mu)} \middle| \Phi_\mu \right\rangle + \frac{1}{2}\left\langle \Phi_{ij}^{ab}(\mu) \middle| \left(\Delta\hat{T}_1^{(\nu/\mu,\mu)}\right)^2 \middle| \Phi_\mu \right\rangle$$
$$= \Delta t_{ij}^{ab}(\nu/\mu,\mu) + \frac{1}{2}P(ij)P(ab)\Delta t_i^a(\nu/\mu,\mu)\Delta t_j^b(\nu/\mu,\mu)$$
$$= t_{ij}^{ab}(\nu/\mu) - t_{ij}^{ab}(\mu) \tag{70}$$
$$+ P(ij)t_i^a(\nu/\mu)t_j^b(\nu/\mu)$$
$$+ P(ij)t_i^a(\mu)t_j^b(\mu)$$
$$- P(ij)P(ab)t_i^a(\nu/\mu)t_j^b(\mu)$$

The coupling terms for the T_3-amplitudes are

$$\left\langle \Phi_{ijk}^{abc}(\mu) \middle| e^{-\hat{T}^\mu} e^{\hat{T}^\nu} \middle| \Phi_\mu \right\rangle = \left\langle \Phi_{ijk}^{abc}(\mu) \middle| \Delta\hat{T}_3^{(\nu/\mu,\mu)} \middle| \Phi_\mu \right\rangle + \left\langle \Phi_{ijk}^{abc}(\mu) \middle| \Delta\hat{T}_1^{(\nu/\mu,\mu)}\Delta\hat{T}_2^{(\nu/\mu,\mu)} \middle| \Phi_\mu \right\rangle$$
$$+ \frac{1}{6}\left\langle \Phi_{ijk}^{abc}(\mu) \middle| \left(\Delta\hat{T}_1^{(\nu/\mu,\mu)}\right)^3 \middle| \Phi_\mu \right\rangle$$
$$= \Delta t_{ijk}^{abc}(\nu/\mu,\mu) \tag{71}$$
$$+ P(i/jk)P(a/bc)\Delta t_i^a(\nu/\mu,\mu)\Delta t_{jk}^{bc}(\nu/\mu,\mu)$$
$$+ \frac{1}{6}P(ijk)P(abc)\Delta t_i^a(\nu/\mu,\mu)\Delta t_j^b(\nu/\mu,\mu)\Delta t_k^c(\nu/\mu,\mu)$$

and may be expanded to give

$$\left\langle \Phi_{ijk}^{abc}(\mu) \middle| e^{-\hat{T}^{\mu}} e^{\hat{T}^{\nu}} \middle| \Phi_{\mu} \right\rangle = \quad -t_{ijk}^{abc}(\mu) + P(a/bc)P(i/jk)t_i^a(\mu)t_{jk}^{bc}(\mu)$$
$$-P(abc)t_i^a(\mu)t_j^b(\mu)t_k^c(\mu)$$
$$-P(a/bc)P(i/jk)t_i^a(\nu/\mu)t_{jk}^{bc}(\mu)$$
$$+P(abc)P_+(ia/jb,kc)t_i^a(\nu/\mu)t_j^b(\mu)t_k^c(\mu)$$
$$-P(a/bc)P(i/jk)t_i^a(\mu)t_{jk}^{bc}(\nu/\mu)$$
$$-P(abc)P_+(ia/jb,kc)t_i^a(\mu)t_j^b(\nu/\mu)t_k^c(\nu/\mu)$$
$$+t_{ijk}^{abc}(\nu/\mu) + P(a/bc)P(i/jk)t_i^a(\nu/\mu)t_{jk}^{bc}(\nu/\mu)$$
$$+P(abc)t_i^a(\nu/\mu)t_j^b(\nu/\mu)t_k^c(\nu/\mu).$$

$$(72)$$

where we have introduced the permutation operators

$$P(abc)f(a,b,c) = f(a,b,c) + f(b,c,a) + f(c,a,b)$$
$$-f(b,a,c) - f(a,c,b) - f(c,b,a)$$

$$(73)$$

$$P(a/bc)f(a,b,c) = f(a,b,c) - f(b,a,c) - f(c,b,a)$$

$$(74)$$

$$P_+(ia/jb,kc)f(i,a,j,b,k,c) = f(i,a,j,b,k,c) + f(j,b,i,a,k,c)$$
$$+f(k,c,j,b,i,a)$$

$$(75)$$

REFERENCES AND NOTES

[1]   B. Jeziorski and H. J. Monkhorst, Phys. Rev. A **24**, 1668 (1981).

[2]   I. Hubač and P. Neogrády, Phys. Rev. A **50**, 4558 (1994).

[3]   U. S. Mahapatra, B. Datta, and D. Mukherjee, J. Chem. Phys. **110**, 6171 (1999).

[4]   L. Adamowicz, J. P. Malrieu, and V. V. Ivanov, J. Chem. Phys. **112**, 10075 (2000).

[5]   D. I. Lyakh, V. V. Ivanov, and L. Adamowicz, J. Chem. Phys. **122**, 024108 (2005).

[6]   J. Olsen, J. Chem. Phys. **113**, 7140 (2000).

[7]   M. Kállay, P. G. Szalay, and P. R. Surján, J. Chem. Phys. **117**, 980 (2002).

[8]   X. Z. Li and J. Paldus, J. Chem. Phys. **107**, 6257 (1997).

[9]   X. Z. Li and J. Paldus, Collect. Czech. Chem. Commun. **63**, 1381 (1998).

10   X. Z. Li and J. Paldus, Chem. Phys. Lett. **286**, 145 (1998).

11   X. Z. Li and J. Paldus, J. Chem. Phys. **108**, 637 (1998).

12   X. Z. Li and J. Paldus, J. Chem. Phys. **110**, 2844 (1999).

13   X. Z. Li, I. Grabowski, K. Jankowski, and J. Paldus, Adv Quantum Chem **36**, 231 (2000).

14   X. Z. Li and J. Paldus, J. Chem. Phys. **113**, 9966 (2000).

15   X. Z. Li and J. Paldus, Int. J. Quantum Chem. **80**, 743 (2000).

16   X. Z. Li and J. Paldus, Mol. Phys. **98**, 1185 (2000).

17   P. Piecuch and L. Adamowicz, J. Chem. Phys. **100**, 5792 (1994).

18   P. Piecuch and L. Adamowicz, Chem. Phys. Lett. **221**, 121 (1994).

19   K. Kowalski and P. Piecuch, J. Chem. Phys. **113**, 8490 (2000).

20   K. Kowalski and P. Piecuch, Chem. Phys. Lett. **344**, 165 (2001).

21   K. Kowalski and P. Piecuch, J. Chem. Phys. **115**, 643 (2001).

22   K. Kowalski, S. Hirata, M. Wloch, P. Piecuch, and T. L. Windus, J. Chem. Phys. **123**, 074319 (2005).

23   P. Piecuch, S. Hirata, K. Kowalski, P. D. Fan, and T. L. Windus, Int. J. Quantum Chem. **106**, 79 (2006).

24   A. I. Krylov, C. D. Sherrill, E. F. C. Byrd, and M. Head-Gordon, J. Chem. Phys. **109**, 10669 (1998).

25   C. D. Sherrill, A. I. Krylov, E. F. C. Byrd, and M. Head-Gordon, J. Chem. Phys. **109**, 4171 (1998).

26   A. I. Krylov, C. D. Sherrill, and M. Head-Gordon, J. Chem. Phys. **113**, 6509 (2000).

27   A. I. Krylov, Abstr Pap Am Chem S **228**, U236 (2004).

28   A. I. Krylov, Accounts Chem Res **39**, 83 (2006).

[29]   A. I. Krylov and L. V. Slipchenko, Abstr Pap Am Chem S **225**, U454 (2003).

[30]   S. V. Levchenko and A. I. Krylov, Abstr Pap Am Chem S **226**, U292 (2003).

[31]   S. V. Levchenko and A. I. Krylov, J. Chem. Phys. **120**, 175 (2004).

[32]   J. S. Sears, C. D. Sherrill, and A. I. Krylov, J. Chem. Phys. **118**, 9084 (2003).

[33]   L. V. Slipchenko and A. I. Krylov, J. Chem. Phys. **117**, 4694 (2002).

[34]   L. V. Slipchenko and A. I. Krylov, Abstr Pap Am Chem S **226**, U287 (2003).

[35]   S. R. Gwaltney and M. Head-Gordon, Abstr Pap Am Chem S **219**, U338 (2000).

[36]   S. R. Gwaltney and M. Head-Gordon, Chem. Phys. Lett. **323**, 21 (2000).

[37]   S. R. Gwaltney, C. D. Sherrill, M. Head-Gordon, and A. I. Krylov, J. Chem. Phys. **113**, 3548 (2000).

[38]   S. R. Gwaltney and M. Head-Gordon, J. Chem. Phys. **115**, 2014 (2001).

[39]   S. R. Gwaltney, E. F. C. Byrd, T. Van Voorhis, and M. Head-Gordon, Chem. Phys. Lett. **353**, 359 (2002).

[40]   K. Jankowski, J. Paldus, and P. Piecuch, Theor. Chim. Acta **80**, 223 (1991).

[41]   K. Kowalski and P. Piecuch, J. Chem. Phys. **113**, 18 (2000).

[42]   K. Kowalski and P. Piecuch, J. Chem. Phys. **116**, 7411 (2002).

[43]   I. S. O. Pimienta, K. Kowalski, and P. Piecuch, J. Chem. Phys. **119**, 2951 (2003).

[44]   P. Piecuch, K. Kowalski, I. S. O. Pimienta, P. D. Fan, M. Lodriguito, M. J. McGuire, S. A. Kucharski, T. Kus, and M. Musial, Theor Chem Acc **112**, 349 (2004).

[45]   P. D. Fan, K. Kowalski, and P. Piecuch, Mol. Phys. **103**, 2191 (2005).

[46]   K. Kowalski and P. Piecuch, J. Chem. Phys. **113**, 5644 (2000).

[47]   P. Piecuch, S. A. Kucharski, V. Spirko, and K. Kowalski, J. Chem. Phys. **115**, 5796 (2001).

[48]   P. Piecuch, S. A. Kucharski, and K. Kowalski, Chem. Phys. Lett. **344**, 176 (2001).

[49]   P. Piecuch, K. Kowalski, I. S. O. Pimienta, and M. J. McGuire, Int Rev Phys Chem **21**, 527 (2002).

[50]   K. Kowalski and P. Piecuch, J. Chem. Phys. **122**, 074107 (2005).

[51]   P. Piecuch and M. Wloch, J. Chem. Phys. **123**, 224105 (2005).

[52]   X. Li and J. Paldus, J. Chem. Phys. **119**, 5320 (2003).

[53]   X. Li and J. Paldus, J. Chem. Phys. **119**, 5346 (2003).

[54]   X. Li and J. Paldus, J. Chem. Phys. **120**, 5890 (2004).

[55]   X. Li and J. Paldus, J. Chem. Phys. **124**, 034112 (2006).

[56]   J. Pittner, P. Nachtigall, P. Čársky, J. Mášik, and I. Hubač, J. Chem. Phys. **110**, 10275 (1999).

[57]   J. Pittner, J. Smydke, P. Carsky, and I. Hubac, J. Mol. Struct. **547**, 239 (2001).

[58]   J. Pittner and O. Demel, J. Chem. Phys. **122**, 181101 (2005).

[59]   S. Chattopadhyay, U. S. Mahapatra, and D. Mukherjee, J. Chem. Phys. **111**, 3820 (1999).

[60]   S. Chattopadhyay, U. S. Mahapatra, and D. Mukherjee, J. Chem. Phys. **112**, 7939 (2000).

[61]   S. Chattopadhyay, P. Ghosh, and U. S. Mahapatra, J. Phys. B **37**, 495 (2004).

[62]   F. A. Evangelista, W. D. Allen, and H. F. Schaefer, J. Chem. Phys. **125**, 154113 (2006).

[63]   G. E. Scuseria, C. L. Janssen, and H. F. Schaefer, J. Chem. Phys. **89**, 7382 (1988).

[64]   J. F. Stanton, J. Gauss, J. D. Watts, and R. J. Bartlett, J. Chem. Phys. **94**, 4334 (1991).

[65]   C. Hampel, K. A. Peterson, and H. J. Werner, Chem. Phys. Lett. **190**, 1 (1992).

[66]   B. Jeziorski and J. Paldus, J. Chem. Phys. **88**, 5673 (1988).

[67]   J. Paldus, L. Pylypow, and B. Jeziorski, in *Many-Body Methods in Quantum Chemistry*, edited by U. Kaldor (Springer, Berlin, 1989), pp. 151.

68   P. Piecuch and J. Paldus, Theor. Chim. Acta **83**, 69 (1992).

69   P. Piecuch and J. Paldus, J. Chem. Phys. **101**, 5875 (1994).

70   J. Paldus, X. Li, and N. D. K. Petraco, J. Math. Chem. **35**, 215 (2004).

71   J. Paldus, P. Piecuch, L. Pylypow, and B. Jeziorski, Phys. Rev. A **47**, 2738 (1993).

72   P. Piecuch and J. Paldus, Phys. Rev. A **49**, 3479 (1994).

73   X. Li and J. Paldus, Int. J. Quantum Chem. **99**, 914 (2004).

74   J. Mášik and I. Hubač, Collect. Czech. Chem. Commun. **62**, 829 (1997).

75   J. Mášik and I. Hubač, Adv. Quantum. Chem. **31**, 75 (1999).

76   I. Hubač, J. Pittner, and P. Čársky, J. Chem. Phys. **112**, 8779 (2000).

77   J. Pittner, J. Chem. Phys. **118**, 10876 (2003).

78   J. Pittner, X. Z. Li, and J. Paldus, Mol. Phys. **103**, 2239 (2005).

79   O. Demel and J. Pittner, J. Chem. Phys. **124**, 144112 (2006).

80   U. S. Mahapatra, B. Datta, B. Bandyopadhyay, and D. Mukherjee, Adv. Quantum Chem. **30**, 163 (1998).

81   U. S. Mahapatra, B. Datta, and D. Mukherjee, Mol. Phys. **94**, 157 (1998).

82   U. S. Mahapatra, B. Datta, and D. Mukherjee, J. Phys. Chem. A **103**, 1822 (1999).

83   U. S. Mahapatra, B. Datta, and D. Mukherjee, Chem. Phys. Lett. **299**, 42 (1999).

84   U. S. Mahapatra, B. Datta, and D. Mukherjee, Chem. Phys. Lett. **301**, 206 (1999).

85   S. Chattopadhyay, U. S. Mahapatra, B. Datta, and D. Mukherjee, Chem. Phys. Lett. **357**, 426 (2002).

86   D. Pahari, S. Chattopadhyay, S. Das, and D. Mukherjee, Chem. Phys. Lett. **381**, 223 (2003).

87 S. Chattopadhyay, D. Pahari, D. Mukherjee, and U. S. Mahapatra, J. Chem. Phys. **120**, 5968 (2004).

88 D. Pahari, S. Chattopadhyay, A. Deb, and D. Mukherjee, Chem. Phys. Lett. **386**, 307 (2004).

89 N. D. K. Petraco, L. Horný, H. F. Schaefer, and I. Hubač, J. Chem. Phys. **117**, 9580 (2002).

90 L. Horný, H. F. Schaefer, I. Hubač, and S. Pal, Chem. Phys. **315**, 240 (2005).

91   See EPAPS Document No. ??? for pdf file containing the spin-factored CCSD equations, ozone energy plots, geometries and vibrational frequencies of the benzynes. This document can be reached via a direct link in the online article's HTML reference section or via the EPAPS homepage http://www.aip.org/pubservs/epaps.html.

92 T. D. Crawford, C. D. Sherrill, E. F. Valeev, J. T. Fermann, R. A. King, M. L. Leininger, S. T. Brown, C. L. Janssen, E. T. Seidl, J. P. Kenny, and W. D. Allen, J. Comp. Chem., (in press) (2007).

93 C. D. Sherrill and H. F. Schaefer, Adv. Quantum. Chem. **34**, 143 (1999).

94 S. A. Kucharski and R. J. Bartlett, J. Chem. Phys. **95**, 8227 (1991).

95 S. Hirata, J. Phys. Chem. A **107**, 9887 (2003).

96 J. Mášik, I. Hubač, and P. Mach, J. Chem. Phys. **108**, 6571 (1998).

97 W. D. Allen and H. F. Schaefer, J. Chem. Phys. **84**, 2212 (1986).

98 W. D. Allen and H. F. Schaefer, J. Chem. Phys. **87**, 7076 (1987).

99 T. J. Lee, W. D. Allen, and H. F. Schaefer, J. Chem. Phys. **87**, 7062 (1987).

100 Y. Osamura, Y. Yamaguchi, and H. F. Schaefer, J. Chem. Phys. **77**, 383 (1982).

101 L. Meissner, J. Gryniakow, and I. Hubač, Mol. Phys. **103**, 2173 (2005).

[102]   V. V. Ivanov, L. Adamowicz, and D. I. Lyakh, Int. J. Quantum Chem. **106**, 2875 (2006).

[103]   S. Chattopadhyay and U. S. Mahapatra, J. Phys. Chem. A **108**, 11664 (2004).

[104]   G. Herzberg, *Molecular Spectra and Molecular Structure I. Spectra of Diatomic Molecules*, 2nd ed. (Van Nostrand, New York, 1950). p. v.

[105]   T. H. Dunning, J. Chem. Phys. **90**, 1007 (1989).

[106]   D. Feller, J. Chem. Phys. **98**, 7059 (1993).

[107]   T. Helgaker, W. Klopper, H. Koch, and J. Noga, J. Chem. Phys. **106**, 9639 (1997).

[108]   J. F. Stanton, J. Gauss, J. D. Watts, W. J. Lauderdale, and R. J. Bartlett, Int. J. Quantum Chem. **44 (S26)**, 879 (1992).

[109]   J.F. Stanton, J. Gauss, J.D. Watts, P.G. Szalay, R.J. Bartlett with contributions from A.A. Auer, D.B. Bernholdt, O. Christiansen, M.E. Harding, M. Heckert, O. Heun, C. Huber, D. Jonsson, J. Jusélius, W.J. Lauderdale, T. Metzroth, C. Michauk, D.R. Price, K. Ruud, F. Schiffmann, A. Tajti, M.E. Varner, J. Vázquez and the integral packages: MOLECULE (J. Almlöf and P.R. Taylor), PROPS (P.R. Taylor), and ABACUS (T. Helgaker, H.J. Aa. Jensen, P. Jørgensen, and J. Olsen). Current version see http://www.aces2.de. .

[110]   J. Yang, Y. S. Hao, J. Li, C. Zhou, and Y. X. Mo, J. Chem. Phys. **122**, 134308 (2005).

[111]   J. L. Dunham, Phys. Rev. **41**, 721 (1932).

[112]   In accord with common usage, we employ the term "size consistency" when a computational method on a molecule AB in the limit of inifinite separation gives the same energy as the sum of the separate computations for A and B. "Size extensivity" is the mathematical property of correct (linear) scaling of the energy with the number of the electrons, a characteristic that applies to any molecular geometry if the method contains no unlinked diagrams.

[113]   J. A. Pople, J. S. Binkley, and R. Seeger, Int. J. Quantum. Chem. Symp. **10**, 1 (1976).

[114]   R. J. Bartlett and G. D. Purvis, Int. J. Quantum Chem. **14**, 561 (1978).

[115]   We confirmed by explicit computations that in the limit r(F-F) $\to \infty$, the supermolecule MkCCSD, BWCCSD, and apBWCCSD energies derived from a CAS(2,2) active space all become coincident *if the orbitals are localized* onto the fragments. In each case the energy is twice the single-reference CCSD energy of an individual F atom obtained with ROHF orbitals. Thus, localization of the active-space orbitals removes the size-consistency errors for all methods, although the BWCCSD and apBWCCSD approaches rertain ther lack of rigorous size extensivity.

[116]   O. Hino, T. Kinoshita, G. K. L. Chan, and R. J. Bartlett, J. Chem. Phys. **124** (2006).

[117]   P. J. Hay and T. H. Dunning, J. Chem. Phys. **67**, 2290 (1977).

[118]   P. J. Hay, T. H. Dunning, and W. A. Goddard, J. Chem. Phys. **62**, 3912 (1975).

[119]   W. D. Laidig and H. F. Schaefer, J. Chem. Phys. **74**, 3411 (1981).

[120]   S. M. Adler-Golden, S. R. Langhoff, C. W. Bauschlicher, and G. D. Carney, J. Chem. Phys. **83**, 255 (1985).

[121]   T. Tanaka and Y. Morino, J. Mol. Spectrosc. **33**, 538 (1970).

[122]   A. Barbe, C. Secroun, and P. Jouve, J. Mol. Spectrosc. **49**, 171 (1974).

[123]   Y. Yamaguchi, M. J. Frisch, T. J. Lee, H. F. Schaefer, and J. S. Binkley, Theor. Chim. Acta **69**, 337 (1986).

[124]   K. A. Peterson, R. C. Mayrhofer, E. L. Sibert, and R. C. Woods, J. Chem. Phys. **94**, 414 (1991).

[125]   A. Banichevich, S. D. Peyerimhoff, and F. Grein, Chem. Phys. Lett. **173**, 1 (1990).

126   P. Borowski, K. Andersson, P. A. Malmqvist, and B. O. Roos, J. Chem. Phys. **97**, 5568 (1992).

127   J. F. Stanton, W. N. Lipscomb, D. H. Magers, and R. J. Bartlett, J. Chem. Phys. **90**, 1077 (1989).

128   D. H. Magers, W. N. Lipscomb, R. J. Bartlett, and J. F. Stanton, J. Chem. Phys. **91**, 1945 (1989).

129   G. E. Scuseria, T. J. Lee, A. C. Scheiner, and H. F. Schaefer, J. Chem. Phys. **90**, 5635 (1989).

130   T. J. Lee and G. E. Scuseria, J. Chem. Phys. **93**, 489 (1990).

131   J. D. Watts, J. F. Stanton, and R. J. Bartlett, Chem. Phys. Lett. **178**, 471 (1991).

132   G. D. Purvis and R. J. Bartlett, J. Chem. Phys. **76**, 1910 (1982).

133   K. Raghavachari, G. W. Trucks, J. A. Pople, and E. Replogle, Chem. Phys. Lett. **158**, 207 (1989).

134   J. D. Watts and R. J. Bartlett, J. Chem. Phys. **108**, 2511 (1998).

135   S. A. Kucharski and R. J. Bartlett, J. Chem. Phys. **110**, 8233 (1999).

136   R. Kobayashi, R. D. Amos, and N. C. Handy, J. Chem. Phys. **100**, 1375 (1994).

137   G. E. Scuseria, Chem. Phys. Lett. **226**, 251 (1994).

138   M. L. Leininger and H. F. Schaefer, J. Chem. Phys. **107**, 9059 (1997).

139   D. Q. Xie, H. Guo, and K. A. Peterson, J. Chem. Phys. **112**, 8378 (2000).

140   P. G. Szalay and R. J. Bartlett, Chem. Phys. Lett. **214**, 481 (1993).

141   K. W. Sattelmeyer, H. F. Schaefer, and J. F. Stanton, Chem. Phys. Lett. **378**, 42 (2003).

142   M. Nooijen and R. J. Bartlett, J. Chem. Phys. **107**, 6812 (1997).

143   K. Kowalski, J. Chem. Phys. **123**, 014102 (2005).

144   T. Kinoshita, O. Hino, and R. J. Bartlett, J. Chem. Phys. **123** (2005).

145   A. Szabo and N. S. Ostlund, *Modern Quantum Chemistry: Introduction to Advanced Electronic Structure Theory. .* (Macmillan; Collier Macmillan, New York, London, 1982). p. 256.

146   H. H. Wenk, M. Winkler, and W. Sander, Angew. Chem. **42**, 502 (2003).

147   C. J. Cramer, J. J. Nash, and R. R. Squires, Chem. Phys. Lett. **277**, 311 (1997).

148   R. Lindh, A. Bernhardsson, and M. Schütz, J. Phys. Chem. A **103**, 9913 (1999).

149   S. P. de Visser, M. Filatov, and S. Shaik, Phys. Chem. Chem. Phys. **2**, 5046 (2000).

150   D. G. Leopold, A. E. S. Miller, and W. C. Lineberger, J. Am. Chem. Soc. **108**, 1379 (1986).

151   P. G. Wenthold, R. R. Squires, and W. C. Lineberger, J. Am. Chem. Soc. **120**, 5279 (1998).

152   This scheme for computing singlet-triplet splittings was tested on methylene. Using the geometries and DZP basis sets of C. W. Bauschlicher Jr. and P. R. Taylor, J. Chem. Phys. **85**, 6510 (1986), we determined the following splittings: 11.97, 11.83, and 12.82 kcal mol^{-1} using FCI, MkCCSD, and SRCCSD, respectively. Moreover, using the geometries and the larger TZ2P basis set of C. D. Sherrill, M. L. Leininger, T. J. Van Huis, and H. F. Schaefer, J. Chem. Phys. **108**, 1040 (1998), we obtain the following splittings: 11.14, 11.11, and 12.24 kcal mol^{-1} using FCI, MkCCSD, and SRCCSD, respectively.

153   T. D. Crawford, E. Kraka, J. F. Stanton, and D. Cremer, J. Chem. Phys. **114**, 10638 (2001).

154   C. E. Smith, T. D. Crawford, and D. Cremer, J. Chem. Phys. **122**, 174309 (2005).

In the case of methylene using the geometries and DZP basis sets of C. W. Bauschlicher Jr. and P. R. Taylor, J. Chem. Phys. **85**, 6510 (1986) we computed MkCC splittings with our arbitrary-order code DETC++ and obtained the following: 11.83, 12.04, and 11.99 kcal mol^{-1} for MkCCSD, MkCCSDT and MkCCSDTQ, respectively. The corresponding errors from FCI are −0.14, 0.07, and 0.02 kcal mol^{-1}.

CHAPTER 4

TRIPLE EXCITATIONS IN STATE-SPECIFIC MULTIREFERENCE COUPLED CLUSTER THEORY.

APPLICATION OF MK-MRCCSDT AND MK-MRCCSDT-N METHODS TO MODEL SYSTEMS[§]

4.1 ABSTRACT

We report the first implementation with correct scaling of the Mukherjee multireference coupled cluster method with singles, doubles, and approximate iterative triples (Mk-MRCCSDT-n, n = 1a, 1b, 2, 3) as well as full triples (Mk-MRCCSDT). These methods were applied to the classic H4, P4, BeH$_2$ and H8 model systems to assess the ability of the Mk-MRCCSDT-n schemes to accurately account for triple excitations. In all model systems the inclusion of triples via the various Mk-MRCCSDT-n approaches greatly reduces the nonparallelism error (NPE) and the mean nonparallelism derivative (MNPD) diagnostics for the potential energy curves, recovering between 59% and 73% of the full triples effect on average. The most complete triples approximation, Mk-MRCCSDT-3, exhibits the best average performance, reducing the mean NPE to below 0.6 mE$_h$, compared to 1.4 mE$_h$ for Mk-MRCCSD. Both linear and quadratic truncations of the Mk-MRCC triples coupling terms are viable simplifications producing no significant errors. If the off-diagonal parts of the occupied-occupied and virtual-virtual blocks of the Fock matrices are ignored, the storage of the triples amplitudes is no longer required for the Mk-MRCCSDT-n methods introduced here. This proves to be an effective approximation that gives results almost indistinguishable from those derived from full consideration of the Fock matrices.

4.2 INTRODUCTION

Despite the remarkable success of the single reference (SR) coupled cluster (CC) approach[1-4] there is one major drawback: low-order truncated CC schemes fail for systems containing quasidegenerate electronic configurations.[5,6] Therefore, potential energy curves closely approximating full configuration interaction (FCI) may be obtained only by the inclusion of

high-order excitations, and even in this case the convergence to the exact answer may be very slow. This limitation makes conventional SRCC methods inapplicable to important areas of chemistry, including homolytic bond breaking, singlet diradicals, many transition metal compounds, certain types of excited electronic states, and various transition states for chemical reactions.

The problem of quasidegenerate electronic configurations has stimulated several new ideas in CC theory. Several approaches have been advanced that remain within the single-reference coupled cluster framework, including: (1) variational CC,[7] extended CC,[8] and quadratic CC[9] schemes; (2) modifications such as the active-space CC approaches,[10-14] the reduced multireference (RM-RCCSD) method,[15,16] orbital-optimized CC schemes,[17,18] and tailored coupled cluster (TCC);[19,20] (3) equation-of-motion (EOM) approaches, in particular double ionization[21] and spin-flip methods;[22] and (4) a broad class of method-of-moments CC (MM-CC) and renormalized CC methods.[23-26] All of these theories are distinct from genuine multireference coupled cluster (MRCC) methods that are specifically designed for multiconfigurational zeroth-order wave functions. In the MRCC family there are multiroot approaches such as the Fock-space (FS)[27-29] and state-universal (SU) coupled-cluster methods,[30-34] as well as state-specific (single-root) multireference theories.[35-44]

Among the genuine MRCC methods, we have recently focused on the state-specific formulation of Mahapatra, Datta, and Mukherjee,[38,39] referred to hereafter as Mk-MRCC. Mk-MRCC theory is derived from the state-specific form of the Jeziorksi and Monkhorst (JM) ansatz[30] for state α

$$\left| \Psi_\alpha \right\rangle = \sum_{\mu=1}^{d} e^{\hat{T}^\mu} \left| \Phi_\mu \right\rangle c_\mu^{(\alpha)} , \tag{1}$$

in which the wave function is a linear combination of exponential functions obtained from reference determinants Φ_μ spanning a d-dimensional model space. The $\hat{T}^\mu$ are excitation

operators that promote electrons from the occupied to the virtual orbital space of Φ_μ and are typically truncated at a certain excitation level n,

$$\hat{T}^\mu = \hat{T}_1^\mu + \hat{T}_2^\mu + \ldots + \hat{T}_n^\mu \, . \tag{2}$$

In Mk-MRCC theory the energy (E_α) is obtained as an eigenvalue of the effective Hamiltonian matrix

$$H_{\mu\nu}^{\mathrm{eff}} = \left\langle \Phi_\mu \left| \hat{H} e^{\hat{T}^\nu} \right| \Phi_\nu \right\rangle , \tag{3}$$

while the expansion coefficients $[c_\mu^{(\alpha)}]$ of the JM wave function [Eq. (1)] are derived from the corresponding eigenvector,

$$\sum_{\nu=1}^{d} H_{\mu\nu}^{\mathrm{eff}} c_\nu^{(\alpha)} = E_\alpha c_\mu^{(\alpha)} \, . \tag{4}$$

When the model space is complete, including all determinants generated by distributing a specified number of electrons in a chosen set of orbitals, then only the connected part of Eq. (3) contributes to the effective Hamiltonian. The conditions for the cluster amplitudes are given in Section II below.

Mk-MRCC shows a number of appealing features:[38,39] (1) It is a genuine MRCC method that treats all references in the model space on an equal footing. (2) It is rigorously size extensive and leads to size-consistent energies when localized orbitals are used. (3) The theory is free from intruder states. (4) The resulting equations can be written in terms of the usual similarity-transformed Hamiltonian matrix elements plus off-diagonal coupling terms. The coupling terms refer to the "same vacuum" and thus are not difficult to implement.[45] (5) Finally, a number of applications to atoms, small molecules, and medium-size molecules using Mk-MRCC truncated to singles and doubles (Mk-MRCCSD) have validated the accuracy of the theory vis-à-vis experiment and other theoretical methods.[39,45,46]

The goal of the present work is to extend the Mk-MRCCSD method and increase its accuracy by including excitations higher than doubles in the cluster operators. In single-reference coupled cluster theory, Paldus, Čížek, and Shavitt[47] were the first to introduce the $\hat{T}_3$ component approximately, by adding linear $\hat{T}_1$ and $\hat{T}_3$ terms to the SR coupled cluster doubles (SRCCD) model. More recent schemes that include connected triple excitations may be classified as perturbative (non-iterative) and iterative methods.[1,2] These methods have computational scaling with a leading term O^3V^4 when the triples are treated only approximately and O^3V^5 for coupled cluster with the full inclusion of single, double and triple excitations (CCSDT),[48-51] where O and V are the number of occupied and virtual orbitals for a given basis set. Therefore, these methods are about O and OV times more expensive than regular SRCCSD, respectively.

Non-iterative methods are widely used because of their low computational cost (only one O^3V^4 step after a CCSD calculation) and high accuracy. The CCSD[T] model of Urban *et al.* [also denoted CCSD + T(CCSD)], contains fourth-order corrections to the energy computed using converged CCSD amplitudes.[52,53] The "gold standard" of quantum chemistry, CCSD(T), was introduced later,[54] improving upon CCSD[T] by including fifth-order terms that balance the overestimated effect of triples by CCSD[T]. More sophisticated variants are based either on the use of the Λ-amplitudes[55,56] or the use of the full similarity-transformed Hamiltonian in the perturbative treatment.[57,58]

The CCSDT-*n* family of iterative triples methods was advanced first by Urban, Noga, Cole, and Bartlett,[52,53,59] and constitutes a hierarchy of approximations to CCSDT. These include the CCSDT-1a, CCSDT-1b, CCSDT-2, and CCSDT-3 schemes. The CCSDT-*n* methods were recently analyzed by Cremer *et al.*[60] in terms of orders of perturbation. It was found that CCSDT-1a contains 75% of the terms that contribute to CCSDT, while CCSDT-1b offers little

further improvement. In the examples analyzed in Ref. 60, the contributions of CCSDT-2 and CCSDT-3 to the total energy showed opposite signs, providing some cancellation of terms beyond CCSDT-1. The CC3 method, another approximation to CCSDT, was introduced in the context of excited states and molecular properties by Koch *et al.*[61] The CCSDT-*n* methods have found use in applications,[62-67] but they have been largely supplanted by the more cost-effective CCSD(T) method for dealing with triples in single-reference systems.

In this paper we investigate the effect of approximate triple excitations in Mk-MRCC theory. Our pilot-code computations[68] on H4, BeH$_2$ and H8 revealed that the inclusion of full connected triples reduces the error in the total energy with respect to FCI to less than 0.15 kcal mol^{-1} (0.24 mE$_h$) across the potential energy curves. These encouraging results provide motivation for investigating the inclusion of triples excitations in Mk-MRCC in more detail. Three goals have to be achieved in this respect: (1) the capability of computing Mk-MRCCSDT energies for the purpose of benchmarking and obtaining high accuracy results on small molecules; (2) the formulation of iterative triples approximations for more economical treatments; and (3) the development of a perturbative triples correction analogous to SRCCSD(T) for general large-scale applications. From a theoretical point of view, the first goal is straightforward and univocal, while the others present some challenges concerning the underlying theoretical formulations.

Several authors have already investigated possible extensions of MRCC methods including triple excitations. Balková and Bartlett[69] proposed a perturbative triples correction to SU-MRCCSD analogous to the single-reference case. Li and Paldus[70,71] formulated a somewhat less elaborated SU-MRCCSD(T) scheme, which involves only symmetric corrections to the diagonal part of the effective Hamiltonian. Demel and Pittner have investigated perturbative[72] triples in the context

of Brillouin-Wigner MRCC. Nonetheless, these approaches are not entirely satisfactory, as their theoretical formulation involves some drastic assumptions; moreover, none of these schemes have been extensively tested and applied. Further work from both the theoretical as well as computational side is needed to improve previous approaches and to find a unifying and rigorous formulation. Thusfar, no (T) correction has been formulated in the context of Mk-MRCC. Concerning iterative triples approaches, Pittner and Demel introduced in the context of Brillouin-Wigner multireference coupled cluster (BW-MRCC) the so-called T-α[73] approximation, which is based on the generalized Bloch equation[37] for the triples amplitudes

$$
\begin{aligned}
\lambda(E_\alpha - H_{\mu\mu}^{\text{eff}})\left\langle \Phi_{ijk}^{abc}(\mu)\middle| e^{\hat{T}_1^\mu + \hat{T}_2^\mu + \hat{T}_3^\mu}\middle| \Phi_\mu \right\rangle &= \left\langle \Phi_{ijk}^{abc}(\mu)\middle| \hat{H}_N(\mu) e^{\hat{T}_1^\mu + \hat{T}_2^\mu + \hat{T}_3^\mu}\middle| \Phi_\mu \right\rangle_{\text{C}} \\
&+ \lambda\left\langle \Phi_{ijk}^{abc}(\mu)\middle| \hat{H}_N(\mu) e^{\hat{T}_1^\mu + \hat{T}_2^\mu + \hat{T}_3^\mu}\middle| \Phi_\mu \right\rangle_{\text{DC,L}}.
\end{aligned}
\tag{5}
$$

In Eq. (5), $\hat{H}_N(\mu)$ is the normal-ordered part of the Hamiltonian operator with respect to the vacuum Φ_μ, $H_{\mu\mu}^{\text{eff}} = \left\langle \Phi_\mu \middle| \hat{H} e^{\hat{T}^\mu}\middle| \Phi_\mu \right\rangle$ is the diagonal part of the effective Hamiltonian, and $\Phi_{ijk}^{abc}(\mu)$ denotes triply excited determinants vis-à-vis Φ_μ. The subscript C denotes connected diagrams, whereas DCL and UL refer, respectively, to disconnected linked diagrams and unlinked diagrams. Setting $\lambda = 1$ recovers the BW-MRCC method, while $\lambda = 0$ yields the Rayleigh-Schrödinger (RS) Bloch equation CC. The BW-MRCCSDT-α approximation neglects the λ-scaled terms on both sides of Eq. (5). This excludes the disconnected linked and the unlinked contributions to the $\hat{T}_3$ amplitudes. Pittner and Demel[73] at the same time investigated the effect of approximating the similarity-transformed Hamiltonian

$$
\bar{H}_\mu = e^{-\hat{T}^\mu} \hat{H} e^{\hat{T}^\mu},
\tag{6}
$$

following the CCSDT-n approach.[52,53,59] Results from a preliminary implementation on O_2 and NF showed an improvement over BW-MRCCSD results.

In the following sections we describe our approach to the iterative triples approximation within Mk-MRCC theory. We outline the underlying theory and present first results for standard model systems used in MRCC theory, H4, P4, BeH$_2$, and H8. In addition, we discuss the prospects for an efficient implementation of the suggested Mk-MRCCSDT-n schemes suitable for large-scale applications. This contribution lays groundwork for future research on a (T) correction in Mk-MRCC theory.

4.3 THEORY

In the following discussion we use indices i, j, k, and m for occupied (occ) orbitals, while a, b, c, and e denote virtual (vir) orbitals, the orbital classes being defined in all cases with respect to some indicated reference determinant. The state specific MRCC method of Mukherjee is obtained assuming the state-specific JM ansatz for the wave function and using a well defined set of sufficiency conditions. Inserting Eq. (1) into the Schrödinger equation gives

$$\sum_{\mu=1}^{d}\left[\hat{H}e^{\hat{T}^{\mu}}\left|\Phi_{\mu}\right\rangle c_{\mu}^{(\alpha)} - E^{(\alpha)}e^{\hat{T}^{\mu}}\left|\Phi_{\mu}\right\rangle c_{\mu}^{(\alpha)}\right] = 0 . \tag{7}$$

It is convenient to introduce a projection operator unto the model space $\hat{P}$ defined as

$$\hat{P} = \sum_{\mu=1}^{d}\left|\Phi_{\mu}\right\rangle\left\langle\Phi_{\mu}\right|, \tag{8}$$

as well as its orthogonal complement $\hat{Q} = 1 - \hat{P}$. If Eq. (7) is multiplied by the identity

$$1 = e^{\hat{T}^{\mu}}e^{-\hat{T}^{\mu}} = e^{\hat{T}^{\mu}}(\hat{P}+\hat{Q})e^{-\hat{T}^{\mu}} = \sum_{\nu=1}^{d} e^{\hat{T}^{\mu}}\left|\Phi_{\nu}\right\rangle\left\langle\Phi_{\nu}\right|e^{-\hat{T}^{\mu}} + e^{\hat{T}^{\mu}}\hat{Q}e^{-\hat{T}^{\mu}} = \hat{P}_{\mu} + \hat{Q}_{\mu}, \tag{9}$$

we obtain

$$\sum_{\mu,\nu} e^{\hat{T}^{\mu}}\left|\Phi_{\nu}\right\rangle H_{\nu\mu}^{\text{eff}}c_{\mu}^{(\alpha)} + \sum_{\mu} e^{\hat{T}^{\mu}}\hat{Q}\bar{H}_{\mu}\left|\Phi_{\mu}\right\rangle c_{\mu}^{(\alpha)} - E^{(\alpha)}\sum_{\mu} e^{\hat{T}^{\mu}}\left|\Phi_{\mu}\right\rangle c_{\mu}^{(\alpha)} = 0 . \tag{10}$$

Upon interchanging the indices μ and ν in the double summation of Eq. (10) and collecting the individual terms, we arrive at

$$\sum_{\mu} \left[\sum_{\nu} e^{\hat{T}^{\nu}} \left| \Phi_{\mu} \right\rangle H_{\mu\nu}^{\text{eff}} c_{\nu}^{(\alpha)} + e^{\hat{T}^{\mu}} \hat{Q} \bar{H}_{\mu} \left| \Phi_{\mu} \right\rangle c_{\mu}^{(\alpha)} - E^{(\alpha)} e^{\hat{T}^{\mu}} \left| \Phi_{\mu} \right\rangle c_{\mu}^{(\alpha)} \right] = 0 . \tag{11}$$

The Mk-MRCC sufficiency conditions are chosen such that Eq. (11) is satisfied by setting the individual terms in the summation over μ to zero. After multiplication by $e^{-\hat{T}^{\mu}}$ and left projection on the excited determinants $\Phi_{ij\ldots}^{ab\ldots}(\mu)$, the final amplitude equations become

$$\left\langle \Phi_{ij\ldots}^{ab\ldots}(\mu) \middle| \bar{H}_{\mu} \middle| \Phi_{\mu} \right\rangle c_{\mu}^{(\alpha)} + \sum_{\nu(\neq\mu)} \left\langle \Phi_{ij\ldots}^{ab\ldots}(\mu) \middle| e^{-\hat{T}^{\mu}} e^{\hat{T}^{\nu}} \middle| \Phi_{\mu} \right\rangle H_{\mu\nu}^{\text{eff}} c_{\nu}^{(\alpha)} = 0 \quad (\mu = 1, 2, \ldots, d) \tag{12}$$

Mukherjee and co-workers[38,39] proved the connected nature of the coupling terms and thus showed that Mk-MRCC is rigorously size extensive. These coupling terms resemble those present in SU-MRCC theory, but with the important difference that both the bra and ket refer to the same reference Φ_{μ}.

The Mk-MRCCSDT method is defined by Eq. (12) with the projection over all singly $\Phi_i^a(\mu)$, doubly $\Phi_{ij}^{ab}(\mu)$, and triply $\Phi_{ijk}^{abc}(\mu)$ excited determinants. The cluster operator is

$$\hat{T}^{\mu} = \hat{T}_1^{\mu} + \hat{T}_2^{\mu} + \hat{T}_3^{\mu}, \tag{13}$$

with the individual components expressed as

$$\hat{T}_1^{\mu} = \sum_i^{\text{occ}(\mu)} \sum_a^{\text{vir}(\mu)} t_i^a(\mu) \hat{a}_a^+ \hat{a}_i , \tag{14}$$

$$\hat{T}_2^{\mu} = \frac{1}{4} \sum_{ij}^{\text{occ}(\mu)} \sum_{ab}^{\text{vir}(\mu)} t_{ij}^{ab}(\mu) \hat{a}_b^+ \hat{a}_j \hat{a}_a^+ \hat{a}_i , \tag{15}$$

and

$$\hat{T}_3^{\mu} = \frac{1}{36} \sum_{ijk}^{\text{occ}(\mu)} \sum_{abc}^{\text{vir}(\mu)} t_{ijk}^{abc}(\mu) \hat{a}_c^+ \hat{a}_k \hat{a}_b^+ \hat{a}_j \hat{a}_a^+ \hat{a}_i . \tag{16}$$

Table 4.1. Approximation of the similarity-transformed Hamiltonian in the SRCCSDT-*n* models. Only the connected part of each term is included.

Projection	$\left\lvert \Phi_i^a \right\rangle$	$\left\lvert \Phi_{ij}^{ab} \right\rangle$	$\left\lvert \Phi_{ijk}^{abc} \right\rangle$
CCSDT-1a	$\hat{H}\exp\left(\hat{T}_1 + \hat{T}_2 + \hat{T}_3\right)$	$\hat{H}\exp\left(\hat{T}_1 + \hat{T}_2\right) + \hat{H}\hat{T}_3$	$\hat{H}\hat{T}_2 + \hat{F}\hat{T}_3$
CCSDT-1b	$\hat{H}\exp\left(\hat{T}_1 + \hat{T}_2 + \hat{T}_3\right)$	$\hat{H}\exp\left(\hat{T}_1 + \hat{T}_2 + \hat{T}_3\right)$	$\hat{H}\hat{T}_2 + \hat{F}\hat{T}_3$
CCSDT-2	$\hat{H}\exp\left(\hat{T}_1 + \hat{T}_2 + \hat{T}_3\right)$	$\hat{H}\exp\left(\hat{T}_1 + \hat{T}_2 + \hat{T}_3\right)$	$\hat{H}\exp\left(\hat{T}_2\right) + \hat{F}\hat{T}_3$
CCSDT-3	$\hat{H}\exp\left(\hat{T}_1 + \hat{T}_2 + \hat{T}_3\right)$	$\hat{H}\exp\left(\hat{T}_1 + \hat{T}_2 + \hat{T}_3\right)$	$\hat{H}\exp\left(\hat{T}_1 + \hat{T}_2\right) + \hat{F}\hat{T}_3$

Here, we have been careful to note that the amplitudes in Eqs. (14)-(16) belong to reference Φ_μ by adding the symbol μ in parentheses. Assuming the model space used to build the zeroth-order wave function is a complete active space (CAS), we can require the wave operator to satisfy intermediate normalization

$$\left\langle \Phi_\nu \left\lvert e^{\hat{T}^\mu} \right\rvert \Phi_\mu \right\rangle = 0 \qquad (\nu \neq \mu). \tag{17}$$

This condition implies that the so-called *internal amplitudes* corresponding to excitations that transform a reference determinant Φ_μ into another reference determinant Φ_ν are set to zero:[30]

$$\cdots \hat{a}_b^\dagger \hat{a}_j \hat{a}_a^\dagger \hat{a}_i \left\lvert \Phi_\mu \right\rangle = \pm \left\lvert \Phi_\nu \right\rangle \quad \Rightarrow \quad t_{ij\cdots}^{ab\cdots}(\mu) = 0. \tag{18}$$

The computational scaling of the Mk-MRCCSDT method has a leading contribution determined by the evaluation of the similarity-transformed Hamiltonian for each reference, requiring $d \times O^3 V^5$ operations.

Our Mk-MRCCSDT-*n* theories introduce simplifications of the $\bar{H}_{ij\cdots}^{ab\cdots}(\mu) = \left\langle \Phi_{ij\cdots}^{ab\cdots}(\mu) \left\lvert \bar{H}_\mu \right\rvert \Phi_\mu \right\rangle$ matrix elements following the analogous SRCCSDT-*n* methods. The similarity-transformed Hamiltonians employed in our CCSDT-*n* schemes are summarized in Table 4.1, where we show explicitly which contributions are included.

We also consider two approximations to our Mk-MRCCSDT-n methods. The first approximation involves the triples coupling terms $\langle \Phi_{ijk}^{abc}(\mu) | e^{-\hat{T}^\mu} e^{\hat{T}^\nu} | \Phi_\mu \rangle$. The full expression for the coupling terms is[45]

$$
\begin{aligned}
\langle \Phi_{ijk}^{abc}(\mu) | e^{-\hat{T}^\mu} e^{\hat{T}^\nu} | \Phi_\mu \rangle &= \langle \Phi_{ijk}^{abc}(\mu) | \Delta\hat{T}_3^{(\nu/\mu,\mu)} | \Phi_\mu \rangle + \langle \Phi_{ijk}^{abc}(\mu) | \Delta\hat{T}_1^{(\nu/\mu,\mu)} \Delta\hat{T}_2^{(\nu/\mu,\mu)} | \Phi_\mu \rangle \\
&\quad + \frac{1}{6} \langle \Phi_{ijk}^{abc}(\mu) | \left(\Delta\hat{T}_1^{(\nu/\mu,\mu)} \right)^3 | \Phi_\mu \rangle \\
&= \Delta t_{ijk}^{abc}(\nu/\mu,\mu) \\
&\quad + P(i/jk)P(a/bc)\Delta t_i^a(\nu/\mu,\mu)\Delta t_{jk}^{bc}(\nu/\mu,\mu) \\
&\quad + P(abc)\Delta t_i^a(\nu/\mu,\mu)\Delta t_j^b(\nu/\mu,\mu)\Delta t_k^c(\nu/\mu,\mu),
\end{aligned}
\tag{19}
$$

where the permutation operators are defined as

$$
P(a/bc)f(a,b,c) = f(a,b,c) - f(b,a,c) - f(c,b,a),
\tag{20}
$$

and

$$
\begin{aligned}
P(abc)f(a,b,c) &= f(a,b,c) + f(b,c,a) + f(c,a,b) \\
&\quad - f(b,a,c) - f(a,c,b) - f(c,b,a).
\end{aligned}
\tag{21}
$$

The $\Delta\hat{T}_k^{(\nu/\mu,\nu)}$ operators and the $\Delta t_{ij\cdots}^{ab\cdots}(\nu/\mu,\mu)$ amplitudes are

$$
\begin{aligned}
\Delta\hat{T}^{(\nu/\mu,\mu)} &= \sum_{k=1}^{n} \frac{1}{(k!)^2} \sum_{ij\cdots}^{\text{occ}(\mu)} \sum_{ab\cdots}^{\text{vir}(\mu)} \left[t_{ij\cdots}^{ab\cdots}(\nu/\mu) - t_{ij\cdots}^{ab\cdots}(\mu) \right] \ldots \hat{a}_b^+ \hat{a}_j \hat{a}_a^+ \hat{a}_i \\
&= \sum_{k=1}^{n} \frac{1}{(k!)^2} \sum_{ij\cdots}^{\text{occ}(\mu)} \sum_{ab\cdots}^{\text{vir}(\mu)} \Delta t_{ij\cdots}^{ab\cdots}(\nu/\mu,\mu) \ldots \hat{a}_b^+ \hat{a}_j \hat{a}_a^+ \hat{a}_i \\
&= \sum_{k=1}^{n} \Delta\hat{T}_k^{(\nu/\mu,\mu)},
\end{aligned}
\tag{22}
$$

with the "common" amplitudes of operator $\hat{T}^\nu$ with respect to $\hat{T}^\mu$ defined as

$$
t_{ij\cdots}^{ab\cdots}(\nu/\mu) =
\begin{cases}
t_{ij\cdots}^{ab\cdots}(\nu) & \text{if } i,j,\ldots \in \text{occ}(\mu) \\
& \text{and } a,b,\ldots \in \text{vir}(\mu) \\
0 & \text{else.}
\end{cases}
\tag{23}
$$

The three contributions to the coupling matrix elements in Eq. (19) are the linear $\Delta t_{ijk}^{abc}(\nu/\mu,\mu)$, the quadratic $P(i/jk)P(a/bc)\Delta t_i^a(\nu/\mu,\mu)\Delta t_{jk}^{bc}(\nu/\mu,\mu)$, and the cubic

$P(abc) \Delta t_i^a(\nu/\mu,\mu) \Delta t_j^b(\nu/\mu,\mu) \Delta t_k^c(\nu/\mu,\mu)$ terms. Assuming the singles and doubles amplitudes are first-order quantities, while the triples are second-order quantities, then the coupling terms may be classified as second-order (linear and quadratic terms) and third order (cubic term).

Our second approximation to the Mk-MRCCSDT-n approaches entails the neglect of off-diagonal Fock matrix elements to enhance computational efficiency. One of the design features of the SRCCSDT-n methods is that they do not require storage of the $\hat{T}_3$ amplitudes, as all terms which couple different $\hat{T}_3$ operators are omitted.[52,53,59] However, storage can be only avoided when these schemes are used together with canonical Hartree-Fock (HF) orbitals. In a more general formulation, which applies also to the present multireference case, the CCSDT-n methods still involve the following contribution

$$\bar{H}_{ijk}^{abc}(\mu) \leftarrow -P(ij/k) \sum_{m}^{occ(\mu)} t_{ijm}^{abc}(\mu) f_{mk}(\mu) + P(ab/c) \sum_{e}^{vir(\mu)} t_{ijk}^{abe}(\mu) f_{ec}(\mu), \qquad (24)$$

which couples different $\hat{T}_3$ amplitudes via the off-diagonal elements [$f_{mk}(\mu)$ and $f_{ec}(\mu)$] of the Fock matrix for reference $|\Phi_\mu\rangle$. In SRCCSDT-n methods based on restricted open-shell HF (ROHF) or localized HF orbitals,[74-77] this problem, which in principal would require storage of $\hat{T}_3$, is resolved either (in the ROHF case) by transforming the orbitals to a semicanonical representation[78] with diagonal occupied-occupied and virtual-virtual blocks of the Fock matrix, or (in the case of localized orbitals) by (partially) neglecting the troublesome off-diagonal elements of $\hat{F}$. Similar ideas have been also pursued in order to avoid the storage of $\hat{T}_3$ amplitudes in perturbative treatments of triple excitations based either on ROHF or localized HF orbitals[75,79] or when using the full similarity-transformed Hamiltonian.[57,58]

Unfortunately, in the multireference case, a solution to the $\hat{T}_3$ coupling problem via orbital transformations seems not to be viable, because it is not possible to diagonalize simultaneously the Fock matrices for all d references. In a rigorous formulation, the MRCCSDT-n schemes thus require storage of the $\hat{T}_3$ amplitudes. The necessity to store $\hat{T}_3$ is solely due to the similarity-transformed Hamiltonian, as the Mk coupling terms just require the simultaneous availability of the same $\hat{T}_3$ amplitudes (*i.e.*, those with the same orbital indices) for the different references.

It is therefore natural to pursue our second approximation, specifically, modified MRCCSDT-n schemes in which the off-diagonal elements of $\hat{F}$ are neglected to eliminate the problematic $\hat{F}\hat{T}_3$ couplings. Such modified schemes can be implemented without storage of $\hat{T}_3$; the resulting equations are then coupled only with respect to amplitudes belonging to the different references but *with the same orbital labels*. Thus, the $\hat{T}_3$ equations may be solved by simultaneously computing the $\hat{T}_3$ amplitudes for all references within a loop over all orbital indices. While such modified MRCCSDT-n methods are less rigorous and clearly not orbital invariant, they may prove to be both computationally feasible and acceptably accurate in practical chemical applications, warranting their investigation here. Furthermore, this issue, *i.e.*, the effect of the off-diagonal part of the Fock operator, is of vital importance for the development of a (T) correction for any MRCC scheme based on the JM ansatz.

4.4 COMPUTATIONAL DETAILS

The similarity-transformed Hamiltonian matrix elements for the CCSDT-n (n = 1a, 1b, 2, 3) and CCSDT models were coded in the LOOPMRCC program, developed at the University of Georgia and the Universität Mainz, using intermediates given by Gauss and Stanton earlier for

the single-reference case.[80,81] The coupling terms and update equations were implemented in

LOOPMRCC according to the equations given in our earlier work.[45] Our implementation of the

Mk-MRCCSDT-n and Mk-MRCCSDT methods has the proper scaling, which is the scaling of

the corresponding single-reference CC methods times the number of references d.

LOOPMRCC was benchmarked on single-reference closed- and open-shell systems against CCSD,

CCSDT-1a, CCSDT-1b, CCSDT-2, CCSDT-3, and CCSDT energies generated with ACESII.[82]

These tests confirmed the correctness of the similarity-transformed Hamiltonian matrix elements.

The implementation of the triples coupling terms in Eq. (19) was benchmarked against our

arbitrary-order Mk-MRCC code DETC++.[68]

All computations were carried with the Psi 3.3 package.[83] The orbitals were generated with either

the CSCF or DETCAS modules, and the atomic integrals were transformed to the MO basis using

the TRANSQT module.

4.5 MK-MRCCSDT-N RESULTS FOR MODEL SYSTEMS

In this section Mk-MRCCSDT-n results are presented for the classic H4, P4, BeH$_2$, and

H8 model systems, constituting the first applications of these new multireference CCSDT-n

methods. The basis sets employed for each system are described in the subsections below and

are fully specified in Supplementary Material.[84] For each level of theory (X), plots are displayed

for the difference between the total electronic energy and the FCI value at a given molecular

geometry $\mathbf{R}$,

$$\Delta E_X(\mathbf{R}) = E_X(\mathbf{R}) - E_{FCI}(\mathbf{R}). \tag{25}$$

The ΔE_X diagnostic is preferable to the percent of the correlation energy recovered, since the

former is independent of the choice for the reference wave function. Another measure employed

here for the quality of the potential energy curves is the nonparallelism error (NPE) with respect to FCI over a range (R) of geometries ($\mathbf{R}$), defined as

$$\text{NPE} = \max_{\mathbf{R} \in R} [\Delta E_X(\mathbf{R})] - \min_{\mathbf{R} \in R} [\Delta E_X(\mathbf{R})]. \tag{26}$$

A final, more sensitive diagnostic quantifying nonparallelism of $E_X(\mathbf{R})$ from the FCI standard is the mean nonparallelism derivative (MNPD),

$$\text{MNPD} = \left\{ \frac{\int_R \left[E'_X(\mathbf{R}) - E'_{\text{FCI}}(\mathbf{R}) \right]^2 d\mathbf{R}}{\int_R \left[E'_{\text{FCI}}(\mathbf{R}) \right]^2 d\mathbf{R}} \right\}^{1/2}. \tag{27}$$

Tables 4.2-4.5 report the NPE and MNPD values for the model systems investigated in this study.

The H4, P4, BeH$_2$, and H8 models all involve only two closed-shell reference determinants. The Mk-MRCC methods were applied with CAS(2,2) orbitals, optimized for the target state. The Mk-MRCC methods applied here are rigorously invariant to all (occupied, occupied) and (virtual, virtual) orbital rotations completely outside the active space, provided that no off-diagonal Fock matrix elements are neglected; however, orbital rotations within the active space do change the MRCC energy, as we have discussed previously.[45] We canonicalized the orbitals as CAS(2,2) natural orbitals. As long as the model systems are not distorted into a lower point-group symmetry, the active space orbitals belong to different irreducible representations (irreps) and automatically come out of the CAS(2,2) computations as natural orbitals.

4.5.1 H4

In the H4 model, four hydrogen atoms are arranged as an isosceles trapezoid with all the nearest-neighbor distances (r) fixed to exactly 2 bohr, considerably longer than the H$_2$

139

equilibrium bond length of around 1.4 bohr. Varying the angle θ in Scheme 1 deforms the trapezoid from a square configuration (90°) to a linear chain (180°).

$$r = 2 \text{ bohr}$$
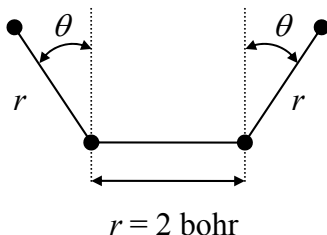
Scheme 4.1. The H4 Model.

The geometry of the H4 model can be parametrized by a continuous parameter $\alpha \in \left[0, \frac{1}{2}\right]$ that specifies $\theta = \pi(\alpha + \frac{1}{2})$. This model system, first introduced by Jankowski and Paldus,[85] has been studied using the SU-MRCC,[33,86,87] BW-MRCC,[35] and Mk-MRCC[39] methods, the multireference coupled cluster theory of Hanrath (MRexpT),[41] and the state-specific perturbation theory based on Mk-MRCC (SS-MRPT).[88]

At the square planar geometry ($\alpha = 0$, D_{4h} symmetry), the H4 system has the electronic configuration $(1a_{1g})^2 (1e_u)^2$, and the zeroth-order wave function is an equal mixture of the two degenerate determinants

$$\left|\Phi_1\right\rangle = \left|(1a_{1g})^2 (1e_{ua})^2\right\rangle, \quad \left|\Phi_2\right\rangle = \left|(1a_{1g})^2 (1e_{ub})^2\right\rangle. \tag{28}$$

For trapezoidal geometries ($0 < \alpha < 1/2$, C_{2v} symmetry) and the linear structure ($\alpha = 1/2$, $D_{\infty h}$ symmetry), the degeneracy is lifted. The two determinants of the zeroth-order wave function map into

$$\left|\Phi_1\right\rangle = \left|(1a_1)^2 (1b_2)^2\right\rangle, \quad \left|\Phi_2\right\rangle = \left|(1a_1)^2 (2a_1)^2\right\rangle, \tag{29}$$

in C_{2v} symmetry and

140

$$\left|\Phi_1\right\rangle = \left|(1\sigma_g^+)^2(1\sigma_u^+)^2\right\rangle, \quad \left|\Phi_2\right\rangle = \left|(1\sigma_g^+)^2(2\sigma_g^+)^2\right\rangle, \tag{30}$$

for the linear geometry ($D_{\infty h}$). For both the trapezoidal and linear geometries $\left|\Phi_1\right\rangle$ is the dominant configuration.

The H4 model was studied using a ($4s1p/2s1p$) double-ζ plus polarization (DZP)[89,90] basis set with α_p(H) = 0.75 bohr^{-2} (see Supplementary Material).[84] The $\left|\Phi_1\right\rangle$ and $\left|\Phi_2\right\rangle$ determinants comprised the reference space, and the molecular orbitals were obtained from the corresponding CAS(2,2) computation. In Fig. 4.1, $\Delta E_X(\alpha)$ curves are presented for the various Mk-MRCCSDT-n methods and compared to our previous Mk-MRCCSD and Mk-MRCCSDT results. The range of the plot is −0.2 to 0.5 mE_h, indicating that even the lowest level of theory (Mk-MRCCSD) is not far removed from FCI. Most importantly, all of the Mk-MRCCSDT-n methods recover most of the triples effect on the energy. As shown in Table 4.2, full inclusion of triples lowers the nonparallelism error (NPE) from 0.677 (Mk-MRCCSD) to 0.107 mE_h (Mk-MRCCSDT), and more than 73% of this reduction is achieved by each of the Mk-MRCCSDT-n methods, if no contributions are omitted from the coupling terms and Fock matrix elements (top row of table). This extent of error reduction is quite uniform in Fig. 4.1, where the Mk-MRCCSDT-n curves (B-E) lie between the Mk-MRCCSD and Mk-MRCCSDT boundaries and are much closer to the full triples result at essentially all geometries. The Mk-MRCCSDT-1a curve (B) happens to be noticeably closer to Mk-MRCCSDT than those of the more complete triples methods, whose performance is hardly distinguishable on the plot.

Figure 4.1. Mk-MRCC/DZP energy curves for the $^1A_1$ ground state of the H4 model system using CAS(2,2) orbitals. The full triples coupling term and off-diagonal Fock matrix elements are included. The lower panel shows the square of the CAS(2,2) CI coefficient of $\left|\Phi_1\right\rangle$ vs. the parameter α.
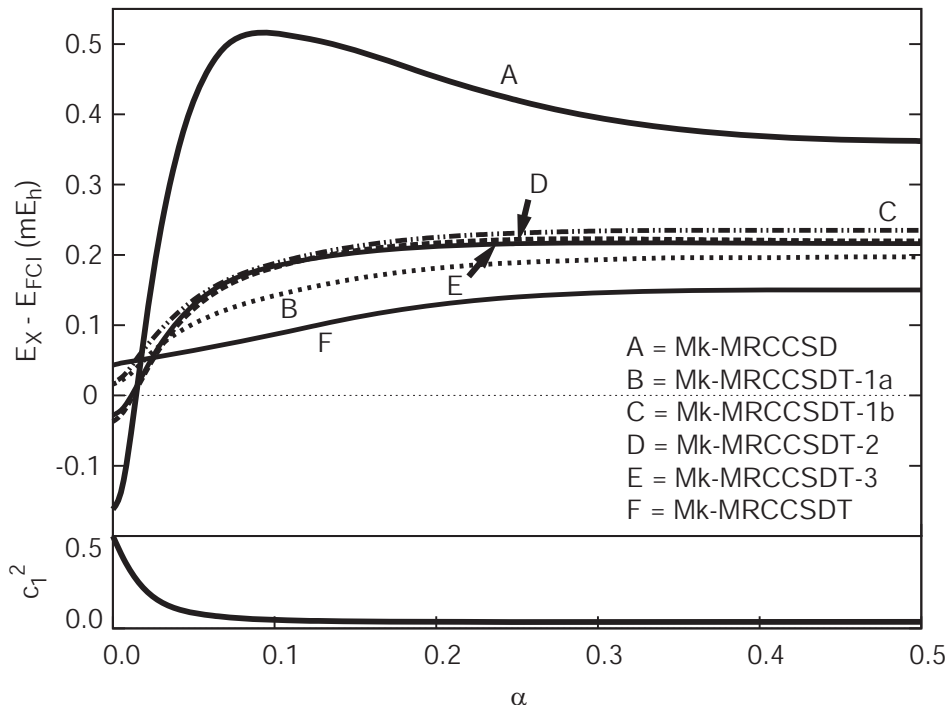
According to the MNPD diagnostic, Mk-MRCCSDT mirrors the FCI curve better than Mk-MRCCSD by a factor of 14. Over 77% of the full triples MNPD reduction is provided by the Mk-MRCCSDT-n methods, with the 1a approximation yielding the best results as before. It is gratifying that all of the Mk-MRCC methods that incorporate connected triples are substantially more accurate in the multireference region of the H4 model ($\alpha < 0.05$) than in the single-reference limit.

Table 4.2. Nonparallelism Error (NPE) in mE$_h$ and Mean Nonparallelism Derivative (MNPD) for the Mk-MRCC /DZP energy curves of the $^1A_1$ ground state of the H4 model system using CAS(2,2) orbitals. Data from calculations including only the diagonal part of the Fock matrices are indicated with ($\hat{F}_{\text{diag}}$).

| | Mk-MRCC method | | | | | |
Triples Coupling	SD	SDT-1a	SDT-1b	SDT-2	SDT-3	SDT
			NPE			
Complete	0.677	0.181	0.217	0.259	0.245	0.107
Quadratic		0.181	0.217	0.259	0.245	
Linear		0.202	0.234	0.276	0.263	
Complete ($\hat{F}_{\text{diag}}$)		0.206	0.243	0.285	0.272	
Quadratic ($\hat{F}_{\text{diag}}$)		0.206	0.243	0.285	0.272	
Linear ($\hat{F}_{\text{diag}}$)		0.227	0.259	0.301	0.289	
			MNPD ($\times 10^3$)			
Complete	8.36	1.34	1.78	2.35	2.31	0.59
Quadratic		1.34	1.78	2.35	2.31	
Linear		1.48	1.88	2.45	2.40	
Complete ($\hat{F}_{\text{diag}}$)		1.47	1.96	2.54	2.49	
Quadratic ($\hat{F}_{\text{diag}}$)		1.47	1.96	2.54	2.49	
Linear ($\hat{F}_{\text{diag}}$)		1.70	2.07	2.65	2.60	

4.5.2 P4

In the P4 model[85] (Scheme 2) four hydrogen atoms form a rectangle with a fixed height of 2 bohr and variable length α (in bohr). The three geometrical regions of the P4 model are (A) compressed, $\alpha < 2$; (B) square, $\alpha = 2$; and (C) elongated, $\alpha > 2$.
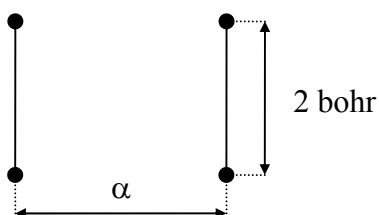
Scheme 4.2. The P4 Model.

For the square configuration (D_{4h}) the zeroth-order wave function is an equal mixture of the two degenerate determinants

$$\left|\Phi_1\right\rangle = \left|(1a_{1g})^2(1e_{ua})^2\right\rangle, \quad \left|\Phi_2\right\rangle = \left|(1a_{1g})^2(1e_{ub})^2\right\rangle, \tag{31}$$

which transform into D_{2h} symmetry as

$$\left|\Phi_1\right\rangle = \left|(1a_1)^2(1b_{3u})^2\right\rangle, \quad \left|\Phi_2\right\rangle = \left|(1a_1)^2(1b_{2u})^2\right\rangle, \tag{32}$$

for both compression and elongation. Thus, the P4 system is multireference in character in the middle of the potential energy curve, whereas the compressed and elongated regions are dominated by $\left|\Phi_1\right\rangle$ and $\left|\Phi_2\right\rangle$, respectively. This feature makes the P4 model a good complement to the H4 model. Previously, the P4 model has been a test case for SU-MRCC[33,86] and Mk-MRCC theories.[39]

Our computations on the P4 model were executed with the same DZP basis set used for the H4 model and with molecular orbitals optimized over the CAS(2,2) space of $\left|\Phi_1\right\rangle$ and $\left|\Phi_2\right\rangle$. The performance of the Mk-MRCCSDT-n methods on the P4 model can be judged from the $\Delta E_X(\alpha)$ curves in Fig. 4.2. The lower panel of this figure plots the square of the largest CI coefficient of the CAS(2,2) wave function, indicating that the multireference region of this system is centered at $\alpha = 2$ and extends roughly from 1.75 to 2.25 bohr.

Figure 4.2. Mk-MRCC/DZP energy curves for the $^1A_1$ ground state of the P4 model system using CAS(2,2) orbitals. The full triples coupling term and off-diagonal Fock matrix elements are included. The lower panel shows the square of the CAS(2,2) CI coefficient of $\left|\Phi_1\right\rangle$ vs. the parameter α.
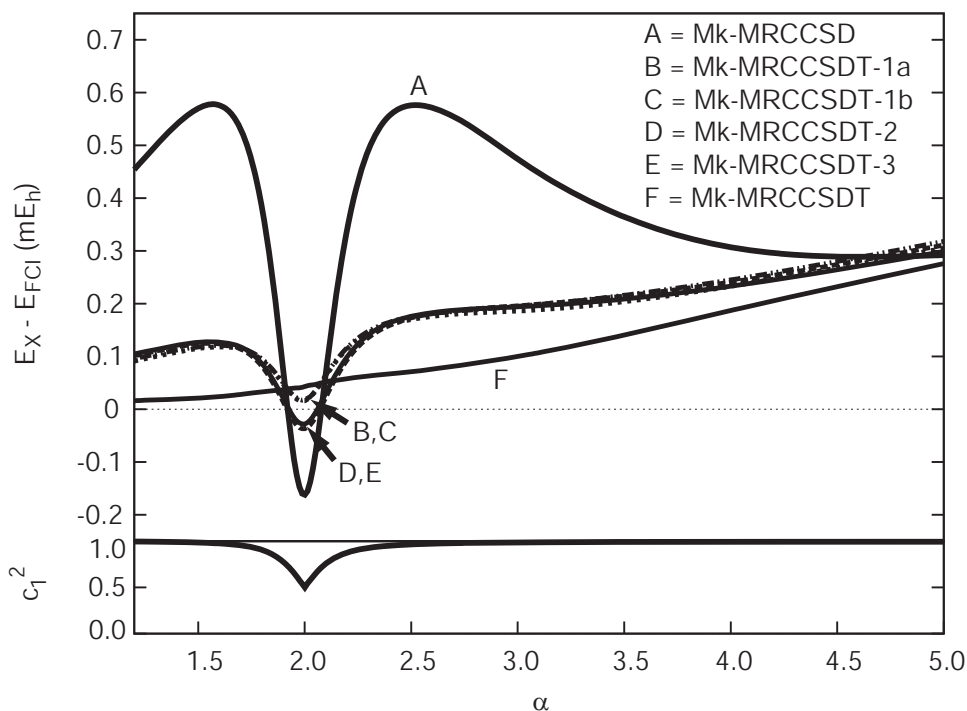
Once again, all of the Mk-MRCCSDT-n methods recover most of the triples effect on the energy. The top row of Table 4.3 shows that more than 80% of the full triples reduction in the nonparallelism error is recovered by each of the Mk-MRCCSDT-n methods.   This NPE characterization is also borne out in Fig. 4.2, where most of the difference between the Mk-MRCCSD and Mk-MRCCSDT curves is uniformly damped out by the Mk-MRCCSDT-n schemes over the entire range of α. Unlike the H4 case, there is very little distinction in the performance of the four approximate triples methods. Among all the methods, Mk-MRCCSDT is the only one in Fig. 4.2 that does not exhibit a pronounced sink in the curve near $\alpha = 2$, the point of maximum multireference character. Thus, while all the Mk-MRCCSDT-n energies lie within 0.1 mE_h of FCI in this region, the full inclusion of triples is necessary to smoothly follow the FCI energy curve near the square-planar configuration of the P4 system. The depth of the sink in the $\Delta E_X(\alpha)$ curves is smaller for the T-1a,1b methods than for T-2,3, as indicated by the MNPD diagnostic. In going from Mk-MRCCSD to Mk-MRCCSDT, the MNPD is cut down by a factor

of 14. The T-1a,1b triples approximations give 89% of this reduction, whereas the T-2,3 schemes recover more than 82% of the triples effect.

Table 4.3. Nonparallelism Error (NPE) in mE_h and Mean Nonparallelism Derivative (MNPD) for the Mk-MRCC/DZP energy curves of the $^1A_1$ ground state of the P4 model system using CAS(2,2) orbitals. Data from calculations including only the diagonal part of the Fock matrices are indicated with ($\hat{F}_{\text{diag}}$).

Triples Coupling	SD	SDT-1a	SDT-1b	SDT-2	SDT-3	SDT
			Mk-MRCC method			
			NPE			
Complete	0.739	0.290	0.300	0.348	0.328	0.259
Quadratic		0.290	0.300	0.348	0.328	
Linear		0.320	0.322	0.370	0.351	
Complete ($\hat{F}_{\text{diag}}$)		0.313	0.324	0.372	0.352	
Quadratic ($\hat{F}_{\text{diag}}$)		0.313	0.324	0.372	0.352	
Linear ($\hat{F}_{\text{diag}}$)		0.344	0.346	0.395	0.376	
			MNPD ($\times 10^3$)			
Complete	11.26	1.98	2.00	2.73	2.66	0.82
Quadratic		1.98	2.00	2.73	2.66	
Linear		2.05	2.06	2.80	2.72	
Complete ($\hat{F}_{\text{diag}}$)		2.18	2.20	2.95	2.88	
Quadratic ($\hat{F}_{\text{diag}}$)		2.18	2.20	2.95	2.88	
Linear ($\hat{F}_{\text{diag}}$)		2.26	2.27	3.02	2.94	

4.5.3 BEH$_2$

The BeH$_2$ model involves the insertion of the beryllium atom into the center of the bond in diatomic H$_2$ to form the linear beryllium hydride molecule. This process was studied at selected points along a C_{2v} path using single-reference coupled cluster theory in 1983.[91] Later, several authors applied various multireference methods to the BeH$_2$ system.[13,39,92-102] Our revision of the original model[91] introduces a continuous path between the reactant and product regions. The beryllium atom is placed at the origin of the axis system, while the two hydrogen atoms move along the lines (Scheme 3)

$$y(x) = \pm(2.54 - 0.46x),\qquad(33)$$

where x varies from 0 to 4 bohr. This path interpolates points A-H of the original model.[91]
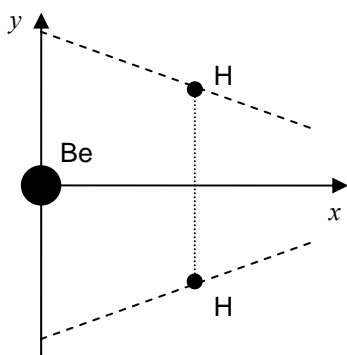
Scheme 4.3. The BeH$_2$ Model.

Molecular BeH$_2$ at its linear ($D_{\infty h}$) equilibrium geometry has the primary configuration

$$\left|\Phi_1\right\rangle = \left|(1\sigma_g)^2(2\sigma_g)^2(1\sigma_u)^2\right\rangle,\qquad(34)$$

which correlates to

$$\left|\Phi_1\right\rangle = \left|(1a_1)^2(2a_1)^2(1b_2)^2\right\rangle,\qquad(35)$$

in C_{2v} symmetry. For dissociated Be + H$_2$ the wave function is predominantly

147

$$\left|\Phi_2\right\rangle = \left|(1a_1)^2(2a_1)^2(3a_1)^2\right\rangle, \tag{36}$$

which transforms to

$$\left|\Phi_2\right\rangle = \left|(1\sigma_g)^2(2\sigma_g)^2(3\sigma_g)^2\right\rangle \tag{37}$$

in $D_{\infty h}$ symmetry. Therefore, the electronic wave function switches from $\left|\Phi_1\right\rangle$ to $\left|\Phi_2\right\rangle$ along the dissociation path, and in the intervening transition state region these determinants are quasidegenerate.[103]

Figure 4.3. Mk-MRCC/[Be(3s2p) /H(2s)] energy curves for the $^1A_1$ ground state of the BeH$_2$ model system using CAS(2,2) orbitals. The full triples coupling term and off-diagonal Fock matrix elements are included. The lower panel shows the square of the CAS(2,2) CI coefficient of $\left|\Phi_1\right\rangle$ vs. the parameter x.
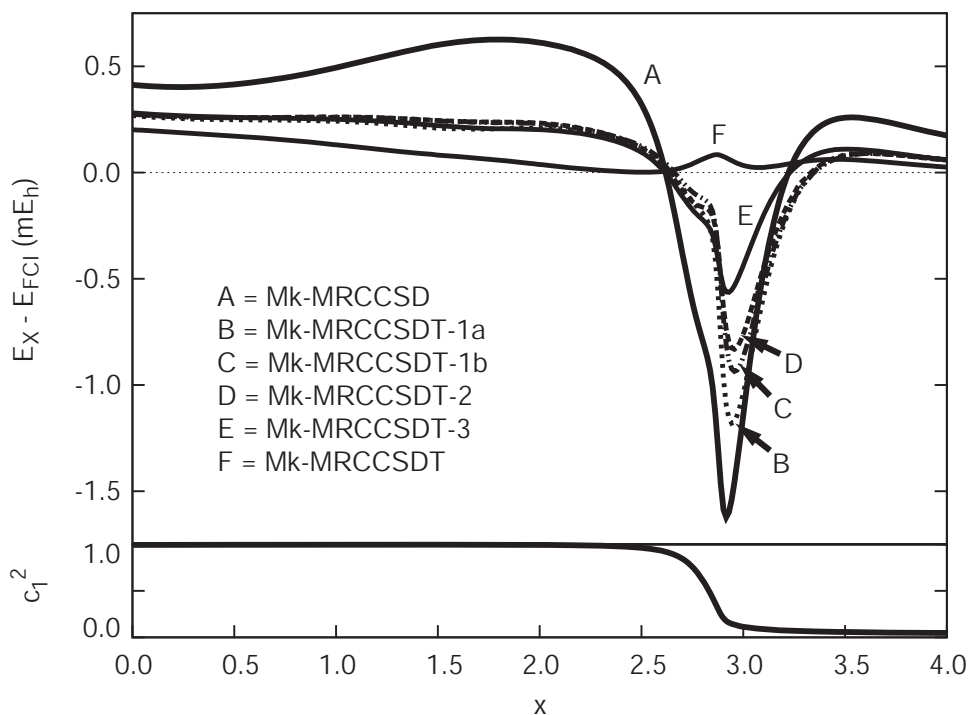
The basis set utilized here for BeH$_2$ (and detailed in the Supplementary Material)[84] is a Be(10s3p/3s2p), H(4s/2s)[89,90] contraction with a tight beryllium p primitive function to describe core correlation. It is a more loosely contracted variant of the double-ζ basis adopted in previous

benchmark studies.[13,39,91-101] The hydrogen basis is identical to the H($4s$/$2s$) manifold employed above for the H4 and P4 models.

The $\Delta E_X(x)$ curves for the BeH$_2$ model are displayed in Fig. 4.3. Unlike the H4 and P4 cases, the performance of the Mk-MRCC methods steadily improves as the level of theory is increased. Indeed, both the NPE and MNPD values in Table 4.4 lie in the order Mk-MRCCSD > Mk-MRCCSDT-1a > Mk-MRCCSDT-1b > Mk-MRCCSDT-2 > Mk-MRCCSDT-3 > Mk-MRCCSDT.   Although this sequence is encouraging, large sinks appear in the multireference region in all of the error curves for the approximate triples schemes. Moreover, none of the Mk-MRCCSDT-n methods recovers more than 70% of the full triples effect, as measured by either the NPE or the MNPD diagnostic. Accordingly, the maximum error with respect to FCI along the BeH$_2$ dissociation path is not reduced below 0.5 mE$_h$ until Mk-MRCCSDT is applied.

The C_{2v} transition state for the insertion of Be into H$_2$ provides a genuine chemical test of multireference theories. In Table 4.6 properties of this transition state predicted by our Mk-MRCC methods are compared to the corresponding FCI benchmarks. The Mk-MRCCSD and Mk-MRCCSDT results for the activation barrier differ by only −0.27 and +0.02 kcal mol^{-1}, respectively, from the FCI value of 100.24 kcal mol^{-1}. This excellent agreement is also achieved by all the approximate triples methods, which yield barriers between 0.01 and 0.06 kcal mol^{-1} below the FCI limit. The H-H and the Be-H distances in the transition state are both underestimated by about 0.026 Å with Mk-MRCCSD, but Mk-MRCCSDT reproduces the FCI geometric parameters within 0.0003 Å! The Mk-MRCCSDT-n methods recover between 54% and 66% of the full triples elongation of the distances in the transition state.   The harmonic vibrational frequencies of the transition state provide the most stringent test. The Mk-MRCCSD

149

frequencies are too large, particularly in the ω_2 case, where the overestimation is almost 20%. However, Mk-MRCCSDT once again proves to be a remarkably accurate theory, giving frequencies within 2 cm^{-1} of the FCI values of $\omega_1 = 3769i$ cm^{-1} and $\omega_2 = 796$ cm^{-1}. The approximate triples methods provide 60%-80% of the full triples effect on ω_2, but only 30%-75% for the imaginary frequency ω_1. The Mk-MRCCSDT-2 scheme performs best for the vibrational frequencies, whereas the T-1a and T-3 approaches are rather disappointing in this instance in that they account for less than 50% of the triples shift on ω_1.

Figure 4.4. Mk-MRCC/[Be(3s2p) /H(2s)] singlet-triplet splittings (ΔE_X^{ST}) of the BeH$_2$ model system using CAS(2,2) orbitals for the $^1A_1$ state and ROHF orbitals for the $^3B_2$ state. The full triples coupling term and off-diagonal Fock matrix elements are included. Curves A-F are referenced to the FCI results and are quantified on the left vertical axis. The absolute FCI splitting is plotted as a dotted line on the scale of the right vertical axis. The lower panel shows the square of the CAS(2,2) CI coefficient of $|\Phi_1\rangle$ vs. the parameter x for the $^1A_1$ state.
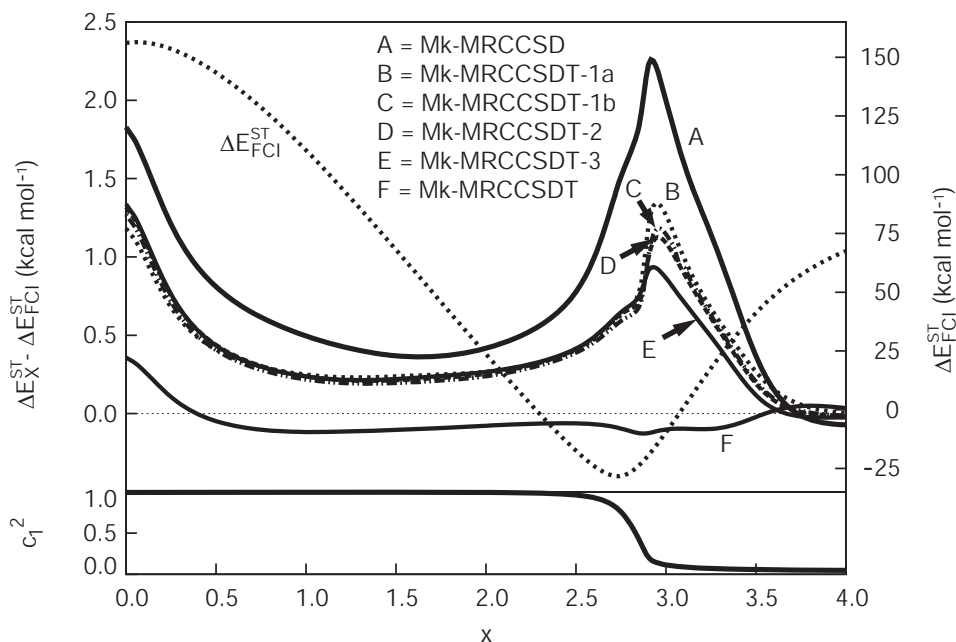
Our final test of methods for the BeH$_2$ model is summarized in Fig. 4.4, where deviations from FCI singlet-triplet splittings are plotted along the BeH$_2$ insertion path. In these computations the $^3B_2$ state of BeH$_2$ was treated consistently within the Mk-MRCC formalisms by converging on the $M_S = 0$ component of the triplet manifold. The error in the Mk-MRCCSD singlet-triplet splitting reaches a maximum of 2.26 kcal mol^{-1} near the point of greatest multireference character ($x = 2.85$). Mk-MRCCSDT almost completely eliminates this error. There is a uniform reduction of the peak in the error curve in progressing from the T-1a to the T-3 approximate triples methods, but the maximum error along the insertion path remains above 1.0 kcal mol^{-1} in all cases.

Table 4.4. Nonparallelism Error (NPE) in mE_h and Mean Nonparallelism Derivative (MNPD) for the Mk-MRCC/[Be(3s2p) /H(2s)] energy curves of the $^1A_1$ ground state of the BeH_2 model system using CAS(2,2) orbitals. Data from calculations including only the diagonal part of the Fock matrices are indicated with ($\hat{F}_{diag}$).

Triples Coupling	SD	SDT-1a	SDT-1b	SDT-2	SDT-3	SDT
			Mk-MRCC method			
			NPE			
Complete	2.238	1.445	1.206	1.104	0.844	0.198
Quadratic		1.498	1.287	1.183	0.906	
Linear		1.481	1.225	1.128	0.863	
Complete ($\hat{F}_{diag}$)		1.432	1.181	1.079	0.819	
Quadratic ($\hat{F}_{diag}$)		1.489	1.221	1.123	0.857	
Linear ($\hat{F}_{diag}$)		1.486	1.264	1.158	0.882	
			MNPD ($\times 10^3$)			
Complete	27.62	22.69	19.03	15.78	10.90	1.13
Quadratic		23.70	20.09	17.28	11.27	
Linear		22.09	17.75	12.16	11.17	
Complete ($\hat{F}_{diag}$)		22.55	18.00	11.32	10.43	
Quadratic ($\hat{F}_{diag}$)		23.57	19.90	17.12	10.90	
Linear ($\hat{F}_{diag}$)		22.05	17.48	11.53	10.71	

4.5.4 H8

The H8 model consists of eight hydrogen atoms arranged in an octagonal configuration with four bond lengths fixed to exactly 2 bohr. A variable distance parameter α (in bohr) determines the deviation from the D_{8h} configuration due to the displacement of a pair of parallel H_2 molecules. Scheme 4 depicts the H8 model and gives the definition of the parameter α.
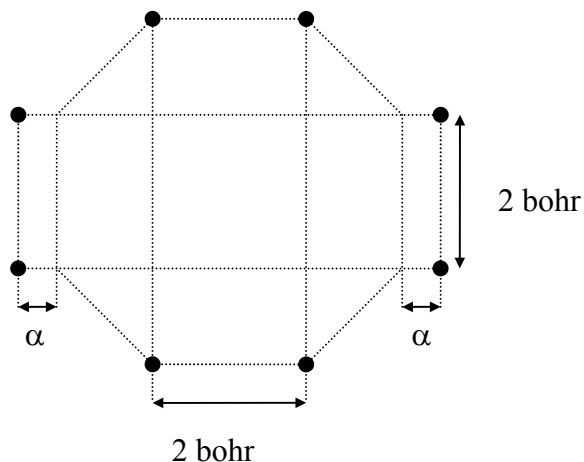
Scheme 4.4. The H8 Model.

This model system was introduced in the 1980s by Jankowski, Meissner and Wasilewski[104] and was later studied intensely by several authors with CASCCSD,[105,106] SU-MRCCSD,[33,86,107] BW-MRCCSD,[108] multireference coupled electron pair approximation (MRCEPA),[109] Mk-MRCCSD[38], and MRexpT[41] theories. As in the P4 model, upon varying the parameter α, the H8 model gives three different types of geometrical configurations: (A) compressed, $\alpha < 0$; (B) octagonal, $\alpha = 0$; and (C) elongated, $\alpha > 0$.

The H8 system is described by a two-dimensional model space with the electronic configurations (in D_{2h} symmetry)

$$
\begin{aligned}
\left| \Phi_1 \right\rangle &= \left| (1a_g)^2 (1b_{3u})^2 (1b_{2u})^2 (1b_{1g})^2 \right\rangle \\
\left| \Phi_2 \right\rangle &= \left| (1a_g)^2 (1b_{3u})^2 (1b_{2u})^2 (2a_g)^2 \right\rangle .
\end{aligned}
\tag{38}
$$

For the compressed geometry the $\left|\Phi_1\right\rangle$ configuration is the restricted Hartree-Fock ground state, while for the elongated geometry, $\left|\Phi_2\right\rangle$ becomes lower in energy than $\left|\Phi_1\right\rangle$. Thus, $\left|\Phi_1\right\rangle$ dominates for $\alpha < 0$ and $\left|\Phi_2\right\rangle$ for $\alpha > 0$. The zeroth-order wave function for the D_{8h} geometry has the electronic configuration

$$(1a_{1g})^2(1e_{1g})^4(1e_{1u})^2 \tag{39}$$

comprising two degenerate determinants.

Figure 4.5. Mk-MRCC/DZ energy curves for the $^1A_1$ ground state of the H8 model system using CAS(2,2) orbitals optimized for the 1 $^1A_1$ state. The full triples coupling term and off-diagonal Fock matrix elements are included. The lower panel shows the square of the CAS(2,2) CI coefficient of $\left|\Phi_1\right\rangle$ vs. the parameter α.
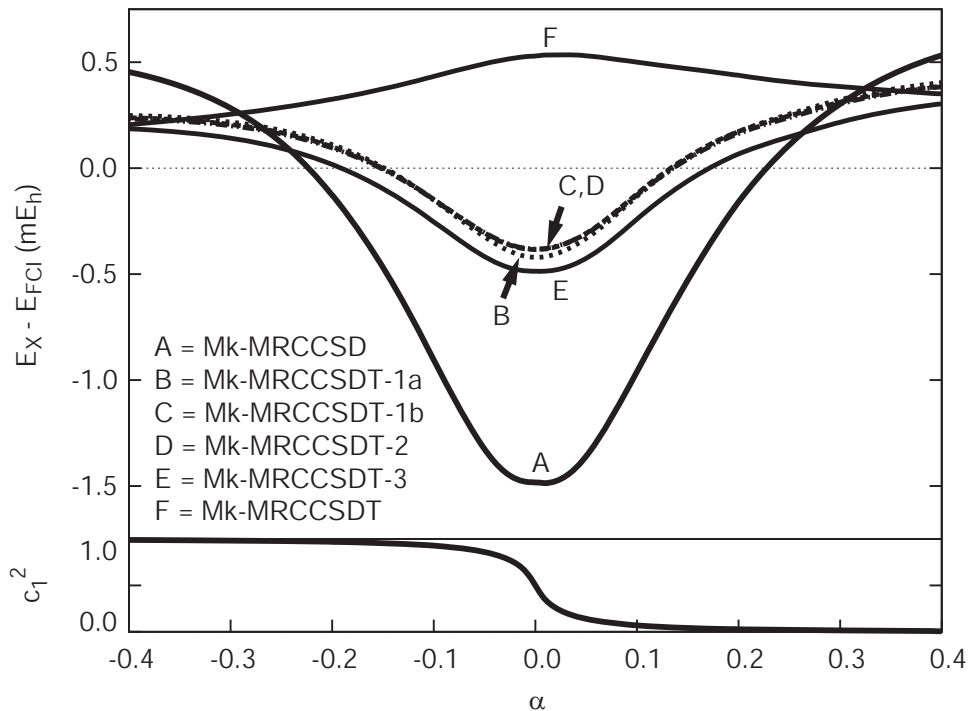
All computations employed ground-state CAS(2,2) orbitals and the s manifold of the DZP basis set utilized above for the H4 and P4 models.[89,90] The $\Delta E_X(\alpha)$ curves in Fig. 4.5 show that all the Mk-MRCCSDT-n schemes perform equally well for the H8 model. The NPE

values in Table 4.5 for the approximate triples methods lie in a narrow range of 0.765-0.825

mE_h, as compared to 2.019 mE_h for Mk-MRCCSD and 0.330 mE_h for Mk-MRCCSDT. The

distribution of the MNPD diagnostics is qualitatively the same. By both the NPE and MNPD

measures, all of the Mk-MRCCSDT-*n* approaches recover between 69% and 74% of the full

triples effect. It is noteworthy in Fig. 4.5 that the curves for the approximate triples methods are

generally closer to FCI than full Mk-MRCCSDT; however, the performance of the latter must be

considered superior because $\Delta E_X(\alpha)$ does not change signs in the multireference region.

Table 4.5. Nonparallelism Error (NPE) in mE_h and Mean Nonparallelism Derivative (MNPD) for the Mk-MRCC/DZ energy curves of the $^1A_1$ ground state of the H8 model system using CAS(2,2) orbitals. Data from calculations including only the diagonal part of the Fock matrices are indicated with ($\hat{F}_{diag}$).

Triples Coupling	SD	SDT-1a	SDT-1b	SDT-2	SDT-3	SDT
			Mk-MRCC method			
			NPE			
Complete	2.019	0.825	0.765	0.771	0.790	0.330
Quadratic		0.825	0.765	0.771	0.790	
Linear		0.819	0.759	0.765	0.785	
Complete ($\hat{F}_{diag}$)		0.823	0.763	0.768	0.788	
Quadratic ($\hat{F}_{diag}$)		0.824	0.763	0.768	0.788	
Linear ($\hat{F}_{diag}$)		0.818	0.758	0.763	0.783	
			MNPD ($\times 10^3$)			
Complete	58.67	23.05	21.19	21.53	22.32	7.31
Quadratic		23.05	21.19	21.53	22.32	
Linear		22.58	20.71	21.05	21.85	
Complete ($\hat{F}_{diag}$)		22.70	20.83	21.14	21.95	
Quadratic ($\hat{F}_{diag}$)		22.70	20.83	21.14	21.95	
Linear ($\hat{F}_{diag}$)		22.48	20.61	20.92	21.73	

Table 4.6. Properties of the transition state for the C_{2v} insertion of Be into H_2 on the $^1A_1$ ground state surface of BeH$_2$, as given by Mk-MRCC theory using CAS(2,2) orbitals. Complete coupling terms are employed. The bond distances r(Be-H) and r(H-H) are in Å. ΔE_R and ΔE_{TS} are the reaction energy and activation barrier (in kcal mol^{-1}) for the C_{2v} insertion.

	Mk-MRCC method						FCI
	SD	SDT-1a	SDT-1b	SDT-2	SDT-3	SDT	
	BeH$_2$ product						
r(Be-H)	1.3803	1.3804	1.3804	1.3804	1.3804	1.3805	1.3808
ΔE_R	-10.19	-10.27	-10.26	-10.26	-10.26	-10.31	-10.44
	$(\text{Be} \cdots \text{H}_2)^\dagger$ transition state						
r(Be-H)	1.6474	1.6626	1.6648	1.6653	1.6635	1.6744	1.6741
r(H-H)	1.3968	1.4105	1.4126	1.4132	1.4114	1.4222	1.4224
$\omega_1(a_1)$	3834i	3815i	3798i	3787i	3806i	3770i	3769i
$\omega_2(a_1)$	952	842	828	831	857	794	796
ΔE_{TS}	99.97	100.21	100.23	100.20	100.18	100.26	100.24

4.6 The Effect of Triples Coupling Terms and Off-Diagonal Fock Matrix Elements

Tables 4.2-4.5 contain our data for assessing the two approximations to Mk-MRCCSDT-*n* theory outlined in Section II: (1) truncation of the triples coupling term in Eq. (19), and (2) neglect of off-diagonal elements of the Fock matrices of the various references to avert the storage of triples amplitudes. The results are best characterized in two sets, the H4, P4, and H8 models collectively and BeH$_2$ separately.

For H4, P4, and H8, truncating to quadratic triples coupling yields results indistinguishable from the complete inclusion of terms. The NPE values for H4, P4, and H8 are affected by less than 1 μE_h in all cases, and the MNPD diagnostics change less than 0.01%. If only linear coupling terms are retained, the accuracy of the Mk-MRCCSDT-*n* schemes deteriorates only slightly. For the NPE measure, the T-*n* methods with linear coupling recover an average of 77.4% of the full triples effect, compared to 80.0% with complete coupling. Likewise, for the MNPD diagnostic, the average recovery of the full triples effect is 79.4% and 79.8% for linear and complete coupling, respectively. Neglecting off-diagonal elements of the Fock matrices in the Mk-MRCCSDT-*n* methods does not change the accuracy of the quadratic and linear coupling approximations in the H4, P4, and H8 models.

The BeH$_2$ results are somewhat more sensitive to the treatment of the Mk-MRCC coupling terms than for the other model systems. In Table 4.4, the largest NPE change arising from truncation of triples coupling is 0.08 mE$_h$. Owing to an advantageous cancellation of errors, the linear coupling approximation actually performs better than quadratic coupling, particularly for the NPE values. Mk-MRCCSDT-2 is the only method for which truncating the triples coupling term substantially alters the percent recovery of the full triples effect on the NPE and

158

MNPD diagnostics. For the other T-n schemes, the accounting of the full triples effect does not change more than 5% regardless of the treatment of the coupling matrix element in Eq. (19).

In the H4, P4, and H8 model systems, the errors in neglecting off-diagonal Fock matrix elements (the $\hat{F}_{\text{diag}}$ approximation) are comparable to those engendered by the truncation to linear coupling. For NPE, $\hat{F}_{\text{diag}}$ with complete coupling in the Mk-MRCCSDT-n schemes recovers on average 76.9% of the full triples effect, which amounts to only a 3.1% reduction in performance compared to incorporation of all off-diagonal Fock matrix elements. For MNPD the average recovery with $\hat{F}_{\text{diag}}$ is 78.6%, within 1% of the corresponding measure without this approximation. For the H4 and P4 systems, the $\hat{F}_{\text{diag}}$ and triples coupling errors are cumulative, but for H8 the combined linear-coupling/$\hat{F}_{\text{diag}}$ NPE and MNPD values in Table 4.5 are the closest to the Mk-MRCCSDT benchmarks of all the entries, indicating another favorable cancellation of errors.

For BeH$_2$, the $\hat{F}_{\text{diag}}$ approximation performs even better than for the H4, P4, and H8 model systems. With complete coupling, $\hat{F}_{\text{diag}}$ actually improves the mean percent recovery of the full triples effect by about 1% for NPE and 2% for MNPD (excepting the T-2 case where $\hat{F}_{\text{diag}}$ improves MNPD dramatically).

Our findings on the $\hat{F}_{\text{diag}}$ approximation may be related to a previous investigation by Crawford and Schaefer[110] on the effect of neglecting the off-diagonal part of the Fock matrix in perturbative triples computations using single reference coupled cluster theory with a restricted open-shell reference. It was found that the accuracy for equilibrium bond lengths, dissociation energies, and harmonic vibrational frequencies of 11 test molecules is basically the same for both

the theory containing the full Fock matrix and the variant that neglects the off-diagonal terms. Further work is required to more fully assess the accuracy of the $\hat{F}_{\text{diag}}$ approximation in both perturbative and iterative MRCC methods; however, our initial results show that even in cases as difficult as the model systems studied here, this approach is valid.

4.7 SUMMARY AND DISCUSSION

In this investigation, several schemes that include triple excitations within the rigorously size-extensive Mukherjee multireference coupled cluster formalism have been implemented for the first time. These consist of a family of approximate triples methods based on CCSDT-n similarity-transformed Hamiltonians[52,53,59] (Mk-MRCCSDT-n) as well as the full Mukherjee multireference coupled cluster method with single, double, and triple excitations (Mk-MRCCSDT). Our implementation of Mk-MRCCSDT-n and Mk-MRCCSDT is not based on a determinantal expansion of the operators, but instead uses intermediates, and therefore has the proper scaling, $d \times O^3V^4$ (N^7) for the Mk-MRCCSDT-n schemes and $d \times O^3V^5$ (N^8) for the Mk-MRCCSDT method.

The performance of these Mk-MRCC methods was tested on four classic model systems for which FCI results are available: H4, P4, BeH$_2$, and H8. The potential energy curves in Figs. 4.1-4.5 clearly demonstrate that the Mk-MRCCSDT-n schemes substantially improve upon the Mk-MRCCSD approach, recovering most of the effects of triples from Mk-MRCCSDT. Two diagnostics were introduced to quantify the performance of the methods – the nonparallelism error (NPE) and the mean nonparallelism derivative (MNPD). The NPE measures the range of deviation from the FCI energy potential curve, while the MNPD is a more precise diagnostic that measures the smoothness of the error with respect to the FCI curve. The average NPE error for

the model systems is reduced from 1.418 mE_h (Mk-MRCCSD) to (0.685, 0.622, 0.620, 0.552) mE_h for (Mk-MRCCSDT-1a, Mk-MRCCSDT-1b, Mk-MRCCSDT-2, Mk-MRCCSDT-3), respectively. Thus, the approximate (Mk-MRCCSDT-1a, Mk-MRCCSDT-1b, Mk-MRCCSDT-2, Mk-MRCCSDT-3) triples methods recover on average (61, 67, 67, 73) % of the triples effect, respectively. The average MNPD value for Mk-MRCCSD is 26.48×10^{-3}, which decreases to $(12.26, 11.00, 10.60, 9.55) \times 10^{-3}$ for (Mk-MRCCSDT-1a, Mk-MRCCSDT-1b, Mk-MRCCSDT-2, Mk-MRCCSDT-3), in order; in comparison it is 2.46×10^{-3} for Mk-MRCCSDT. According to the MNPD diagnostic, the approximate triples schemes (Mk-MRCCSDT-1a, Mk-MRCCSDT-1b, Mk-MRCCSDT-2, Mk-MRCCSDT-3) recover on average (59, 64, 66, 71) % of the triples effects, respectively. The combined NPE and MNPD results indicate that these CC methods form a hierarchy of increasing accuracy following the general order: Mk-MRCCSD < Mk-MRCCSDT-1a < Mk-MRCCSDT-1b < Mk-MRCCSDT-2 < Mk-MRCCSDT-3 < Mk-MRCCSDT. Of course, this order is not always maintained in individual cases.

We further scrutinized BeH_2 to probe the performance of the various Mk-MRCC theories in a more representative chemical application. The transition state for the C_{2v} insertion path of Be + H_2 is a severe multireference case, whereas the linear BeH_2 molecule is single-reference in character and hence is an ideal complement. For the BeH_2 stationary points, we optimized the geometries and computed harmonic vibrational frequencies and reaction energies. Our Mk-MRCCSDT-n methods achieve very good agreement (within 0.1 kcal mol^{-1}) with the FCI activation barrier and reaction energy, performing comparably to Mk-MRCCSDT. The vibrational frequencies at the transition state represent a much sterner test for the theory, as is evident from Table 4.6. In this case the Mk-MRCCSDT method gives errors less than 2 cm^{-1}

with respect to FCI. Of the approximate triple excitations models, CCSDT-2 is the most accurate, matching ω_1 and ω_2 within $18i$ and 35 cm^{-1}, respectively.

Finally, two excellent approximations in Mk-MRCCSDT-n treatments have been substantiated. First, we find that the triples coupling matrix elements in Eq. (19) can be truncated at either the quadratic or linear level without significant loss of accuracy. In our model systems, the NPE value always changed less than 0.1 mE_h regardless of the level of truncation. Second, neglecting the off-diagonal part of the Fock matrices in evaluating matrix elements of the similarity-transformed Hamiltonian introduces negligible errors, and in some cases actually yields more accurate results than if the full Fock matrices are employed. For example, the $\hat{F}_{diag}$ approximation increases the average NPE for our model systems by only (1.3, 0.9, 0.9, 1.1) % for (Mk-MRCCSDT-1a, Mk-MRCCSDT-1b, Mk-MRCCSDT-2, Mk-MRCCSDT-3), respectively. The consequences of these findings are far reaching, particularly for constructing a viable perturbative triples correction [(T)] to Mk-MRCCSD. Not only may the (T) scheme be formulated by including only the linear triples coupling terms, but a non-iterative algorithm can be devised analogous to the single-reference case, whereby the storage of $\hat{T}_3$ amplitudes is avoided. Given the remarkable accuracy we have documented for the full Mk-MRCCSDT theory, the development of an efficient and robust Mk-MRCCSD(T) theory promises many rewards in the study of multireference systems.

R<small>EFERENCES</small>

1   R. J. Bartlett, *Recent Advances in Coupled-Cluster Methods*. (World Scientific, Singapore, 1997).

2   J. Gauss, in *The Encyclopedia of Computational Chemistry*, edited by P.v. R. Schleyer, N. L. Allinger, T. Clark, J. Gasteiger, P. A. Kollman, H. F.Schaefer III, and a. P. R. Scheiner (Wiley, Chichester, 1998), pp. 615.

3   T. D. Crawford and H. F. Schaefer, Rev. Comp. Chem. **14**, 33 (2000).

4   R. J. Bartlett and M. Musial, Rev. Mod. Phys. **79**, 291 (2007).

5   P. R. Surján and M. Kállay, J. Mol. Struct. **547**, 145 (2001).

6   G. K. L. Chan, M. Kállay, and J. Gauss, J. Chem. Phys. **121**, 6110 (2004).

7   T. Van Voorhis and M. Head-Gordon, J. Chem. Phys. **113**, 8873 (2000).

8   R. F. Bishop and J. S. Arponen, Int. J. Quantum. Chem. Symp. **38**, 197 (1990).

9   T. Van Voorhis and M. Head-Gordon, Chem. Phys. Lett. **330**, 585 (2000).

10   P. Piecuch, N. Oliphant, and L. Adamowicz, J. Chem. Phys. **99**, 1875 (1993).

11   V. V. Ivanov and L. Adamowicz, J. Chem. Phys. **112**, 9258 (2000).

12   J. Olsen, J. Chem. Phys. **113**, 7140 (2000).

13   M. Kállay, P. G. Szalay, and P. R. Surján, J. Chem. Phys. **117**, 980 (2002).

14   P. Piecuch, S. A. Kucharski, and R. J. Bartlett, J. Chem. Phys. **110**, 6103 (1999).

15   X. Z. Li and J. Paldus, J. Chem. Phys. **107**, 6257 (1997).

16   X. Z. Li and J. Paldus, J. Chem. Phys. **108**, 637 (1998).

17   A. I. Krylov, C. D. Sherrill, E. F. C. Byrd, and M. Head-Gordon, J. Chem. Phys. **109**, 10669 (1998).

18   A. Köhn and J. Olsen, J. Chem. Phys. **122**, 084116 (2005).

19   O. Hino, T. Kinoshita, G. K. L. Chan, and R. J. Bartlett, J. Chem. Phys. **124**, 114311 (2006).

20   T. Kinoshita, O. Hino, and R. J. Bartlett, J. Chem. Phys. **123**, 074106 (2005).

21   M. Nooijen and R. J. Bartlett, J Chem Phys **107**, 6812 (1997).

22   S. V. Levchenko and A. I. Krylov, J. Chem. Phys. **120**, 175 (2004).

23   K. Jankowski, J. Paldus, and P. Piecuch, Theor. Chim. Acta **80**, 223 (1991).

24   K. Kowalski and P. Piecuch, J. Chem. Phys. **113**, 18 (2000).

25   P. Piecuch, K. Kowalski, I. S. O. Pimienta, and M. J. McGuire, Int. Rev. Phys. Chem. **21**, 527 (2002).

26   M. D. Lodriguito, K. Kowalski, M. Wloch, and P. Piecuch, J. Mol. Struct. **771**, 89 (2006).

27   I. Lindgren, Int. J. Quantum. Chem. Symp. **12**, 33 (1978).

28   D. Mukherjee, R. K. Moitra, and A. Mukhopadhyay, Mol. Phys. **33**, 955 (1977).

29   M. A. Haque and D. Mukherjee, J. Chem. Phys. **80**, 5058 (1984).

30   B. Jeziorski and H. J. Monkhorst, Phys. Rev. A **24**, 1668 (1981).

31   S. A. Kucharski and R. J. Bartlett, J. Chem. Phys. **95**, 8227 (1991).

32   S. A. Kucharski, A. Balkova, P. G. Szalay, and R. J. Bartlett, J. Chem. Phys. **97**, 4289 (1992).

33   J. Paldus, P. Piecuch, L. Pylypow, and B. Jeziorski, Phys. Rev. A **47**, 2738 (1993).

34   P. Piecuch and J. Paldus, Phys. Rev. A **49**, 3479 (1994).

35   J. Mášik and I. Hubač, Adv. Quantum. Chem. **31**, 75 (1999).

36   I. Hubač, J. Pittner, and P. Čársky, J. Chem. Phys. **112**, 8779 (2000).

37   J. Pittner, J. Chem. Phys. **118**, 10876 (2003).

38   U. S. Mahapatra, B. Datta, and D. Mukherjee, Mol. Phys. **94**, 157 (1998).

39   U. S. Mahapatra, B. Datta, and D. Mukherjee, J. Chem. Phys. **110**, 6171 (1999).

40   M. Hanrath, J. Chem. Phys. **123**, 084102 (2005).

41   M. Hanrath, Chem. Phys. Lett. **420**, 426 (2006).

42   I. D. Petsalakis, G. Theodorakopoulos, C. A. Nicolaides, R. J. Buenker, and S. D. Peyerimhoff, J. Chem. Phys. **81**, 3161 (1984).

43   C. A. Nicolaides, Int. J. Quantum Chem. **60**, 119 (1996).

44   C. A. Nicolaides, Int. J. Quantum Chem. **102**, 250 (2005).

45   F. A. Evangelista, W. D. Allen, and H. F. Schaefer, J. Chem. Phys. **127**, 024102 (2007).

46   S. Chattopadhyay, P. Ghosh, and U. S. Mahapatra, J. Phys. B **37**, 495 (2004).

47   J. Paldus, I. Shavitt, and J. Čížek, Phys. Rev. A **5**, 50 (1972).

48   J. Noga and R. J. Bartlett, J. Chem. Phys. **86**, 7041 (1987).

49   J. Noga and R. J. Bartlett, J. Chem. Phys. **89**, 3401 (1988).

50   G. E. Scuseria and H. F. Schaefer, Chem. Phys. Lett. **152**, 382 (1988).

51   J. D. Watts and R. J. Bartlett, J. Chem. Phys. **93**, 6104 (1990).

52   M. Urban, J. Noga, S. J. Cole, and R. J. Bartlett, J. Chem. Phys. **83**, 4041 (1985).

53   M. Urban, J. Noga, S. J. Cole, and R. J. Bartlett, J. Chem. Phys. **85**, 5383 (1986).

54   K. Raghavachari, G. W. Trucks, J. A. Pople, and M. Head-Gordon, Chem. Phys. Lett. **157**, 479 (1989).

55   T. D. Crawford and J. F. Stanton, Int. J. Quantum Chem. **70**, 601 (1998).

56   S. A. Kucharski and R. J. Bartlett, J. Chem. Phys. **108**, 5243 (1998).

57   S. R. Gwaltney and M. Head-Gordon, Chem. Phys. Lett. **323**, 21 (2000).

58   S. R. Gwaltney and M. Head-Gordon, J. Chem. Phys. **115**, 2014 (2001).

59   J. Noga, R. J. Bartlett, and M. Urban, Chem. Phys. Lett. **134**, 126 (1987).

60   Y. He, Z. He, and D. Cremer, Theor. Chem. Acc. **105**, 182 (2001).

61   H. Koch, O. Christiansen, P. Jørgensen, A. M. S. de Meras, and T. Helgaker, J. Chem. Phys. **106**, 1808 (1997).

62   J. D. Watts, J. F. Stanton, and R. J. Bartlett, Chem. Phys. Lett. **178**, 471 (1991).

63   M. Urban, J. D. Watts, and R. J. Bartlett, Int. J. Quantum Chem. **52**, 211 (1994).

64   O. Christiansen, H. Koch, A. Halkier, P. Jørgensen, T. Helgaker, and A. S. de Meras, J. Chem. Phys. **105**, 6921 (1996).

65   O. Christiansen, J. Gauss, J. F. Stanton, and P. Jørgensen, J. Chem. Phys. **111**, 525 (1999).

66   N. J. DeYonker, Y. Yamaguchi, W. D. Allen, C. Pak, H. F. Schaefer, and K. A. Peterson, J. Chem. Phys. **120**, 4726 (2004).

67   J. M. Turney, L. Sari, Y. Yamaguchi, and H. F. Schaefer, J. Chem. Phys. **122**, 094304 (2005).

68   F. A. Evangelista, W. D. Allen, and H. F. Schaefer, J. Chem. Phys. **125**, 154113 (2006).

69   A. Balková and R. J. Bartlett, J. Chem. Phys. **101**, 8972 (1994).

70   X. Li and J. Paldus, J. Chem. Phys. **124**, 034112 (2006).

71   X. Z. Li and J. Paldus, Mol. Phys. **104**, 2047 (2006).

72   O. Demel and J. Pittner, J. Chem. Phys. **124**, 144112 (2006).

73   J. Pittner and O. Demel, J. Chem. Phys. **122**, 181101 (2005).

74   M. Rittby and R. J. Bartlett, J. Phys. Chem. **92**, 3033 (1988).

75   J. D. Watts, J. Gauss, and R. J. Bartlett, J. Chem. Phys. **98**, 8718 (1993).

76   C. E. Smith, R. A. King, and T. D. Crawford, J. Chem. Phys. **122**, 054110 (2005).

[77]   M. Schütz, J. Chem. Phys. **116**, 8772 (2002).

[78]   N. C. Handy, J. A. Pople, M. Head-Gordon, K. Raghavachari, and G. W. Trucks, Chem. Phys. Lett. **164**, 185 (1989).

[79]   M. Schütz and H. J. Werner, Chem. Phys. Lett. **318**, 370 (2000).

[80]   J. Gauss and J. F. Stanton, Phys. Chem. Chem. Phys. **2**, 2047 (2000).

[81]   J. Gauss and J. F. Stanton, J. Chem. Phys. **116**, 1773 (2002).

[82]   J.F. Stanton, J. Gauss, J.D. Watts, P.G. Szalay, R.J. Bartlett with contributions from A.A. Auer, D.B. Bernholdt, O. Christiansen, M.E. Harding, M. Heckert, O. Heun, C. Huber, D. Jonsson, J. Jusélius, W.J. Lauderdale, T. Metzroth, C. Michauk, D.R. Price, K. Ruud, F. Schiffmann, A. Tajti, M.E. Varner, J. Vázquez and the integral packages: MOLECULE (J. Almlöf and P.R. Taylor), PROPS (P.R. Taylor), and ABACUS (T. Helgaker, H.J. Aa. Jensen, P. Jørgensen, and J. Olsen). Current version see http://www.aces2.de. .

[83]   T. D. Crawford, C. D. Sherrill, E. F. Valeev, J. T. Fermann, R. A. King, M. L. Leininger, S. T. Brown, C. L. Janssen, E. T. Seidl, J. P. Kenny, and W. D. Allen, J. Comp. Chem. **28**, 1610 (2007).

[84]   (See EPAPS Document No. ??? for pdf file containing the basis sets and energy error curves. This document can be reached via a direct link in the online article's HTML reference section or via the EPAPS homepage http://www.aip.org/pubservs/epaps.htm).

[85]   K. Jankowski and J. Paldus, Int. J. Quantum Chem. **18**, 1243 (1980).

[86]   P. Piecuch and J. Paldus, J. Phys. Chem. **99**, 15354 (1995).

[87]   P. Piecuch and J. Paldus, J. Chem. Phys. **101**, 5875 (1994).

[88]   U. S. Mahapatra, B. Datta, and D. Mukherjee, J. Phys. Chem. A **103**, 1822 (1999).

[89]   T. H. Dunning, Jr., J. Chem. Phys. **53**, 2823 (1970).

[90] S. Huzinaga, J. Chem. Phys. **42**, 1293 (1965).

[91] G. D. Purvis, R. Shepard, F. B. Brown, and R. J. Bartlett, Int. J. Quantum Chem. **23**, 835 (1983).

[92] R. K. Chaudhuri, J. P. Finley, and K. F. Freed, J. Chem. Phys. **106**, 4067 (1997).

[93] S. B. Sharp and G. I. Gellene, J. Phys. Chem. A **104**, 10951 (2000).

[94] U. S. Mahapatra, B. Datta, B. Bandyopadhyay, and D. Mukherjee, Adv. Quantum Chem. **30**, 163 (1998).

[95] J. Ma, S. H. Li, and W. Li, J. Comp. Chem. **27**, 39 (2006).

[96] P. J. A. Ruttink, J. H. van Lenthe, and P. Todorov, Mol. Phys. **103**, 2497 (2005).

[97] S. Chattopadhyay and U. S. Mahapatra, J. Phys. Chem. A **108**, 11664 (2004).

[98] J. Pittner, H. V. Gonzalez, R. J. Gdanitz, and P. Čársky, Chem. Phys. Lett. **386**, 211 (2004).

[99] A. Banerjee and J. Simons, Chem. Phys. **81**, 297 (1983).

[100] R. J. Gdanitz and R. Ahlrichs, Chem. Phys. Lett. **143**, 413 (1988).

[101] R. J. Gdanitz, Int. J. Quantum Chem. **85**, 281 (2001).

[102] D. I. Lyakh, V. V. Ivanov, and L. Adamowicz, Theor. Chem. Acc. **116**, 427 (2006).

[103] For linear BeH_2, the Hartree-Fock orbital energy of the unoccupied 1π orbital is lower than that of the $3\sigma_g^*$ antibonding orbital. A proper multireference description of the dissociation process requires continuous following of the $(1\sigma_u)^2 \leftrightarrow (3\sigma_g^*)^2$ zeroth-order wave function solution. We were careful to ensure that this solution was obtained for both the CAS(2,2) orbitals and the multireference coupled cluster wave functions at all points along the BeH_2 dissociation path.

[104] K. Jankowski, L. Meissner, and J. Wasilewski, Int. J. Quantum Chem. **28**, 931 (1985).

[105] P. Piecuch and L. Adamowicz, J. Chem. Phys. **100**, 5792 (1994).

[106] P. Piecuch and L. Adamowicz, Chem. Phys. Lett. **221**, 121 (1994).

[107] X. Li and J. Paldus, J. Chem. Phys. **103**, 1024 (1995).

[108] I. Hubač, P. Mach, and S. Wilson, Int. J. Quantum Chem. **104**, 387 (2005).

[109] S. Chattopadhyay, D. Pahari, D. Mukherjee, and U. S. Mahapatra, J. Chem. Phys. **120**, 5968 (2004).

[110] T. D. Crawford and H. F. Schaefer, J. Chem. Phys. **104**, 6259 (1996).

CHAPTER 5

CONCLUSION

We have developed and implemented a state-specific multireference coupled cluster (MRCC) theory first suggested by Mukherjee and co-workers (Mk-MRCC). Mk-MRCC is a fully size extensive and intruder-free approach aimed at computing accurate thermodynamic, kinetic, and spectroscopic data for multireference open-shell states of atoms and molecules.

In the initial stage of our research, in order to avoid the mathematical difficulties encountered in MRCC theory, we solved the corresponding equations using a new arbitrary-order string-based code capable of computing energies. This advancement allowed us, for the first time, to compare the accuracy of various MRCC approaches and benchmark the results against full configuration interaction. For ground electronic states we found that Mk-MRCC is clearly superior to the state-universal MRCC (SU-MRCC) method at all levels of truncation of the cluster operator. Our results on model systems also indicate that Mk-MRCC is in general more accurate than Brillouin-Wigner MRCC (BW-MRCC) theory.

We then proceeded to solve the mathematical difficulties found in Mk-MRCC theory and derived closed expressions for the "same vacuum" coupling terms. This allowed us to develop the first production-level code capable of performing Mk-MRCC with singles and doubles computations (Mk-MRCCSD) on molecular systems. Mk-MRCCSD benchmark calculations of the potential energy curve of F_2 and the harmonic vibrational frequencies of ozone support the

accuracy and reliability of Mk-MRCC when compared to single-reference coupled cluster and BW-MRCC. While the dissociation energy and harmonic vibrational frequency of F_2 computed with Mk-MRCC using localized orbitals are within 0.2 kcal mol^{-1} and 2 cm^{-1} from experimental values, respectively, the harmonic vibrational frequencies for ozone were found to be problematic. For example, the antisymmetric stretching frequency of ozone, $\omega_3(b_2)$, remains a problem for all the MRCC methods investigated, moreover, ω_3 is extremely sensitive to the choice of orbital canonicalization. Mk-MRCCSD was also tested on the singlet-triplet energy splitting of *ortho*-, *meta*-, and *para*-benzyne. In all cases our results are in close agreement (within 1.5 kcal mol^{-1}) with the experimental values.

In the last part of our dissertation we advanced the Mk-MRCCSDT-n ($n = $ 1a,1b,2,3) models. These are new approximate methods based on the full Mk-MRCCSDT approach which includes triple excitations aimed at improving the accuracy of Mk-MRCCSD. The Mk-MRCCSDT-n methods have a computational cost which scales as N^7 (N being the number of electrons) and thus are less expensive than the full Mk-MRCCSDT model which scales as N^8. Our computations on model systems show that the Mk-MRCCSDT-n methods recover on average 60-70% of the effect of full triples excitations.

This dissertation establishes Mk-MRCC as the method of choice for accurate description of multireference open-shell states of atoms and molecules. However, further work is required to extend the range of problems that can be treated with Mk-MRCC. For example, to study polyradicals, multiple bond dissociation processes, and transition metal compounds, a generalization of Mk-MRCC to arbitrary active spaces is required. Furthermore, other desirable advances would include the formulation of an internally contracted approximation to reduce the computational cost and the formulation of a perturbative triples approach akin to the "gold

standard" of single-reference methods, CCSD(T). From the formal point of view, the most important limitation of Mk-MRCC is the sensitivity with respect to orbital canonicalization. This problem seems to be intimately connected to the form of the Jeziorski-Monkhorst ansatz, and therefore its solution might require the formulation of a completely new MRCC ansatz.